2nd Department of Medicine and Cardiology Center, Medical Faculty,
Albert Szent-Györgyi Clinical Center,
University of Szeged

Mitral annular dimensions and function in certain disorders and their relationship to left ventricular function

Zsolt Kovács MD

PhD thesis

Tutor:

Prof. Attila Nemes MD, PhD, DSc

2019

Relevant publications

Full papers

I. Kovács Z, Kormányos Á, Domsik P, Kalapos A, Lengyel C, Ambrus N, Ajtay Z, Piros GÁ, Forster T, Nemes A. Left ventricular longitudinal strain is associated with mitral annular fractional area change in healthy subjects-Results from the three-dimensional speckle tracking echocardiographic MAGYAR-Healthy Study. Quant Imaging Med Surg. 2019; 9: 304-311. **(impact factor: 3.074)**

II. Kovács Z, Kormányos Á, Domsik P, Kalapos A, Lengyel C, Ajtay Z, Forster T, Nemes A. Borderline left ventricular ejection fraction is associated with alterations in mitral annular size and function. Results from the three-dimensional speckle-tracking echocardiographic MAGYAR-Healthy Study. Orv Hetil. 2018; 159: 2129-2135. **(impact factor: 0.564)**

III. Nemes A, Kovács Z, Kormányos Á, Domsik P, Kalapos A, Piros GÁ, Kemény L, Forster T, Szolnoky G. The Mitral Annulus in Lipedema: Insights from the Three-Dimensional Speckle Tracking Echocardiographic MAGYAR-Path Study. Echocardiography 2019; 36: 1482-1491. **(impact factor: 1.287)**

IV. Nemes A, Kormányos Á, Havasi K, Kovács Z, Domsik P, Kalapos A, Hartyánszky I, Ambrus N, Forster T. Mitral annulus is enlarged and functionally impaired in adult patients with repaired tetralogy of Fallot as assessed by three-dimensional speckle-tracking echocardiography – Results from the CSONGRAD Registry and MAGYAR-Path Study. Cardiovasc Diagn Ther. (in press) **(impact factor: 2.006)**

Table of contents

Abbreviations

2D – two-dimensional

3D – three-dimensional

2DSTE – two-dimensional speckle-tracking echocardiography

3DSTE – three-dimensional speckle-tracking echocardiography

AP2CH – apical 2-chamber view

AP4CH – apical 4-chamber view

BMI – body mass index

CHD – congenital heart disease

CI – confidence interval

CSONGRÁD Registry – Registry for **C(S)ONG**enital ca**R**di**A**c **D**isease patients at the University of Szeged

E and A – early and late diastolic transmitral flow velocities

EF – emptying fraction

LA – left atrium

LS – longitudinal strain

LV – left ventricle

MAGYAR-Healthy Study – **M**otion **A**nalysis of the heart and **G**reat vessels b**Y** three-dimension**A**l speckle-t**R**acking echocardiography in **Healthy** subjects Study

MAGYAR-Path Study – **M**otion **A**nalysis of the heart and **G**reat vessels b**Y** three-dimension**A**l speckle-t**R**acking echocardiography in **Path**ological cases Study

MA – mitral annulus

MAA – mitral annular area

MAD – mitral annular diameter

MAFAC – mitral annular fractional area change

MAFS – mitral annular fractional shortening

MAP – mitral annular perimeter

MCS – medical compression stocking

MRI – magnetic resonance imaging

MV – mitral valve

RA – right atrium

ROC – receiver operator characteristics

RT3DE – real-time three-dimensional echocardiography

SD – standard deviation

STE – speckle-tracking echocardiography

TOF – tetralogy of Fallot

etrTOF – patient with early total reconstructed TOF

pcTOF – patient with early palliated, late corrected TOF

1. Introduction

The mitral valve (MV) apparatus is a saddle-shaped, complex three-dimensional (3D) functional unit which separates the left atrium (LA) and the left ventricle (LV), and has a critical role in the regulation of normally unidirectional blood flow (1,2). Significant parts of MV are mitral annulus (MA), valvular leaflets, papillary muscles and tendines (1,2). MA morphology and function could show significant alterations in several valvular (for instance in mitral prolapse, mitral regurgitation) and non-valvular disorders (for instance in certain cardiomyopathies, cardiac amyloidosis)(3-6).

Three-dimensional speckle-tracking echocardiography (3DSTE) is a new non-invasive imaging method with 3D capability of volumetric and strain-based functional assessment not only of certain heart chambers (for instance LV, LA), but using the same 3D virtual heart chamber model, MA dimensions could be easily assessed respecting cardiac cycle (7).

Alterations in MA size and function are known to be important parameters in different disorders with alterations in LV size and function. Due to technical reasons, 3DSTE-derived ***LV ejection fraction (EF)*** could be different to routinely assessed LV-EF using two-dimensional (2D) echocardiography (7,8). Theoretically some cases could have 3DSTE-derived borderline LV-EF (50-55%) with early alterations in MA dimensions and functional properties.

Compared to the LV-EF, ***LV longitudinal systolic function*** was found to be more sensitive in the detection of cardiac depression in several disorders (9,10). 3DSTE is a clinical tool of choice for simultaneous quantification of longitudinal LV deformation and MV morphology and function (7,11). LV-MV interactions are not clearly understood at this moment, therefore the relationship between LV quantitative features of longitudinal contractility and MA size and function would be interesting in healthy subjects.

Lipedema is a poorly recognized disease with female predominance, it is characterized by bilateral, symmetrical disproportional fatty deposits in the lower body and commonly in the upper extremities (12). It is usually mistaken with obesity or lymphedema. Lipedema is characterized by non-pitting edema, susceptibility to bruising, tenderness, and it usually it does not respond to various dietary approaches. Underlying causes are mostly unknown,

however hormonal influence is strongly suspected (12). A recent investigation showed increased aortic stiffness and altered LV rotational mechanics among patients with lipedema (13,14). However, alterations in MA morphology and function have never been assessed in these patients.

Tetralogy of Fallot (TOF) is a cyanotic congenital heart disease (CHD) consisting of ventricular septal defect, overriding aorta, pulmonary stenosis, and right ventricular hypertrophy (15,16). Due to the opportunity of early total reconstruction, there is an increasing number of patients with repaired TOF in the adult clinical practice (17). 3DSTE-derived deformation analyses confirmed deteriorated left (18-20) and right (21-23) heart chambers including ventricles (18,19,21,23) and atria (20,22,23). Similarly to lipedema, morphological and functional assessment of the MA has never been performed in adult patients with repaired TOF.

2. Aims

To investigate the relationship between LV strains, quantitative features of longitudinal contractility and MA size and function in healthy subjects.

To examine the relationship between MA morphologic and functional properties and 3DSTE-derived LV-EF in subjects with normal versus borderline LV-EF.

To examine lipedema-associated cardiac implications and to compare MA size and function between lipedema patients and age-, gender-, and body mass index (BMI) - matched healthy controls by 3DSTE. It was also determined whether one-hour use of medical compression stockings (MCS) has any effect on MA morphology and functional properties.

To test whether repaired TOF is associated with morphological and functional alterations of the MA. The role of the type of treatment (early total reconstruction vs. early palliation, late correction) was also aimed to be assessed.

3. Methods

Patient population (general considerations). Complete 2D Doppler echocardiography and 3DSTE have been performed in all cases. Results of the adult repaired TOF patients are from the CSONGRAD Registry (Registry for C(S)ONGenital caRdiAc Disease patients at the University of Szeged)(17). The results are parts of the MAGYAR-Healthy and MAGYAR-Path Studies (Motion Analysis of the heart and Great vessels bY three-dimensionAl speckle-tRacking echocardiography in Healthy subjects and Pathological cases). These studies were organized at the 2nd Department of Medicine and Cardiology Center, University of Szeged to evaluate usefulness, diagnostic and prognostic value of 3DSTE-derived volumetric, strain, rotational etc. parameters in pathological cases and to establish their normal values and their physiological relationship with other normal parameters in healthy adults (’magyar’ means ’Hungarian’ in Hungarian language)(7). Informed consent was obtained from each patient and the study protocol conformed to the ethical guidelines of the 1975 Declaration of Helsinki, as reflected in a prior approval by the institution’s human research committee (71/2011).

Two-dimensional echocardiography. Toshiba Artida^{TM} (Toshiba Medical Systems, Tokyo, Japan) echocardiography equipment using a PST-30SBP (1-5 MHz) phased-array transducer was used for standard transthoracic Doppler examinations. Concerning guidelines, LV-EF was calculated by the Simpson’s method (8,24). Valvular regurgitations were visually assessed by color Doppler echocardiography. Early and late mitral inflow E and A were measured by pulsed Doppler echocardiography. To assess LV function, 2D speckle-tracking echocardiographic evaluation of peak systolic LV longitudinal strain (LS) and LS rate were measured in each subject in apical four-chamber view (AP4CH) in the lipedema study (8,24).

3DSTE-derived data acquisition and quantitative analysis. The same Toshiba Artida^{TM} echocardiography equipment was used with a fully sampled PST-25SX matrix-array transducer (Toshiba Medical Systems, Tokyo, Japan) with 3D capability. Pyramidal 3D full volumes were formed by the software using the R-wave triggered LV subvolumes from the 3D pyramidal data acquired during six consecutive cardiac cycles during one breath-hold from apical views in accordance with recent practices (7,25). Depth and angle were adjusted for optimal temporal and spatial resolution. 3D Wall Motion Tracking software version 2.7

(Toshiba Artida^{TM}; Toshiba Medical Systems, Tokyo, Japan) was used for quantitative analysis.

3DSTE-derived LV ejection fraction and longitudinal strain parameters. Three short-axis views acquired at different LV levels and the apical two-chamber (AP2CH) and AP4CH views were selected automatically from the 3D echocardiographic pyramidal dataset at end-diastole by the software (7,25). For 3D reconstruction of the LV endocardial surface, the examiner selected two points at the edges of the mitral valve and one point at the apex on the 3D reconstruction of the endocardial surface on the AP2CH and AP4CH views. Then the endocardial surface was manually adjusted in all apical and short-axis views. After these adjustments were made, the software automatically reconstructed and tracked the endocardial surface in 3D space throughout the cardiac cycle, and generated LV volumetric data including LV-EF and curves for global and mean segmental LV-LSs (Figure 1).

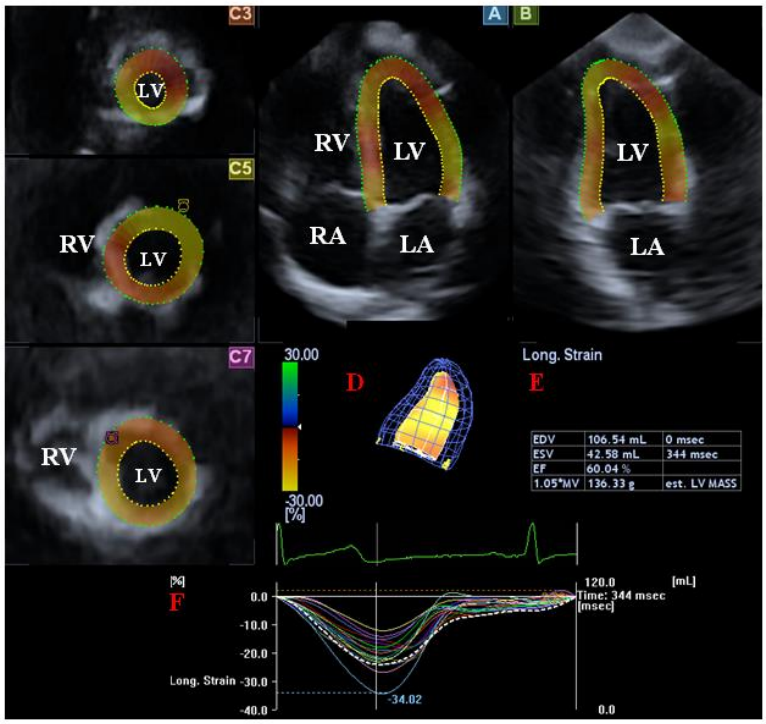

Figure 1. The apical four- (A) and two-chamber (B) views and 3 short axis views at different left ventricular (LV) levels (C3, C5, C7) are presented in a healthy case. The three-dimensional LV cast (D) together with LV volumetric data (E) and LV segmental longitudinal strains (coloured lines) and LV volume-change (dashed line) regarding the cardiac cycle (F) are also presented.
Abbreviations: LA = left atrium, LV = left ventricle, RA = right atrium, RV = right ventricle

3DSTE-derived LA longitudinal strain parameters. In the lipedema study, to create a 3D virtual LA model, the reader set markers on orthogonal AP2CH and AP4CH views. Following detection of the edge of the septum-MA ring, markers were set in counterclockwise direction around the LA to the edge of the lateral wall-MA ring. LA appendage and pulmonary veins were excluded from the LA cavity. Then LA was automatically reconstructed and tracked in 3D space throughout the entire cardiac cycle. Using 3D LA-cast, peak LA-LS characterizing LA reservoir function was calculated for each patient (Figure 2)(7,25).

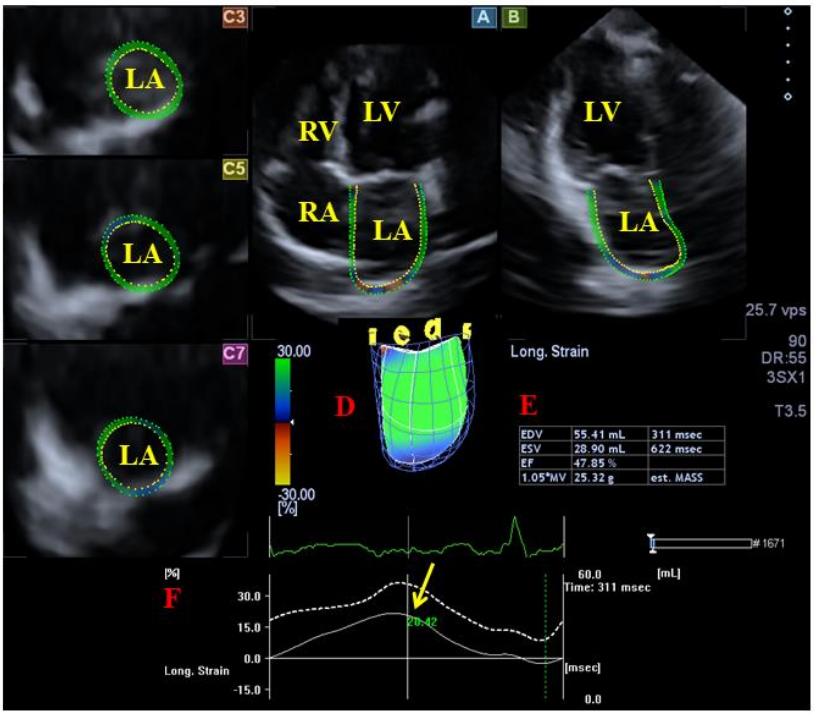

Figure 2. Three-dimensional (3D) speckle-tracking echocardiographic evaluation of the left atrium (LA) is displayed in a patient with lipedema. Apical four-chamber (A) and two-chamber (B) views, short-axis view at basal (C3), midatrial (C5) and superior LA level (C7) are shown together with a 3D cast of the LA (D) and calculated volumetric LA data (E). Time – global LA volume change (dashed line) and time – global LA longitudinal strain curves (white line) are also demonstrated (F). The yellow arrow represents global peak LA-LS featuring LA reservoir function.
Abbreviations: EDV = end-diastolic volume, ESV = end-systolic volume, EF = ejection fraction, LA = left atrium, LV = left ventricle, RA =right atrium, RV = right ventricle

3DSTE-derived mitral annular measurements. MA measurements were performed in accordance with a simple method recently demonstrated by our working group. Briefly, from short-axis views, C7 was positioned at the level of the MA with the help of AP2CH and

AP4CH views to find the optimal endpoints of the MA at end-diastole and end-systole (Figure 3)(6):

MA morphologic parameters

- MA diameter (MAD) was defined as the perpendicular line drawn from the peak of MA curvature to the middle of the straight MA border both at end-systole and at end-diastole
- MA area (MAA) was measured at end-diastole, just before mitral valve closure, and at end-systole, just before mitral valve opening
- MA perimeter (MAP) was measured by planimetry both at end-systole and at end-diastole

MA functional parameters

- MA fractional shortening (MAFS) = (end-diastolic MAD - end-systolic MAD) / (end-diastolic MAD × 100)
- MA fractional area change (MAFAC) = (end-diastolic MAA_{3D} - end-systolic MAA) / (end-diastolic MAA × 100)

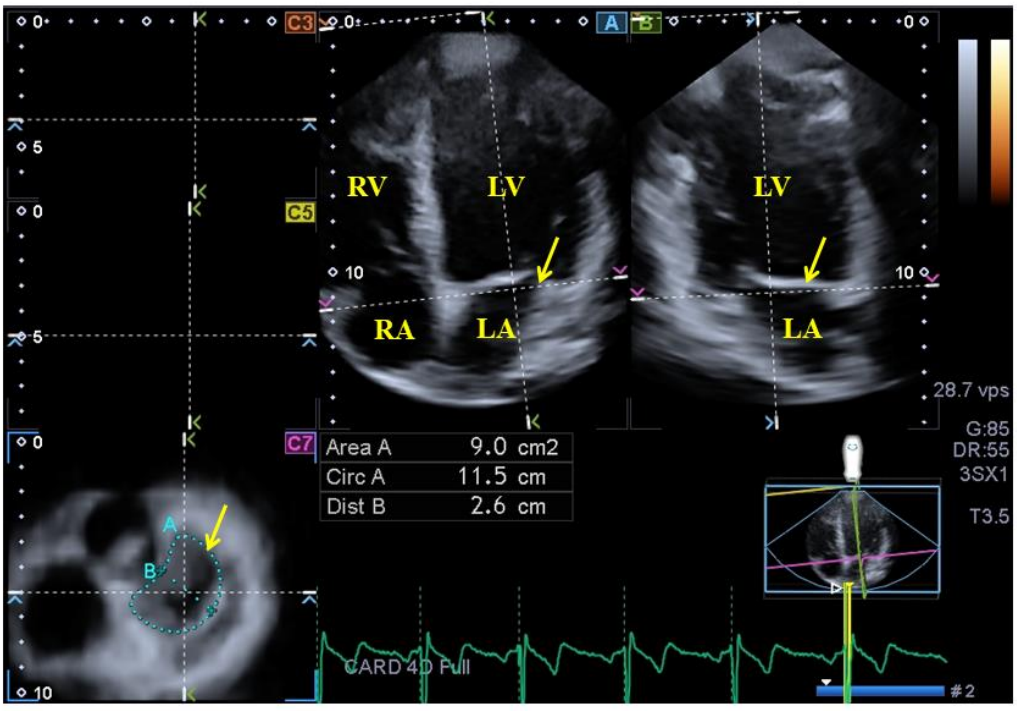

Figure 3. Images from three-dimensional full-volume echocardiographic dataset: apical four-chamber view (A), apical two-chamber view (B) and a cross-sectional view at the level of the mitral annulus (C7) optimized on apical four- and two-chamber views. Mitral annular data in end-systole and end-diastole are also presented.
Abbreviations: Area = MA area, Circ = MA perimeter, Dist = MA diameter, LA = left atrium, LV = left ventricle, RA = right atrium, RV = right ventricle

Experimental protocol for the lipedema study. First, patients underwent 2D echocardiography and consecutively 3DSTE. After the echocardiographic measurements, the patients donned their MCSs and applied them for 60 minutes (26). Postprocedural echocardiography was scheduled at the end of the 60-min MCS application before the patients took off the MCSs. Patients were not allowed to do any kind of physical exercise or to consume any meal or beverage until the second echocardiographic procedure had been done. During the 60-min stocking application period, they could sit with straight legs or stand. Room temperature and relative humidity were stable at 21-22 °C and 45-50%, respectively. Each garment was used for the first time and our physiotherapist colleagues assisted donning and doffing, if needed. Participants were informed precisely about the study protocol when the study started.

During study, Bauerfeind VenoTrain CuraFlow black colored flat-knitted ccl 2 (23-32 mmHg) (Bauerfeind, Zeulenroda, Germany) stocking consisting of 73% polyamide and 27% elastane was used. Interface pressure measurement between skin and compression material using Picopress device (Microlab Elettronica, Nicolò, Italy) (27) at B1 point (28) in standing position revealed a mean pressure of 22.79±3.75 mmHg among patients with lipedema.

Statistical analysis. Continuous data were presented as mean values ± standard deviation, while categorical data were summarized as a count and percentage. Kolmogorov-Smirnov test was used for normality of distribution of datasets and were analyzed by Student's *t*-test. Non-normally distributed datasets were tested with Mann-Whitney-Wilcoxon test. Fisher's exact test was used for categorical variables. Two-sided p <0.05 was defined as statistical significance. Pearson's coefficient was calculated to examine correlations between parameters. Inter- and intraobserver reproducibility of measurements was tested and agreements were verified using the Bland–Altman method. To assess the predictive power of MAFAC, receiver operator curve (ROC) was constructed and the area under the curve was reported with sensitivity and specificity values with 95% confidence intervals. MedCalc software (MedCalc, Mariakerke, Belgium) and RStudio (RStudio Team (2015) RStudio: Integrated Development for R. RStudio, Inc., Boston, MA) was used for statistical analysis. MATLAB version 8.6 software package was used for data analysis (The MathWorks Inc., Natick, MA, 2015).

4. Results

4.1. Left ventricular longitudinal strain is associated with mitral annular fractional area change in healthy subjects

Patient populations. The present study comprised 295 healthy adults; 117 subjects were excluded due to inferior image quality (40%). Finally, 178 healthy adults (mean age: 32.0 ± 11.3 years, 92 males) have been included without risk factors, known diseases or other conditions which theoretically could have affected the results. None of them take any medications at the time of examination.

Clinical data. Demographic data are presented in Table 1. Average height and weight proved to be 172.3 ± 11.1 cm and 71.8 ± 17.7 kg, respectively.

Two-dimensional echocardiographic data. Routine two-dimensional Doppler echocardiography showed normal results including left atrial diameter (36.8 ± 4.0 mm), interventricular septum thickness (9.1 ± 1.5 mm), systolic and diastolic LV diameter (38.4 ± 23.5 mm and 48.0 ± 3.9 mm, respectively) and LV volume (36.4 ± 9.1 ml and 97.4 ± 29.4 ml, respectively), LV ejection fraction (65.6 ± 4.7 %), transmitral flow velocity E (72.8 ± 26.0 cm/s) and A (64.3 ± 19.0 cm/s) and their ratio (1.25 ± 0.52). None of the healthy subjects had grade ≥ 1 valvular regurgitation or significant valvular stenosis.

Table 1. Three-dimensional speckle-tracking echocardiographic data of healthy subjects and their relationship to left ventricular longitudinal strain and mitral annular fractional area change

	All	global LV-LS > -13%	global LV-LS ≤ -13%	MAFAC >44%	MAFAC ≤44%
Demographic data					
n	178 (100)	163 (92)	15 (8)	117 (66)	61 (34)
Age (years)	32.0 ± 11.3	32.7 ± 11.5	23.9 ± 4.6	32.1 ± 11.1	31.8 ± 11.8
Male gender (%)	92 (52)	84 (52)	8 (53)	34 (58)	59 (50)
LV volumetric data					
LV end-diastolic volume (ml)	86.1 ± 23.0	85.0 ± 22.2	94.7 ± 28.1*	85.5 ± 23.0	87.3 ± 22.9
LV end-systolic volume (ml)	36.2 ± 10.5	35.7 ± 10.0	42.2 ± 13.9*	35.4 ± 10.5	38.0 ± 10.3
LV ejection fraction (%)	58.2 ± 5.6	58.4 ± 5.5	55.1 ± 5.7	58.6 ± 5.7	57.4 ± 5.3
LV mass (mg)	158.0 ± 31.9	156.3 ± 31.5	168.8 ± 31.1*	156.5 ± 30.9	160.6 ± 33.7
LV longitudinal strain					
global LV-LS (%)	-16.1 ± 2.5	-16.50 ± 2.10	-11.6 ± 1.6*	-16.5 ± 2.4	-15.5 ± 2.5†
mean segmental LV-LS (%)	-16.9 ± 2.4	-17.24 ± 2.12	-12.9 ± 1.5*	-17.3 ± 2.4	-16.2 ± 2.2†
MA parameters					
MA end-diastolic diameter (cm)	2.38 ± 0.44	2.45 ± 0.44	2.29 ± 0.45	2.47 ± 0.45	2.21 ± 0.38†
MA end-diastolic area (cm^2)	7.12 ± 2.22	7.39 ± 2.23	6.70 ± 2.62	7.73 ± 2.21	5.93 ± 1.85†
MA end-diastolic perimeter (cm)	10.22 ± 1.49	10.27 ± 1.50	9.89 ± 1.66	10.56 ± 1.47	9.57 ± 1.33†
MA end-systolic diameter (cm)	1.59 ± 0.38	1.59 ± 0.38	1.65 ± 0.41	1.49 ± 0.36	1.80 ± 0.37†
MA end-systolic area (cm^2)	3.44 ± 1.26	3.41 ± 1.26	3.86 ± 1.19	3.09 ± 1.13	4.16 ± 1.23†
MA end-systolic perimeter (cm)	7.08 ± 1.23	7.04 ± 1.23	7.59 ± 1.17	6.74 ± 1.18	7.75 ± 1.06†
MA fractional area change (%)	51.3 ± 15.7	52.5 ± 15.3	39.3 ± 15.3*	60.5 ± 9.2	33.6 ± 9.0†
MA fractional shortening (%)	34.2 ± 15.1	34.3 ± 15.0	27.4 ± 15.2	40.0 ± 13.0	21.4 ± 10.7†
Global LV-LS ≤ -13%	15 (8)	0 (0)	15 (100)	5 (4)	10 (16)†
MAFAC ≤ 44%	117 (66)	51 (31)	10 (67)*	0 (0)	61 (100)†

Abbreviations: LS – longitudinal strain, LV – left ventricular, MA – mitral annular, MAFAC – mitral annular fractional area change, *p <0.05 vs. global LV-LS > 13%, p<0.01 vs. MAFAC > 44

Three-dimensional speckle-tracking echocardiographic data. The global and mean segmental LV-LS proved to be -16.1 ± 2.5% and 16.9 ± 2.4%, respectively (Table 1). 3DSTE-derived LV volumetric, LS and MA data are presented in Table 1. In the present study, LV-LS ≤ 13% was considered to be reduced. In ROC analysis, the cut-off value for MAFAC to predict impaired LV-LS was ≤ 44%, with 67% sensitivity (95% confidence interval [CI] 38–88%) and 69% specificity (95% CI 61–76%) and ROC area under curve 0.73 (p = 0.0005) (Figure 4).

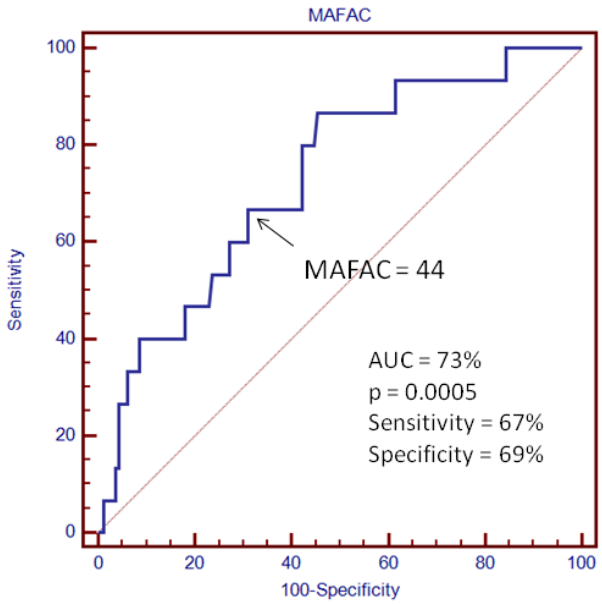

Figure 4. Receiver operating characteristic analysis illustrating the diagnostic accuracy of mitral annular fractional area change (MAFAC) in predicting reduced (≤ 13%) left ventricular longitudinal strain is demonstrated.

Significantly increased LV volumes and LV mass and reduced MAFAC could be demonstrated in healthy subjects with ≤ -13 % global LV-LS as compared to cases with > -13% global LV-LS. Significantly larger ratio of subjects with global LV-LS ≤ -13% had MAFAC ≤ 44% as compared to cases with > -13 % global LV-LS (31% vs. 67%, p =0.009). Patients with MAFAC ≤ 44% had significantly reduced global and mean segmental LV-LS, reduced end-diastolic and increased end-systolic MA sizes and reduced MAFS. Significantly larger ratio of subjects with MAFAC ≤ 44% had global LV-LS ≤ -13% as compared to cases

with >44% MAFAC (4% vs. 16%, p = 0.009). MAFAC showed no correlations with global or mean segmental LV-LS.

Reproducibility measurements. Table 2 shows the mean±standard deviation difference in values obtained by two measurements of the same observer and two observers for the measurements of 3DSTE-derived end-diastolic and end-systolic MA parameters and LV-LS in 20 healthy subjects, along with the respective correlation coefficients.

Table 2 Intra- and interobserver variability for the most important parameters

	Intraobserver agreement		**Interobserver agreement**	
	mean ± 2SD difference in values obtained by 2 measurements of the same observer	**correlation coefficient between measurements of the same observer**	**mean ± 2SD difference in values obtained by 2 observers**	**correlation coefficient between independent measurements of 2 observers**
End-diastolic MAD	0.01 ± 0.25 cm	0.96 (p <0.0001)	0.02 ± 0.21 cm	0.97 (p <0.0001)
End-diastolic MAA	-0.01 ± 1.08 cm^2	0.98 (p <0.0001)	0.00 ± 0.86 cm^2	0.98 (p <0.0001)
End-diastolic MAP	-0.02 ± 1.00 cm	0.93 (p <0.0001)	-0.14 ± 1.06 cm	0.92 (p <0.0001)
End-systolic MAD	-0.02 ± 0.27 cm	0.96 (p <0.0001)	0.01 ± 0.29 cm	0.96 (p <0.0001)
End-systolic MAA	-0.01 ± 0.35 cm^2	0.99 (p <0.0001)	-0.07 ± 0.41 cm^2	0.99 (p <0.0001)
End-systolic MAP	0.08 ± 0.56 cm	0.98 (p <0.0001)	0.07 ± 0.49 cm	0.99 (p <0.0001)
LV-LS	0.08 ± 0.95%	0.98 (p <0.0001)	0.06 ± 1.06%	0.96 (p <0.0001)

Abbreviations: MAD = mitral annular diameter, MAA = mitral annular area, MAP = mitral annular perimeter, LV-LS = left ventricular longitudinal strain, SD = standard deviation

4.2. Borderline left ventricular ejection fraction is associated with alterations in mitral annular size and function

Patient population. The present study comprised 146 healthy volunteers (mean age: 32.0 ± 11.4 years, 74 males), in whom complete 2D Doppler echocardiography has been performed with a negative result. In all cases routine echocardiography has been extended with 3DSTE. All subjects had no any symptoms, they had no cardiovascular disorders or risk factors, and did not take any medicine. Subjects were divided into two subgroups according to their 3DSTE-derived LV-EF: it proved to be normal (LV-EF ≥ 55%) or borderline (LV-EF = 50-54%).

Two-dimensional Doppler echocardiographic data. During 2D echocardiography normal cardiac dimensions could be measured (LA: 39.5 ± 2.2 mm, LV end-diastolic diameter: 47.8 ± 2.3 mm, LV end-systolic diameter: 33.1 ± 2.2 mm, interventricular septum: 9.1 ± 0.8 mm, LV posterior wall: 9.0 ± 0.7 mm, LV-EF: 64.5 ± 2.2%). None of healthy subjects showed more than grade 1 valvular regurgitation or had significant valvular stenosis

Three-dimensional speckle-tracking echocardiographic data. 3DSTE-derived LV volumetric, LV-LS and MA data are presented in Table 3. In patients with borderline LV-EF increased LV end-systolic volume and lower LV-LS could be measured. End-systolic and end-diastolic MA diameter, area and perimeter proved to be increased in patients with borderline (50-54%) LV-EF as compared to cases with ≥55% LV-EF. In these cases MA functional parameters were lower.

Table 3. Relationship between three-dimensional speckle-tracking echocardiography-derived left ventricular volumetric data, longitudinal strain and mitral annular parameters

	All data	**LV-EF 50 - 54%**	**LV-EF ≥ 55%**
n	146	33	113
Age (years)	32.0 ± 11.4	28.6 ± 9.0*	33.0 ± 11.9
Male gender (%)	74 (51)	23 (70)*	51 (45)
3DSTE-derived LV volumetric data			
LV end-diastolic volume (ml)	87.0 ± 23.9	84.1 ± 26.6	87.8 ± 23.1
LV end-systolic volume (ml)	36.4 ± 10.8	40.9 ± 10.6*	35.1 ± 10.5
LV ejection fraction (%)	58.5 ± 5.3	52.6 ± 1.3*	60.3 ± 4.8
3DSTE-derived LV strain data			
LV global longitudinal strain (%)	-16.0 ± 2.5	-15.0 ± 2.3*	-16.3 ± 2.4
LV mean segmental longitudinal strain (%)	-16.8 ± 2.4	-15.9 ± 2.1*	-17.1 ± 2.4
3DSTE-derived MA data			
MA end-diastolic diameter (cm)	2.44 ± 0.43	2.55 ± 0.45†	2.40 ± 0.42
MA end-diastolic area (cm^2)	7.31 ± 2.21	7.90 ± 2.61†	7.13 ± 2.06
MA end-diastolic perimeter (cm)	10.2 ± 1.5	10.61 ± 1.71†	10.1 ± 1.4
MA end-systolic diameter (cm)	1.60 ± 0.39	1.79 ± 0.40*	1.54 ± 0.37
MA end-systolic area (cm^2)	3.45 ± 1.27	4.21 ± 1.34*	3.23 ± 1.16
MA end-systolic perimeter (cm)	7.06 ± 1.23	7.82 ± 1.25*	6.84 ± 1.14
MA fractional area change (%)	51.5 ± 15.5	44.7 ± 14.8*	53.6 ± 15.1
MA fractional shortening (%)	34.0 ± 15.1	29.7 ± 12.2*	35.2 ± 15.6

Abbreviations: 3DSTE = three-dimensional speckle-tracking echocardiography**,** MA = mitralis annulus, LV = left ventricular

*p <0.05 vs. LV-EF ≥55%,

†p=0.08 vs. LV-EF ≥55%

Correlations. LV-EF did not show correlations neither with systolic and diastolic MA dimensions, nor with MAFAC (r =0.21, p =0.24) and MAFS (r =0.19, p =0.31). Similarly, correlations could not be detected during subgroup analyses.

4.3. The mitral annulus in lipedema

Patient population. The present study comprised 24 patients with stage 2 lipedema without known cardiovascular symptoms. Forty-eight age-, BMI-, and gender-matched healthy volunteers were used as control group (Table 4). All lipedema patients and matched controls have undergone two-dimensional Doppler echocardiography and 3DSTE.

Table 4 Baseline demographic and two-dimensional echocardiographic data in patients with lipedema and controls

	Controls	**Lipedema patients**
n	**48**	**24**
Risk factors		
Age (years)	41.0 ± 14.0	43.4 ± 11.7
Male gender (%)	0 (0)	0 (0)
Hypertension (%)	0 (0)	0 (0)
Diabetes mellitus (%)	0 (0)	0 (0)
Hypercholesterolemia (%)	0 (0)	0 (0)
Two-dimensional echocardiography		
LA diameter (mm)	35.3 ± 4.2	40.1 ± 4.3*
LV end-diastolic diameter (mm)	46.7 ± 3.6	50.3 ± 3.4*
LV end-diastolic volume (ml)	97.4 ± 21.2	121.4 ± 18.7*
LV end-systolic diameter (mm)	31.3 ± 3.4	31.5 ± 2.7
LV end-systolic volume (ml)	33.4 ± 8.3	40.2 ± 8.4*
Interventricular septum (mm)	8.8 ± 1.6	8.6 ± 0.9
LV posterior wall (mm)	9.1 ± 1.8	8.6 ± 0.9
LV ejection fraction (%)	65.4 ± 4.3	67.4 ± 3.4
E/A	1.3 ± 0.4	1.1 ± 0.3

Abbreviations: E and A = early and late diastolic transmitral flow velocities, LA=left atrial, LV=left ventricular
*$p<0.05$ vs. Controls

Demographic and two-dimensional echocardiographic data. Enlarged left atrial diameter, LV dimensions and volumes respecting cardiac cycle could be demonstrated with preserved LV ejection fraction in lipedema patients as compared to controls (Table 4). None of the lipedema patients and controls showed ≥ grade 1 mitral or tricuspid regurgitation. Higher mitral inflow early-diastolic E (77.9 ± 17.4 cm vs. 88.2 ± 17.7 cm/s, $p < 0.05$) and late-diastolic A (67.0 ± 17.4 cm/s vs. 80.0 ± 16.8 cm/s, $p < 0.05$) velocities could be demonstrated in lipedema patients as compared to controls, which did not change significantly following the use of compression stockings (85.2 ± 16.4 cm/s and 77.1 ± 15.9 cm, $p = 0.62$ and $p = 0.56$, respectively). 2D speckle-tracking echocardiography-derived peak systolic LV-LS (-17.8 ± 1.2%. vs. -20.5 ± 0.3%, $p < 0.05$) and LV-LS rate (0.79 ± 0.03 1/s vs. 0.90 ± 0.04 1/s, $p < 0.05$) proved to be reduced in lipedema patients as compared to controls.

Three-dimensional speckle-tracking echocardiography. Dilated end-systolic and end-diastolic MAD, MAA and MAP could be demonstrated in lipedema patients as compared to matched controls which was accompanied with impaired MAFAC at rest. Following one hour use of MCS, these parameters did not show any significant improvement (Table 5).

Table 5 Comparison of three-dimensional speckle-tracking echocardiography-derived mitral annular morphological and functional parameters between patients with lipedema and controls

	Controls (n= 48)	**Lipedema patients at rest (n= 24)**	**Lipedema patients one hour after the use of MCS (n= 24)**
Morphological parameters			
End-diastolic MAD (cm)	2.42 ± 0.39	2.54 ± 0.51	2.68 ± 0.56*
End-diastolic MAA (cm^2)	7.33 ± 2.21	8.45 ± 2.43*	9.01 ± 2.77*
End-diastolic MAP (cm)	10.17 ± 1.54	10.92 ± 1.46*	11.24 ± 1.73*
End-diastolic MAD (cm)	1.55 ± 0.39	1.75 ± 0.46*	1.82 ± 0.35*
End-diastolic MAA (cm^2)	3.21 ± 1.12	4.30 ± 1.72*	4.41 ± 1.60*
End-diastolic MAP (cm)	6.75 ± 1.10	7.84 ± 1.40*	8.04 ± 1.38*
Functional parameters			
MAFAC (%)	55.39 ± 14.01	47.78 ± 18.18*	49.08 ± 16.24
MAFS (%)	34.57 ± 15.01	30.16 ± 14.07	30.57 ± 12.53

Abbreviations: MAA = mitral annular area, MAD = mitral annular diameter, MAFAC = mitral annular fractional area change, MAFS = mitral annular fractional shortening, MAP = mitral annular perimeter, MCS = medical compression stocking

*$p<0.05$ vs. Controls

3DSTE-derived peak global LA-LS characterizing LA reservoir function proved to be 27.6 ± 8.5% at rest and 29.8 ± 7.5% one hour after the use of MCS in lipedema patients ($p = 0.14$). At rest, significant correlations could be demonstrated between peak LA-LS and end-systolic MAD ($r =-0.48$, $p =0.02$), MAA ($r =-0.49$, $p =0.02$) and MAP ($r =-0.47$, $p =0.02$) and functional parameters MAFAC ($r =0.50$, $p =0.01$) and MAFS ($r =0.52$, $p =0.01$). End-diastolic MA parameters did not show any correlations [MAD ($r =-0.07$, $p =0.75$), MAA ($r =-0.03$, $p =0.84$) and MAP ($r =-0.02$, $p =0.91$)]. One hour after the use of MCS, only MAFAC ($r =0.47$, $p =0.02$) and MAFS ($r =0.50$, $p =0.01$) correlated with LA-LS, none of end-systolic [MAD (r

=-0.35, p =0.09), MAA (r =-0.33, p =0.12) and MAP (r =-0.36, p =0.08)] and end-diastolic [MAD (r =0.15, p =0.48), MAA (r =0.20, p =0.35) and MAP (r =0.18, p =0.4)] morphological MA parameters correlated with it.

3DSTE-derived peak LA-RS was -19.8 ± 8.8% at rest and -17.5 ± 6.5% one hour after the use of MCS (p =0.30). LA-RS did not correlate with end-systolic and end-diastolic MAD (r =0.01, p =0.96 and r =0.02, p =0.92, respectively), MAA (r =-0.03, p =0.91 and r =0.25, p =0.24, respectively), MAP (r =-0.04, p =0.86 and r =0.26, p =0.22, respectively), MAFAC (r =0.25, p =0.24) and MAFS (r =-0.03, p =0.90) at rest. Similarly, significant correlations could not be detected between LA-RS and end-systolic and end-diastolic MAD (r =0.18, p =0.40 and r =0.07, p =0.75, respectively), MAA (r =0.18, p =0.40 and r =0.04, p =0.85, respectively), MAP (r =0.21, p =0.32 and r =0.09, p =0.68, respectively), MAFAC (r =-0.16, p =0.46) and MAFS (r =-0.11, p =0.61) one hour after the use of MCS.

3DSTE-derived peak LA-CS was found to be 32.8 ± 10.6% at rest and 34.2 ± 15.9% one hour after the use of MCS (p =0.61). Resting LA-CS did not show correlations with end-systolic and end-diastolic MAD (r =-0.33, p =0.12 and r =-0.21, p =0.33, respectively), MAA (r =-0.24, p =0.25 and r =-0.03, p =0.89, respectively), MAP (r =-0.25, p =0.25 and r =-0.07, p =0.73, respectively), MAFAC (r =0.23, p =0.28) and MAFS (r =0.13, p =0.56). One hour after the use of MCS, LA-CS correlated with end-systolic MAA (r =-0.48, p =0.02) and end-systolic and end-diastolic MAP (r =-0.52, p =0.009 and r =-0.48, p =0.02, respectively). End-systolic and end-diastolic MAD (r =-0.38, p =0.07 and r =-0.21, p =0.32, respectively) and end-diastolic MAA (r =-0.39, p =0.06) did not correlate with LA-CS.

Reproducibility measurements. At rest, the mean ± standard deviation differences in values obtained by two observers for the measurements of end-diastolic MAD, MAA and MAP were 0.00 ± 0.22 cm, -0.02 ± 0.83 cm^2 and –0.17 ± 1.01 cm, respectively with a correlation coefficient between these independent measurements of 0.98 (p <0.0001), 0.98 (p <0.0001) and 0.94 (p <0.0001), respectively (interobserver variability) (Figures 5, 6, and 7). At rest, the mean ± standard deviation differences in values obtained by 2 measurements of observer 1 proved to be -0.01 ± 0.25 cm, 0.01 ± 1.00 cm^2 and -0.04 ± 0.97 cm, respectively with a correlation coefficient between these independent measurements of 0.97 (p <0.0001), 0.98 (p <0.0001) and 0.94 (p <0.0001), respectively (intraobserver variability) (Figures 8, 9 and 10).

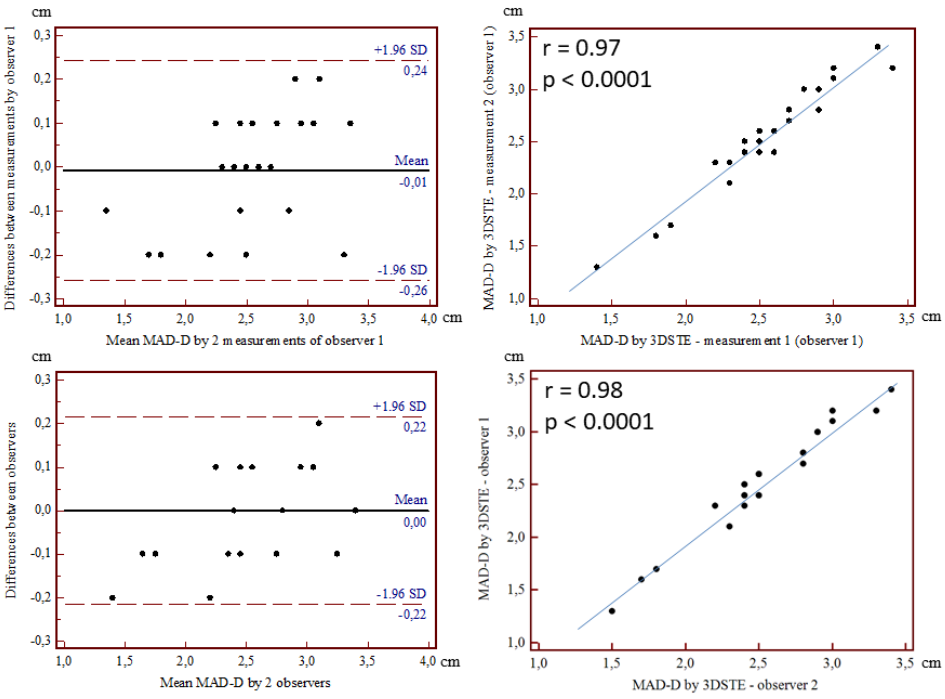

Figure 5. Intraobserver (upper graphs) and interobserver (lower graphs) agreements and correlations for measuring end-diastolic mitral annular diameter (MAD-D) by three-dimensional speckle tracking echocardiography (3DSTE) are presented.

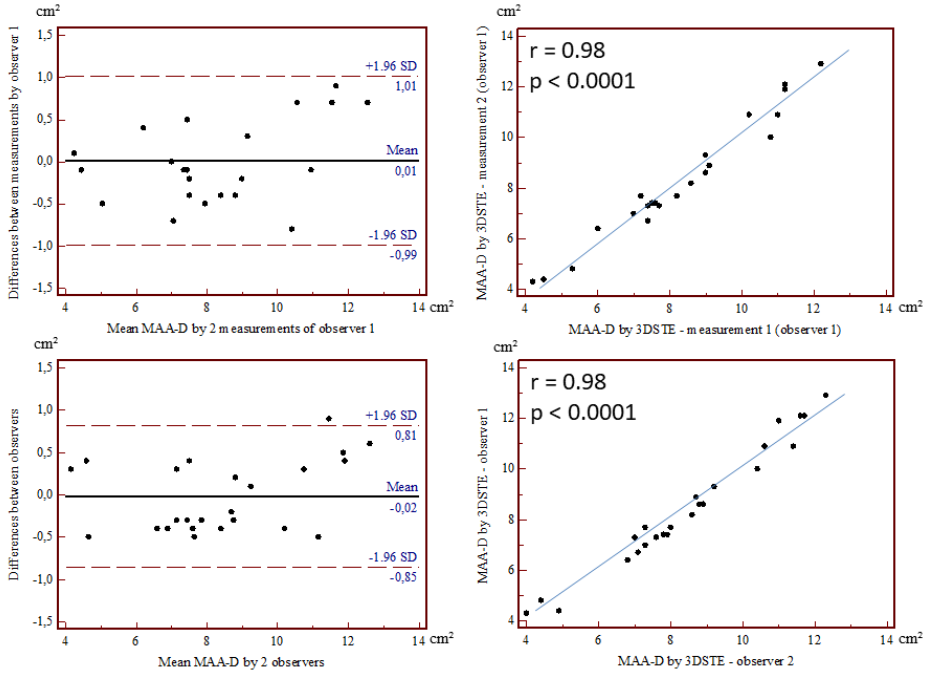

Figure 6. Intraobserver (upper graphs) and interobserver (lower graphs) agreements and correlations for measuring end-diastolic mitral annular area (MAA-D) by three-dimensional speckle tracking echocardiography (3DSTE) are presented.

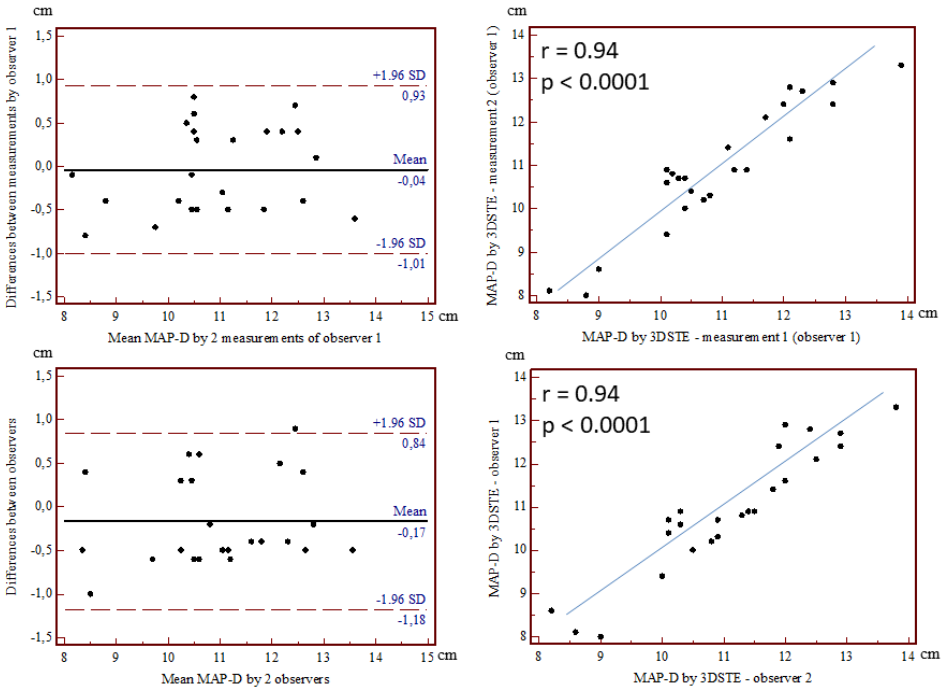

Figure 7. Intraobserver (upper graphs) and interobserver (lower graphs) agreements and correlations for measuring end-diastolic mitral annular perimeter (MAP-D) by three-dimensional speckle tracking echocardiography (3DSTE) are presented.

The same parameters for end-systolic MAD, MAA and MAP were 0.01 ± 0.25 cm, -0.05 ± 0.42 cm^2 and 0.06 ± 0.47 cm with correlation coefficients of 0.96 ($p < 0.0001$), 0.99 ($p < 0.0001$) and 0.99 ($p < 0.0001$), respectively (interobserver variability) (Figures 5, 6 and 7). The same values for 2 measurements of observer 1 proved to be -0.01 ± 0.23 cm, -0.02 ± 0.37 cm^2 and 0.04 ± 0.56 cm, respectively with correlation coefficients between these independent measurements of 0.97 ($p < 0.0001$), 0.99 ($p < 0.0001$) and 0.98 ($p < 0.0001$), respectively (intraobserver variability) (Figures 8, 9 and 10).

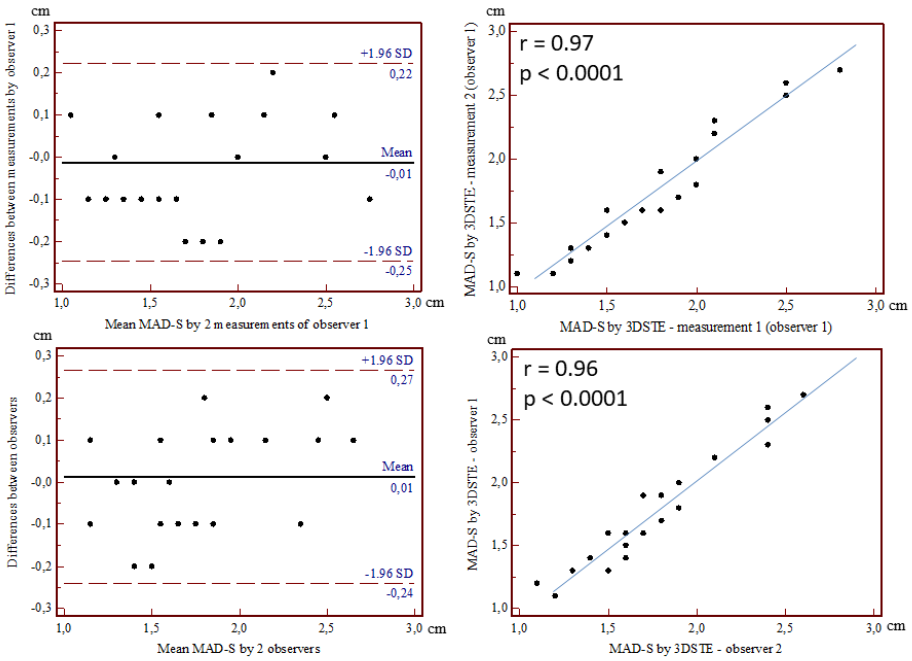

Figure 8. Intraobserver (upper graphs) and interobserver (lower graphs) agreements and correlations for measuring end-systolic mitral annular diameter (MAD-S) by three-dimensional speckle tracking echocardiography (3DSTE) are presented.

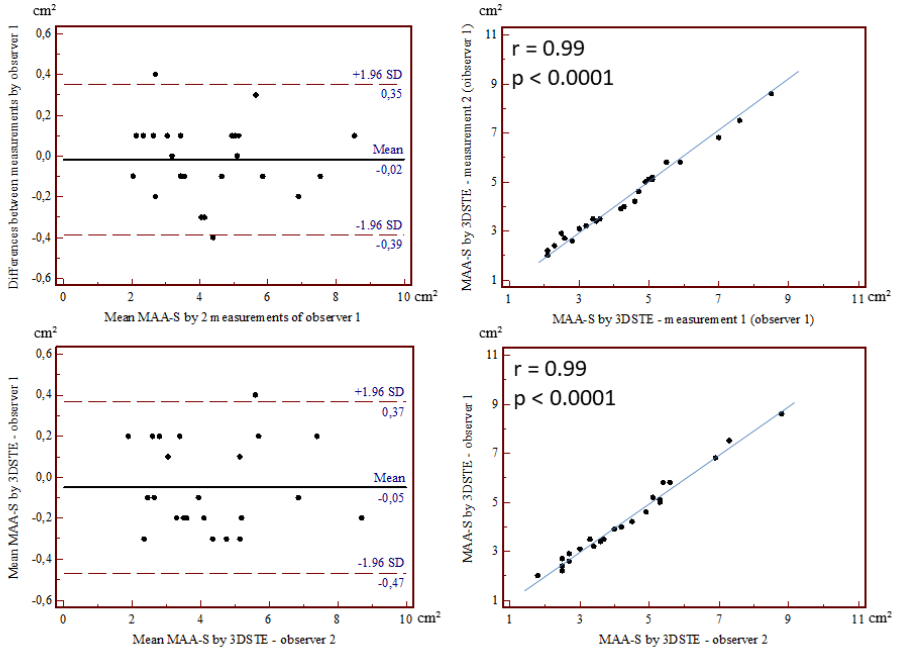

Figure 9. Intraobserver (upper graphs) and interobserver (lower graphs) agreements and correlations for measuring end-systolic mitral annular area (MAA-S) by three-dimensional speckle tracking echocardiography (3DSTE) are presented.

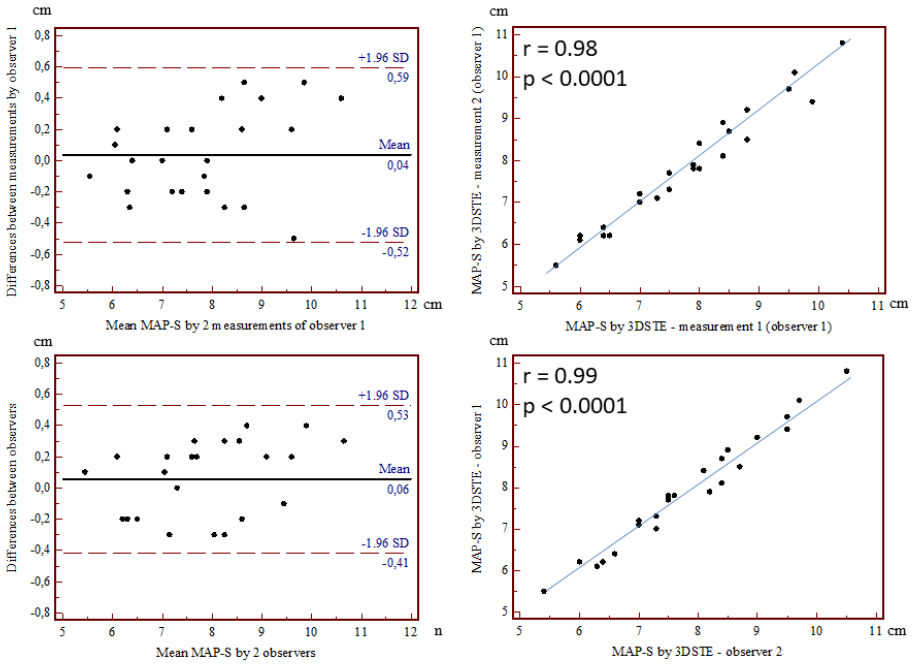

Figure 10. Intraobserver (upper graphs) and interobserver (lower graphs) agreements and correlations for measuring end-systolic mitral annular perimeter (MAP-S) by three-dimensional speckle tracking echocardiography (3DSTE) are presented.

4.4. The Mitral Annulus in adult patients with corrected tetralogy of Fallot

Patient population. From the CSONGRAD Registry, 29 consecutive adult repaired TOF patients (mean age: 35.4 ± 15.5 years, 18 men) were recruited, from which 13 patients underwent early total reconstruction (etrTOF), while 16 patients were firstly palliated and later corrected (pcTOF). Early total reconstruction was performed at the age of 5.3 ± 3.2 years in etrTOF patients (mean follow-up period: 29.0 ± 12.0 years). Blalock-Taussig operation (n=15), Brock surgery (n=2), Brock surgery and Blalock-Taussig operation (n=1) were performed as a palliation in pcTOF patients at the age of 4.4 ± 4.2 years. Late correction was performed in pcTOF patients at the age of 12.6 ± 13.1 years (mean follow-up period from early palliation to late correction was 33.7 ± 14.2 years and 25.0 ± 11.6 years, respectively). Their data were compared to that of 76 age- and gender-matched adult healthy controls (mean age: 35.9 ± 7.6 years, 33 men). All repaired TOF patients and controls were in sinus rhythm and assessed by two-dimensional Doppler echocardiography and 3DSTE.

Demographic and two-dimensional echocardiographic data. Enlarged left atrial diameter and normal LV dimensions and volumes with preserved LV ejection fraction were found in repaired TOF patients regardless of the type of correction as compared to controls (Table 6). Tricuspid annular plane systolic excursion (18.4 ± 4.8 mm vs. 16.7 ± 3.5 mm, p =ns) and right ventricular fractional area change (37.1 ± 21.7% vs. 43.4 ± 10.6%, p =ns) did not differ between etrTOF and pcTOF patients. Valvular regurgitations and the ratio of their grades are presented in Table 6.

Table 6 Baseline demographic and two-dimensional Doppler echocardiographic data in patients with tetralogy of Fallot and controls

Data	Controls	All repaired TOF patients	etrTOF patients	pcTOF patients
n	76	29	13	16
Risk factors				
Age (years)	35.9 ± 7.6	35.4 ± 15.5	33.5 ± 14.2	37.1 ± 16.8
Male gender (%)	33 (43)	18 (62)	7 (54)	11 (69)
Hypertension (%)	0 (0)	8 (28)*	4 (30)*	4 (25)*
Diabetes mellitus (%)	0 (0)	0 (0)	0 (0)	0 (0)
Hypercholesterolaemia (%)	0 (0)	1 (3)	1 (8)	0 (0)
Two-dimensional echocardiography				
LA diameter (mm)	36.1 ± 3.8	42.0 ± 6.9*	42.0 ± 7.5*	41.9 ± 6.6*
LV end-diastolic diameter (mm)	47.6 ± 4.2	50.3 ± 13.2	47.8 ± 5.8	52.4 ± 17.3*
LV end-diastolic volume (ml)	104.8 ± 23.7	110.1 ± 32.9	108.8 ± 32.7	111.3 ± 34.3
LV end-systolic diameter (mm)	35.5 ± 20.6	31.5 ± 6.3	31.2 ± 5.3	31.7 ± 7.3
LV end-systolic volume (ml)	36.7 ± 9.5	42.2 ± 26.4	39.5 ± 20.3	44.5 ± 31.3
Interventricular septum (mm)	9.3 ± 1.5	9.8 ± 1.5	9.5 ± 1.1	9.9 ± 1.8
LV posterior wall (mm)	9.5 ± 1.7	9.5 ± 1.4	9.4 ± 1.1	9.6 ± 1.5
LV ejection fraction (%)	64.7 ± 3.8	63.9 ± 11.0	65.5 ± 6.1	62.5 ± 14.0
Aortic regurgitation				
grade 1 (%)	0 (0)	3 (10)*	1 (8)	2 (13)*
Mitral regurgitation				
grade 1 (%)	0 (0)	5 (17)*	2 (15)*	3 (19)*
grade 2 (%)	0 (0)	2 (7)	1 (8)	1 (6)
Tricuspid regurgitation				
grade 1 (%)	0 (0)	12 (41)*	6 (46)*	6 (38)*
grade 2 (%)	0 (0)	5 (17)*	3 (23)*	2 (13)*
grade 3 (%)	0 (0)	2 (7)†	0 (0)	2 (13)*
grade 4 (%)	0 (0)	1 (3)	0 (0)	1 (6)

Abbreviations: LA=left atrial, LV=left ventricular, TOF=tetralogy of Fallot, etrTOF=TOF – early total reconstruction, pcTOF=TOF – early palliation, late correction

*$p < 0.05$ vs. Controls, †$p = 0.07$ vs. Controls

Three-dimensional speckle-tracking echocardiography. Dilated end-systolic and end-diastolic MAD, MAA and MAP could be demonstrated in repaired TOF patients as compared to controls (Table 7). MAFAC and MAFS were reduced regardless the type of treatment. Both BSA-indexed and non-indexed end-systolic MAD, MAA, and MAP were significantly increased in etrTOF patients as compared to that of healthy controls. Almost all BSA-indexed and non-indexed MA parameters were enlarged in pcTOF patients as compared to controls. Increased BSA-indexed end-diastolic and end-systolic MAD and MAP could be demonstrated in pcTOF patients as compared to that of etrTOF cases.

Correlations. MA functional properties (MAFAC, MAFS) did not correlate with 3DSTE-derived LV-EF neither in controls, nor in repaired TOF patients. End-systolic MAA and MAP showed correlations with age at the time of the total reconstruction in etrTOF patients ($r = 0.57$, $p = 0.04$ and $r = 0.57$, $p = 0.04$, respectively). The other MA parameters did not show correlations with ages. Similar relationships between ages at the time of early palliation, late correction or difference between these ages and MA dimensions and functional properties could not be confirmed in pcTOF patients.

Table 7 Comparison of three-dimensional speckle-tracking echocardiography-derived mitral annular morphological and functional parameters between patients with tetralogy of Fallot and controls

Data	Controls	All repaired TOF patients	etrTOF patients	pcTOF patients
Morphological parameters				
MAD-D (cm)	2.47 ± 0.40	2.65 ± 0.42*	2.62 ± 0.44	2.68 ± 0.41
MAD-D/BSA (cm/m^2)	1.34 ± 0.22	1.48 ± 0.23*	1.40 ± 0.16	1.59 ± 0.25*†
MAA-D (cm^2)	7.62 ± 2.21	8.93 ± 3.09*	8.49 ± 3.03	9.29 ± 3.18*
MAA-D/BSA (cm/m^2)	4.14 ± 1.10	4.88 ± 1.53*	4.47 ± 1.19	5.39 ± 1.76*
MAP-D (cm)	10.41 ± 1.50	11.35 ± 1.93*	11.05 ± 1.91	11.60 ± 1.98*
MAP-D/BSA (cm/m^2)	5.63 ± 0.82	6.29 ± 1.03*	5.88 ± 0.74	6.80 ± 1.08*†
MAD-S (cm)	1.66 ± 0.42	2.16 ± 0.38*	2.08 ± 0.42*	2.22 ± 0.35*
MAD-S/BSA (cm/m^2)	0.90 ± 0.23	1.19 ± 0.22*	1.09 ± 0.17*	1.30 ± 0.21*†
MAA-S (cm^2)	3.55 ± 1.29	6.44 ± 2.54*	5.89 ± 1.96*	6.89 ± 2.92*
MAA-S/BSA (cm/m^2)	1.92 ± 0.66	3.43 ± 1.25*	3.01 ± 0.79*	3.89 ± 1.52*
MAP-S (cm)	7.10 ± 1.19	9.77 ± 1.77*	9.52 ± 1.60*	9.98 ± 1.91*
MAP-S/BSA (cm/m^2)	3.83 ± 0.64	5.36 ± 0.86*	5.01 ± 0.67*	5.78 ± 0.89*†
Functional parameters				
MAFAC (%)	52.25 ± 14.24	27.60 ± 13.50*	29.38 ± 13.75*	26.14 ± 13.56*
MAFS (%)	31.98 ± 15.66	18.25 ± 10.56*	20.45 ± 10.40*	16.47 ± 10.68*

Abbreviations: MAA-D=end-diastolic mitral annular area, MAA-S=end-systolic mitral annular area, MAD-D=end-diastolic mitral annular diameter, MAD-S=end-systolic mitral annular diameter, MAFAC=mitral annular fractional area change, MAFS=mitral annular fractional shortening, MAP-D=end-diastolic mitral annular perimeter, MAP-S=end-systolic mitral annular perimeter, TOF=tetralogy of Fallot, etrTOF=TOF – early total reconstruction, pcTOF=TOF – early palliation, late correction

*$p < 0.05$ vs. Controls, †< 0.05 vs. etrTOF

5. Discussion

5.1. Left ventricular longitudinal strain is associated with mitral annular fractional area change in healthy subjects

The normal MV apparatus is a dynamic 3D structure which allows normal blood flow during the cardiac cycle: LV inflow from the LA during diastole and LV outflow into the aorta during systole. The key components are the MA, the valve leaflets, the chordae tendineae, and the LV wall with its attached papillary muscles (1). MA plays a significant role in promoting LA and LV filling and emptying, which is dependent on LV functional properties (29). LV strains are quantitative features of LV myocardial contractility. Global LV-LS characterizes LV deformation (lengthening or shortening) in longitudinal direction and has good prognostic value in various disorders (30,31). Moreover, LV-LS is more sensitive than LV-EF in detecting abnormalities in LV systolic function as noted by Carasso *et al* (10). 3DSTE allows complete non-invasive assessment of the heart chambers in 3D space including parallel evaluation of MA and LV morphology and function (at the same time) from the same 3D dataset. This advantage enables physiologic studies assessing the effects of these components on each other.

In recent studies global LV-LS and MV function have been demonstrated to be associated in several pathological states (32). However, to the best of the authors' knowledge, no clinical studies are available directly assessing a relationship between LV longitudinal deformation and MA functional properties in healthy subjects. Lower global LV-LS was found to be associated with lower MA function. Moreover, impaired LV longitudinal deformation proved to have a prognostic role in the prediction of MAFAC, as well. These results could suggest that subclinical impairment of LV longitudinal function is associated with reduced MA function in otherwise healthy subjects without risk factors or overt cardiovascular diseases. This result is against what could be demonstrated in different disorders. For instance, although type 1 diabetes mellitus is associated with impaired global LV-LS (33), MA functional properties proved to be significantly increased suggesting a compensatory mechanism in these patients (34). Our results suggest that demand for this compensatory mechanism did not reach a certain level required for the mechanism to develop in our healthy subject. Further studies are warranted to confirm our findings and to reveal pathophysiological background of this compensation.

Limitation section. The most important limitations occurring during the 3DSTE studies are listed below:

- Spatial and temporal resolution of the relatively new 3DSTE is low which could affect the results and should be considered when interpreting the results.
- Although 3DSTE could measure LV volumes, its accuracy depends on the quality of the acquired image and particularly on enlargement of the LV (35). This study tried to mirror real life experience, therefore 3DSTE-derived LV volumetric data could be somewhat lower as expected.
- Early stage diseases were not excluded by other imaging or laboratory tests, although lower strain values could indicate subclinical changes.
- LV strain and volumetric and functional data of heart chambers other than the LV were not examined in this study.
- Although the MA geometric shape approximates a hyperbolic paraboloid, only one-plane MA motion and function was analysed in this study. Although spatial longitudinal analysis of the MA movement along its long-axis is also possible (8), it was not aimed to be measured and compared to other parameters in this particular study.

5.2. Borderline left ventricular ejection fraction is associated with alterations in mitral annular size and function

The most important indication of echocardiographic examinations is the assessment of LV systolic pumping function with the most frequently used LV-EF (8). It is due to the fact, that several clinical studies confirmed the prognostic role of LV-EF in various patient groups (36). LV-EF could be measured by several echocardiographic methods including M-mode, 2D, 2DSTE, volumetric RT3DE and 3DSTE (36). According to the guidelines the recently suggested 2D echocardiographic method for measurement of LV-EF is the modified Simpson-method and the as called area-length method (8,24). According to the same guideline, RT3DE-derived LV-EF is accurate and reproducible, and if there is an opportunity, usable (24).

It is known, that 2D echocardiography underestimates the real MA diameter, if these parameters are compared to RT3DE- and magnetic resonance imaging-derived values (37,38).

The 3D echocardiographic method is accurate, and well correlate with magnetic resonance imaging (MRI)-derived values (39). Due to the fact that MA is not real circle-shaped, but more similar to the letter D, it could show deformation is certain disorders with rounding, therefore MA diameter-derived parameters could show further torsions like MA area or perimeter. These facts could highlight attention on the importance of echocardiographic 3D imaging, although 3D saddle-shape of MA is not taken into consideration, only its 2D projected image (2).

3DSTE is a new non-invasive diagnostic method, which merge together advantages of volumetric 3D echocardiography and STE. With the virtual 3D cast created about a heart chamber like LV, volumetric and strain parameters could be calculated at the same time respecting cardiac cycle (7). According to Kleijn *et al,* although 3DSTE-derived LV volumes are lower as compared to MRI-derived ones, LV-EF shows perfect accordance (39). It was also confirmed that 3DSTE is reliable in the assessment of LV volumes and LV-EF (40), and measured data are interchangeable with RT3DE-derived ones (41). According to the international guidelines cut-off of 2D echocardiography-derived LV-EF is ≥55% (24), while according to literature data borderline values are 47-55% as assessed by 3D echocardiography, and shows age- and gender-dependency (42). LV-EF is reduced if less than 50%, therefore 3DSTE-derived 50-54% LV-EF could be considered as a borderline value.

In the present study the relationship between LV-EF and MA morphology and function was examined. For this aim two patient groups were created, 3DSTE-derived 50-54% LV-EF could be measured in the first group, while LV-EF proved to be equal or more than 55% in the second group. Our results confirmed that in patients with borderline LV-EF MA is more dilated and functionally impaired regardless the cardiac cycle as compared to subjects with 3DSTE-derived normal LV-EF. This result could highlight on the fact, that early MA remodelation could be detected in cases with borderline LV function. Over heart chamber volumetric changes LV and LA functional alterations could play a role in these changes as suggested by subclinical reduced global LV-LS. However, further investigations are warranted in patients showing borderline LV-EF to explore reasons of subclinical changes. According to these facts further examinations are warranted to understand complexity of the above mentioned physiological facts.

Limitation section. Over above mentioned limitations the following specific concerns should be considered:

- The present study did not aim to validate 3DSTE-derived LV volumetric data and LV-EF (7). It is important to know, that there was no direct validation study to compare LV volumes and LV-EF measured by 2D echocardiography with Teichholz- or Simpson-method and 3DSTE-derived ones. Validation studies were performed against cardiac MRI (39) and RT3DE (41).
- According to own experiences lower LV-EF (mean 6-8%) could be measured with the recently available 3DSTE imaging tool as compared to that of assessed by 2D echocardiographic Teichholz-method. Regarding to these facts cases with 3DSTE-derived 50-54% LV-EF had more than 55% 2D echocardiography-derived LV-EF in all cases.
- During subgroup analyses differences could be detected in the age and gender distributions, which could affect our findings.

5.3. The mitral annulus in lipedema

To the best of the authors' knowledge, this is the first time to assess MA morphology and function in lipedema. Moreover, the effects of lower body compression on MA size and function have not been assessed yet. In spite of the absence of valvular regurgitations and stenosis, LV dysfunction and heart failure; dilated MA parameters and reduced MA functional properties could be demonstrated in lipedema patients as compared to those of controls. These MA morphological and functional alterations showed correlations with LA reservoir function. However, the use of MCS does not have any beneficial effects on these alterations.

Lipedema is a barely known bilateral, symmetrical, disproportional fatty edema which is usually mistaken by obesity or primary or secondary lymphedema. It almost always affects women with a common familial accumulation and fails to respond to standard dietary approaches, but the pathomechanism is still not known. Clinically, lipedema is characterized by non-pitting edema, susceptibility to bruising and spontaneous or minor trauma-induced pain. Limited number of information is available about lipedema-related cardiac abnormalities. Lipedema patients were found to have increased aortic stiffness and notably altered left ventricular rotational mechanics (13,14,26). These results gave rise to further investigations regarding lipedematous cardiovascular implications, therefore we focused on MA morphology and function. The saddle-shaped MA is an essential part of the mitral valve,

it is a fibrous ring that represents an anatomical junction between the LV and LA. Its shape and size change throughout the cardiac cycle (29). Similarly to the present findings, MA dilation and functional impairment could be demonstrated in dilated (38) and noncompaction cardiomyopathies (5) and cardiac amyloidosis (6). Our results could be theoretically explained by deformation abnormalities of the left heart chambers due to increased fluid accumulation capacity of the vascularized lipedematous fatty tissue and interlobular septae (43). However, the role of increased number of non-cardiomyocytes with mesenchymal cells (44) and subclinical epicardial fat deposition of the heart could not be excluded either. Based on the present results, LA and LV dilation and functional impairment could be detected as indirect signs of these alterations (26). Furthermore, direct infiltration of the fibrous annulus of the mitral valve by lipedematous tissue could not be excluded either. These alterations could lead to further morphological and functional impairment of the heart chambers and MA acting as a vicious circle theoretically leading to earlier development of symptoms in lipedema.

At this moment, limited information is available not only about alterations in MA morphology and function in lipedema, but also about changes during the progression of the disease. Therefore, exact guideline for its periodic evaluation is not available, but based on the results, annual follow-up could be suggested. Moreover, further diagnostic and prognostic studies are warranted to examine MA-related LV and LA morphological and functional alterations as well.

Limitation section. Only projection of the MA to a selected 2D plane could be assessed by the presented method, not the real 3D shape which could be considered as an important limitation of this study.

5.4. The Mitral Annulus in adult patients with corrected tetralogy of Fallot

According to recent findings from imaging studies, significant alterations could be detected in the left heart including LV and LA morphology and function in addition to right heart abnormalities in adults with repaired TOF (18-23). Most repaired TOF patients show a normal LV twisting pattern, but with a significantly lower LV twist mainly due to decreased apical rotation (19). Almost one-third of the subjects had an abnormal twist pattern due to both

abnormal apical and/or basal LV rotations. Over a quarter of the patients had abnormal apical rotation that was associated with larger LV dimensions and decreased biventricular systolic function. Regarding to LV global longitudinal function in repaired TOF, global LV-LS was found to be reduced mainly due to the interventricular septum probably by mechanical coupling of the ventricles (18). In recent 3DSTE-derived atrial studies, both right atrial (RA) and LA volumes seemed to be increased in adult patients with repaired TOF with almost similar deformational abnormalities of RA and LA (20,22).

Mitral valve and its annulus play an important role in regulating blood flow between LV and LA. According to the above mentioned alterations it could be theoretized, that MA could show significant remodelling in repaired TOF. 3DSTE was found to be a valuable tool not only for volumetric and functional assessment of different cardiac chambers (7), but also for the evaluation of MA dimensions and functional properties respecting the cardiac cycle (6,11). Although 3DSTE-derived methodology does not assess the 3D spatial saddle shape of MA directly, but only its projection to the chosen 2D plane, dilation of MA dimensions and MA functional impairment could be demonstrated in adult repaired TOF patients, regardless of the type of correction. Moreover, patients who were treated with the two-step way (early palliation, late correction) showed worse results suggesting clinical benefits of early total reconstruction on late MA morphology and function. Moreover, correlation between the age of early total reconstruction and MA systolic dimensions could confirm these findings. However, further studies are warranted to confirm our findings in a larger patient population evaluating their prognostic significance, as well.

Limitation section. Several important limitations have arisen during the assessments:

- A relatively small number of patients from a single center by a single observer (DP) were examined. However, it should be considered that repaired TOF is a relatively rare disease.
- Moreover, adult patients with some risk factors were assessed, therefore their effects could also be taken into considerations when interpreting results.

6. Conclusions (new observations)

There is a strong relationship between mitral annular and LV longitudinal function. MA fractional area change predicts global LV-LS.

3DSTE-derived borderline LV-EF is associated with MA dilatation and functional impairment.

Lipedema is associated with MA enlargement and functional impairment. The use of compression stockings does not improve these alterations.

MA enlargement and functional impairment could be detected in adult patients with repaired TOF regardless of the type of correction. However, pcTOF patients have worse results.

7. References

1. Dal-Bianco JP, Levine RA. Anatomy of the Mitral Valve Apparatus – Role of 2D and 3D Echocardiography. Cardiol Clin 2013; 31: 10.
2. Nemes A, Geleijnse ML, Soliman OI, Vletter WB, McGhie JS, Forster T, Ten Cate FJ. Evaluation of the mitral valve by transthoracic real-time three-dimensional echocardiography. Orv Hetil 2010; 151: 854-863.
3. Apor A, Nagy AI, Kovács A, Manouras A, Andrássy P, Merkely B. Three-dimensional dynamic morphology of the mitral valve in different forms of mitral valve prolapse - potential implications for annuloplasty ring selection. Cardiovasc Ultrasound 2016; 14: 32.
4. Antoine C, Mantovani F, Benfari G, Mankad SV, Maalouf JF, Michelena HI, Enriquez-Sarano M. Pathophysiology of Degenerative Mitral Regurgitation: New 3-Dimensional Imaging Insights. Circ Cardiovasc Imaging 2018; 11: e005971.
5. Nemes A, Anwar AM, Caliskan K, Soliman OI, van Dalen BM, Geleijnse ML, ten Cate FJ. Non-compaction cardiomyopathy is associated with mitral annulus enlargement and functional impairment: a real-time three-dimensional echocardiographic study. J Heart Valve Dis 2008; 17: 31-5.
6. Nemes A, Földeák D, Kormányos Á, Domsik P, Kalapos A, Borbényi Z, Forster T. Cardiac Amyloidosis Associated with Enlargement and Functional Impairment of the Mitral Annulus: Insights from the Three-Dimensional Speckle Tracking Echocardiographic MAGYAR-Path Study. J Heart Valve Dis 2017; 26: 304-308.
7. Nemes A, Kalapos A, Domsik P, Forster T. Three-dimensional speckle-tracking echocardiography -- a further step in non-invasive three-dimensional cardiac imaging. Orv Hetil 2012; 153: 1570-1577.
8. Nemes A, Forster T. Recent echocardiographic examination of the left ventricle – from M-mode to 3D speckle-tracking imaging. Orv Hetil 2015; 156: 1723-1740.
9. Zhang HM, Wang XT, Zhang LN, He W, Zhang Q, Liu DW; Chinese Critical Ultrasound Study Group. Left Ventricular Longitudinal Systolic Function in Septic Shock Patients with Normal Ejection Fraction: A Case-control Study. Chin Med J (Engl) 2017; 130: 1169–1174.
10. Carasso S, Cohen O, Mutlak D, Adler Z, Lessick J, Reisner SA, Rakowski H, Bolotin G, Agmon Y. Differential effects of afterload on left ventricular long- and short-axis

function: Insights from a clinical model of patients with aortic valve stenosis undergoing aortic valve replacement. Am Heart J 2009; 158: 540–545.

11. Nemes A, Piros GÁ, Domsik P, Kalapos A, Lengyel C, Várkonyi TT, Orosz A, Forster T. Changes in mitral annular morphology and function in young patients with type 1 diabetes mellitus-results from the three-dimensional speckle tracking echocardiographic MAGYAR-Path Study. Quant Imaging Med Surg 2015; 5: 815-821.
12. Lee BB, Andrade M, Antignani PL, Boccardo F, Bunke N, Campisi C, Damstra R, Flour M, Forner-Cordero I, Gloviczki P, Laredo J, Partsch H, Piller N, Michelini S, Mortimer P, Rabe E, Rockson S, Scuderi A, Szolnoky G, Villavicencio JL; International Union of Phlebology. Diagnosis and treatment of primary lymphedema. Consensus document of the International Union of Phlebology (IUP)-2013. International Union of Phlebology. Int Angiol 2013; 32: 541-574.
13. Szolnoky G, Nemes A, Gavallér H, Forster T, Kemény L. Lipedema is associated with increased aortic stiffness. Lymphology 2012; 45: 71-79.
14. Nemes A, Kalapos A, Domsik P, Lengyel C, Orosz A, Forster T. Correlations between echocardiographic aortic elastic properties and left ventricular rotation and twist--insights from the three-dimensional speckle-tracking echocardiographic MAGYAR-Healthy Study. Clin Physiol Funct Imaging 2013; 33: 381-385.
15. Swamy P, Bharadwaj A, Varadarajan P, Pai RG. Echocardiographic evaluation of tetralogy of Fallot. Echocardiography 2015; 32 Suppl 2: S148-56.
16. Bedair R, Iriart X. Educational series in congenital heart disease: Tetralogy of Fallot: diagnosis to long-term follow-up. Echo Res Pract 2019; 6: R9-R23.
17. Havasi K, Kalapos A, Berek K, Domsik P, Kovács G, Bogáts G, Hartyánszky I, Kertész E, Katona M, Rácz K, Csanády M, Forster T, Nemes A. More than 50 years' experience in treatment of patients with congenital heart disease at a Hungarian university hospital. The basics of the CSONGRAD Registry. Orv Hetil 2015; 156: 794-800.
18. Menting ME, van den Bosch AE, McGhie JS, Eindhoven JA, Cuypers JA, Witsenburg M, Geleijnse ML, Helbing WA, Roos-Hesselink JW. Assessment of ventricular function in adults with repaired Tetralogy of Fallot using myocardial deformation imaging. Eur Heart J Cardiovasc Imaging 2015; 16: 1347-1357.
19. Menting ME, Eindhoven JA, van den Bosch AE, Cuypers JA, Ruys TP, van Dalen BM, **McGhie JS**, Witsenburg M, Helbing WA, Geleijnse ML, Roos-Hesselink JW.

Abnormal left ventricular rotation and twist in adult patients with corrected tetralogy of Fallot. Eur Heart J Cardiovasc Imaging 2014; 15: 566-574.

20. Havasi K, Domsik P, Kalapos A, McGhie JS, Roos-Hesselink JW, Forster T, Nemes A. Left Atrial Deformation Analysis in Patients with Corrected Tetralogy of Fallot by 3D Speckle-Tracking Echocardiography (from the MAGYAR-Path Study). Arq Bras Cardiol 2017; 108: 129-134.
21. Yu HK, Li SJ, Ip JJ, Lam WW, Wong SJ, Cheung YF. Right ventricular mechanics in adults after surgical repair of tetralogy of Fallot: insights from three-dimensional speckle-tracking echocardiography. J Am Soc Echocardiogr 2014; 27: 423-429.
22. Nemes A, Havasi K, Domsik P, Kalapos A, Forster T. Evaluation of right atrial dysfunction in patients with corrected tetralogy of Fallot using 3D speckle-tracking echocardiography. Insights from the CSONGRAD Registry and MAGYAR-Path Study. Herz 2015; 40: 980-988.
23. Timóteo AT, Branco LM, Rosa SA, Ramos R, Agapito AF, Sousa L, Galrinho A, Oliveira JA, Oliveira MM, Ferreira RC. Usefulness of right ventricular and right atrial two-dimensional speckle tracking strain to predict late arrhythmic events in adult patients with repaired Tetralogy of Fallot. Rev Port Cardiol 2017; 36: 21-29.
24. Lang RM, Badano LP, Mor-Avi V, Afilalo J, Armstrong A, Ernande L, Flachskampf FA, Foster E, Goldstein SA, Kuznetsova T, Lancellotti P, Muraru D, Picard MH, Rietzschel ER, Rudski L, Spencer KT, Tsang W, Voigt JU. Recommendations for cardiac chamber quantification by echocardiography in adults: an update from the American Society of Echocardiography and the European Association of Cardiovascular Imaging. Eur Heart J Cardiovasc Imaging 2015; 16: 233-271.
25. Biswas M, Sudhakar S, Nanda NC, Buckberg G, Pradhan M, Roomi AU, Gorissen W, Houle H. Two- and three-dimensional speckle tracking echocardiography: clinical applications and future directions. Echocardiography 2013; 30: 88-105.
26. Nemes A, Kormányos A, Domsik P, Kalapos A, Kemény L, Forster T, Szolnoky G. Left ventricular rotational mechanics differ between lipedema and lymphedema: Insights from the three-dimensional speckle tracking echocardiographic MAGYAR-Path study. Lymphology 2018; 51: 102-108.
27. Partsch H, Mosti G. Comparison of three portable instruments to measure compression pressure. Int Angiol 2010; 29: 426–430.

28. Chassagne F, Helouin-Desenne C, Molimard J, Convert R, Badel P, Giraux P. Superimposition of elastic and nonelastic compression bandages. J Vasc Surg Venous Lymphat Disord 2017; 5: 851-858.
29. Silbiger JJ. Anatomy, mechanics, and pathophysiology of the mitral annulus. Am Heart J 2012; 164: 163-176.
30. Dandel M, Lehmkuhl H, Knosalla C, Suramelashvili N, Hetzer R. Strain and Strain Rate Imaging by Echocardiography – Basic Concepts and Clinical Applicability. Curr Cardiol Rev 2009; 5: 133–148.
31. Ng ACT, Prihadi EA, Antoni ML, Bertini M, Ewe SH, Ajmone Marsan N, Leung DY, Delgado V, Bax JJ. Left ventricular global longitudinal strain is predictive of all-cause mortality independent of aortic stenosis severity and ejection fraction. Eur Heart J Cardiovasc Imaging 2018; 19: 859-867.
32. Witkowski TG, Thomas JD, Debonnaire PJ, Delgado V, Hoke U, Ewe SH, Versteegh MI, Holman ER, Schalij MJ, Bax JJ, Klautz RJ, Marsan NA. Global longitudinal strain predicts left ventricular dysfunction after mitral valve repair. Eur Heart J Cardiovasc Imaging 2013; 14: 69-76.
33. Jensen MT, Risum N, Rossing P, Jensen JS. Self-reported dyspnea is associated with impaired global longitudinal strain in ambulatory type 1 diabetes patients with normal ejection fraction and without known heart disease - The Thousand & 1 Study. J Diabetes Complications 2016; 30: 28-34.
34. Nemes A, Piros GÁ, Domsik P, Kalapos A, Lengyel C, Várkonyi TT, Orosz A, Forster T. Changes in mitral annular morphology and function in young patients with type 1 diabetes mellitus-results from the three-dimensional speckle tracking echocardiographic MAGYAR-Path Study. Quant Imaging Med Surg 2015; 5: 815-821.
35. Kawamura R, Seo Y, Ishizu T, Atsumi A, Yamamoto M, Machino-Ohtsuka T, Nakajima H, Sakai S, Tanaka YO, Minami M, Aonuma K. Feasibility of left ventricular volume measurements by three-dimensional speckle tracking echocardiography depends on image quality and degree of left ventricular enlargement: validation study with cardiac magnetic resonance imaging. J Cardiol 2014; 63: 230-238.
36. Prastaro M, Pirozzi E, Gaibazzi N, Paolillo S, Santoro C, Savarese G, Losi MA, Esposito G, Perrone Filardi P, Trimarco B, Galderisi M. Expert Review on

the Prognostic Role of Echocardiography after Acute Myocardial Infarction. J Am Soc Echocardiogr 2017; 30: 431-443.

37. Anwar AM, Soliman OI, ten Cate FJ, Nemes A, McGhie JS, Krenning BJ, van Geuns RJ, Galema TW, Geleijnse ML. True mitral annulus diameter is underestimated by two-dimensional echocardiography as evidenced by real-time three-dimensional echocardiography and magnetic resonance imaging. Int J Cardiovasc Imaging 2007; 23: 541-547.
38. Anwar AM, Soliman OI, Nemes A, Germans T, Krenning BJ, Geleijnse ML, Van Rossum AC, ten Cate FJ. Assessment of mitral annulus size and function by real-time 3-dimensional echocardiography in cardiomyopathy: comparison with magnetic resonance imaging. J Am Soc Echocardiogr 2007; 20: 941-948.
39. Kleijn SA, Brouwer WP, Aly MF, Rüssel IK, de Roest GJ, Beek AM, van Rossum AC, Kamp O. Comparison between three-dimensional speckle-tracking echocardiography and cardiac magnetic resonance imaging for quantification of left ventricular volumes and function. Eur Heart J Cardiovasc Imaging 2012; 13: 834-839.
40. Kleijn SA, Aly MF, Terwee CB, van Rossum AC, Kamp O. Reliability of left ventricular volumes and function measurements using three-dimensional speckle tracking echocardiography. Eur Heart J Cardiovasc Imaging 2012; 13: 159-168.
41. Kleijn SA, Aly MF, Terwee CB, van Rossum AC, Kamp O. Comparison between direct volumetric and speckle tracking methodologies for left ventricular and left atrial chamber quantification by three-dimensional echocardiography. Am J Cardiol 2011; 108: 1038-1044.
42. Wood PW, Choy JB, Nanda NC, Becher H. Left Ventricular Ejection Fraction and Volumes: It Depends on the Imaging Method. Echocardiography 2014; 31: 87–100.
43. Forner-Cordero I, Szolnoky G, Forner-Cordero A, Kemény L. Lipedema: an overview of its clinical manifestations, diagnosis and treatment of the disproportional fatty deposition syndrome – systematic review. Clin Obes 2012; 2: 86-95.
44. Varga I, Kyselovič J, Galfiova P, Danisovic L. The Non-cardiomyocyte Cells of the Heart. Their Possible Roles in Exercise-Induced Cardiac Regeneration and Remodeling. Adv Exp Med Biol 2017; 999: 117-136.

8. Acknowledgements

The studies reported in this work were performed at the 2nd Department of Medicine and Cardiology Center, Medical Faculty, Albert Szent-Györgyi Clinical Center, University of Szeged, Hungary.

First of all, I express my heartfelt gratitude to Prof. Dr. Attila Nemes for his continuous support during my work, who was my tutor and scientific adviser. Without his support and encouragement, this thesis would have not been performed.

I would like to thank very much also Prof. Dr. Tamás Forster, the former head of the 2nd Department of Medicine and Cardiology Center, who supported me in my work.

I would like to thank all co-authors, Dr. Péter Domsik, Dr. Anita Kalapos, Dr. Árpád Kormányos, Dr. Nóra Ambrus, Dr. Györgyike Á. Piros, Dr. Zénó Ajtay, Dr. Győző Szolnoky, Prof. Dr. István Hartyánszky and Prof. Dr. Lajos Kemény.

I thank all my colleagues as well as nurses, assistants and all the members of the Institute.

Photocopies of essential publications

Original Article

Left ventricular longitudinal strain is associated with mitral annular fractional area change in healthy subjects—Results from the three-dimensional speckle tracking echocardiographic MAGYAR-Healthy Study

Zsolt Kovács[1], Árpád Kormányos[2], Péter Domsik[2], Anita Kalapos[2], Csaba Lengyel[3], Nóra Ambrus[2], Zénó Ajtay[4,5], Györgyike Á. Piros[2], Tamás Forster[2], Attila Nemes[2]

[1]Department of Cardiology, Szent Rókus Hospital, Baja, Hungary; [2]2nd Department of Medicine and Cardiology Centre, [3]1st Department of Medicine, Medical Faculty, Albert Szent-Györgyi Clinical Center, University of Szeged, Szeged, Hungary; [4]Vilmos Zsigmondy SPA Hospital, Harkány, Hungary; [5]Heart Institute, Medical School, University of Pécs, Pécs, Hungary

Correspondence to: Attila Nemes, MD, PhD, DSc, FESC. 2nd Department of Medicine and Cardiology Center, Medical Faculty, Albert Szent-Györgyi Clinical Center, University of Szeged, H-6725 Szeged, Semmelweis street 8, Hungary. Email: nemes.attila@med.u-szeged.hu.

Background: The mitral annulus (MA) plays a significant role in promoting left atrial and left ventricular (LV) filling and emptying, which is dependent on LV functional properties. The present study aimed to investigate the relationship between LV strains, quantitative features of longitudinal contractility and MA size and function in healthy subjects.

Methods: The present study comprised 295 healthy adults; 117 subjects were excluded due to inferior image quality (40%). Finally, 178 healthy adults (mean age: 32.0±11.3 years, 92 males). Complete two-dimensional Doppler echocardiography and three-dimensional speckle-tracking echocardiography were performed in all cases.

Results: The global and mean segmental left ventricular longitudinal strain (LV-LS) proved to be –16.1%±2.5% and –16.9%±2.4%, respectively. In the present study, LV-LS ≤–13% was considered to be reduced. In ROC analysis, the cut-off value for MA fractional area change (MAFAC) to predict impaired LV-LS was ≤44%, with 67% sensitivity and 69% specificity and ROC area under curve 0.73 (P=0.0005). Significantly increased LV volumes and LV mass and reduced MAFAC could be demonstrated in healthy subjects with global LV-LS ≤–13%. Significantly larger ratio of subjects with global LV-LS ≤–13% had MAFAC ≤44% (31% *vs.* 67%, P=0.009). Patients with MAFAC ≤44% had significantly reduced global and mean segmental LV-LS. Significantly larger ratio of subjects with MAFAC ≤44% had global LV-LS ≤–13% (4% *vs.* 16%, P=0.009).

Conclusions: There is a strong relationship between MA and LV longitudinal function. MA fractional area change predicts global LV-LS.

Keywords: Healthy; left ventricular (LV); strain; mitral annulus (MA); three-dimensional; speckle-tracking; echocardiography

Submitted Oct 13, 2018. Accepted for publication Feb 07, 2019.
doi: 10.21037/qims.2019.02.06
View this article at: http://dx.doi.org/10.21037/qims.2019.02.06

Introduction

The mitral valve (MV) apparatus is a complex three-dimensional (3D) functional unit which separates the left atrium and the left ventricle (LV), and has a critical role in the regulation of normally unidirectional blood flow (1). Compared to the LV ejection fraction (EF), LV longitudinal systolic function was found to be more sensitive in the detection of cardiac depression in several disorders (2,3). Three-dimensional speckle-tracking echocardiography (3DSTE) is a clinical tool of choice for simultaneous quantification of longitudinal LV deformation and mitral valve (MV) morphology and function (4,5). LV-MV interactions are not clearly understood at this moment, therefore the relationship between LV quantitative features of longitudinal contractility and MA size and function was aimed to be investigated in healthy subjects in this study.

Methods

Subjects

The present study comprised 295 healthy adults; 117 subjects were excluded due to inferior image quality (40%). Finally, 178 healthy adults (mean age: 32.0±11.3 years, 92 males) have been included without risk factors, known diseases or other conditions which theoretically could have affected the results. None of them take any medications at the time of examination. Complete two dimensional (2D) Doppler echocardiography and 3DSTE were performed in all cases at the same time by the same echocardiography machines. The results of the present study are a part of the MAGYAR-Healthy Study (Motion Analysis of the heart and Great vessels bY three-dimensionAl speckle-tRacking echocardiography in Healthy subjects). It was organized at the Cardiology Center of the University of Szeged to assess the clinical role of 3DSTE-derived echocardiographic parameters in healthy subjects ('magyar' means 'Hungarian' in Hungarian language) among others. Informed consent was obtained from each patient and the study protocol conformed to the ethical guidelines of the 1975 Declaration of Helsinki.

Two-dimensional echocardiography

Toshiba Artida™ (Toshiba Medical Systems, Tokyo, Japan) echocardiography equipment using a PST-30SBP (1–5 MHz) phased-array transducer was used for standard transthoracic Doppler examinations. Concerning guidelines, LV-EF was calculated by the Simpson's method (6). Visual grading and Doppler assessments were used to exclude valvular abnormalities.

3DSTE-derived data acquisition and quantitative analysis

The same Toshiba Artida™ echocardiography equipment was used with a fully sampled PST-25SX matrix-array transducer (Toshiba Medical Systems, Tokyo, Japan) with 3D capability. Pyramidal 3D full volumes were formed by the software using the R-wave triggered LV subvolumes from the 3D pyramidal data acquired during six consecutive cardiac cycles during one breath-hold from apical views in accordance with recent practices (4,7). Depth and angle were adjusted for optimal temporal and spatial resolution. 3D Wall Motion Tracking software version 2.7 (Toshiba Artida™; Toshiba Medical Systems, Tokyo, Japan) was used for quantitative analysis.

3DSTE-derived LV longitudinal strain assessments

Three short-axis views acquired at different LV levels and the apical two- (AP2CH) and four-chamber (AP4CH) views were selected automatically from the 3D echocardiographic pyramidal dataset at end-diastole by the software (4,7). For 3D reconstruction of the endocardial surface, the examiner selected two points at the edges of the mitral valve and one point at the apex on the 3D reconstruction of the endocardial surface on the AP2CH and AP4CH views. Then the endocardial surface was manually adjusted in all apical long- and short-axis. After these adjustments were made, the software automatically reconstructed and tracked the endocardial surface in 3D space throughout the cardiac cycle, and generated curves for global and mean segmental LV longitudinal strains (LSs) (*Figure 1*). LS is expressed as a negative number.

3DSTE-derived mitral annular measurements

MA measurements were performed in accordance with a simple method recently demonstrated by our working group. Briefly, from short-axis views, C3 was positioned at the level of the MA with the help of AP2CH and AP4CH views to find the optimal endpoints of the MA at end-diastole and end-systole (*Figure 2*) (5):

MA morphologic parameters

- MA diameter (MAD) was defined as the perpendicular line drawn from the peak of MA curvature to the

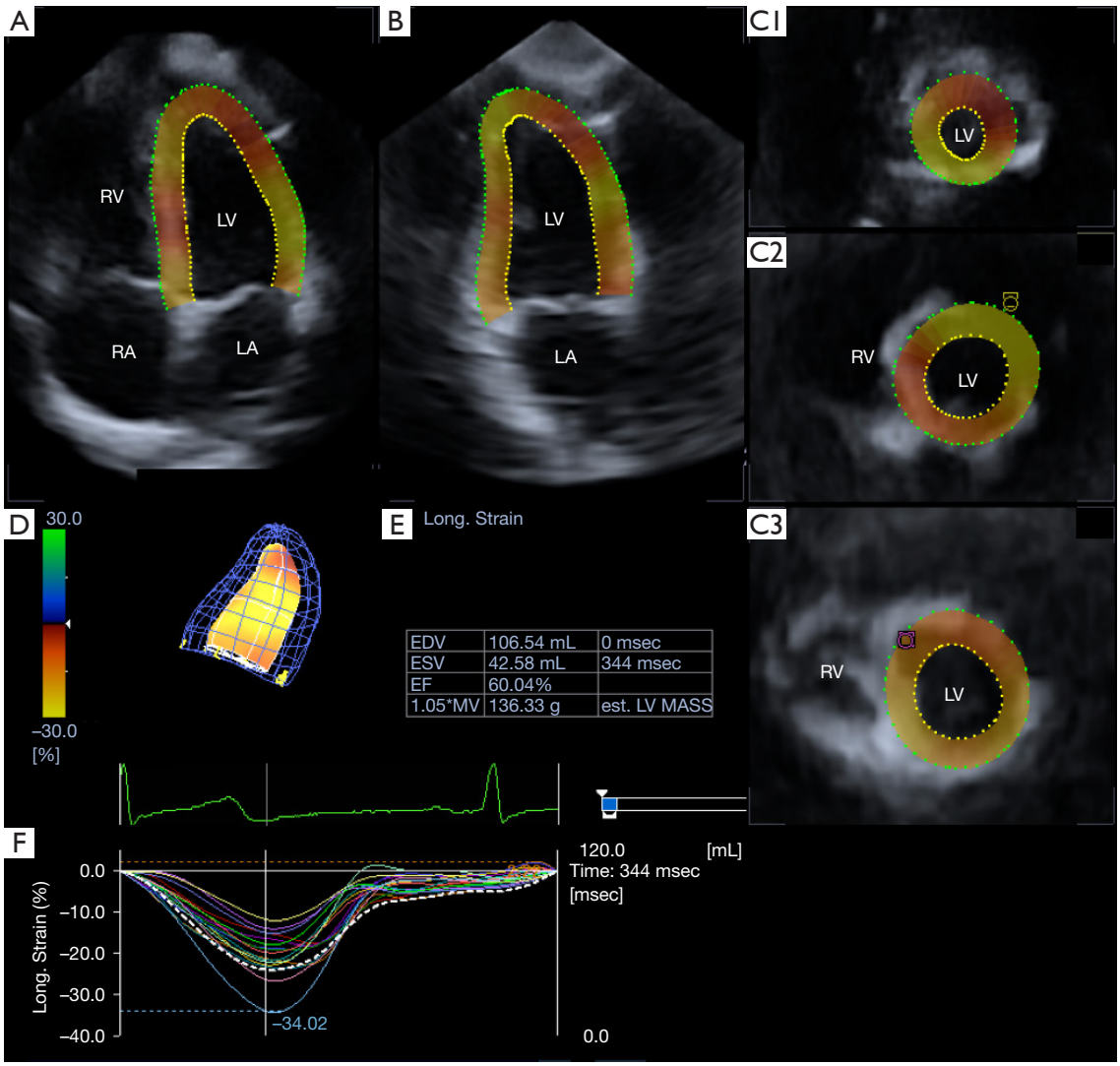

Figure 1 The apical four- (A) and two-chamber (B) views and 3 short-axis views at different left ventricular (LV) levels (C1, C2, C3) are presented in a healthy case. The three-dimensional LV cast (D) together with LV volumetric data (E) and LV segmental longitudinal strains (coloured lines) and LV volume-change (dashed line) regarding the cardiac cycle (F) are also presented. LA, left atrium; LV, left ventricle; RA, right atrium; RV, right ventricle.

middle of the straight MA border both at end-diastole, just before mitral valve closure, and at end-systole, just before mitral valve opening;

- ❖ MA area (MAA) was measured by planimetry both at end-diastole and at end-systole;
- ❖ MA perimeter (MAP) was measured by planimetry both at end-diastole and at end-systole.

MA functional parameters

- ❖ MA fractional shortening (MAFS) = (end-diastolic MAD – end-systolic MAD) / (end-diastolic MAD × 100);
- ❖ MA fractional area change (MAFAC) = (end-diastolic MAA – end-systolic MAA) / (end-diastolic MAA × 100).

Statistical analysis

All values were expressed as mean ± standard deviation. Group comparisons were made with unpaired Student's t-test. For the dichotomous variables, chi-square analysis and Fisher's exact test were performed. Two-sided $P<0.05$ was defined as statistical significance. Pearson's coefficient was calculated to examine correlations between parameters

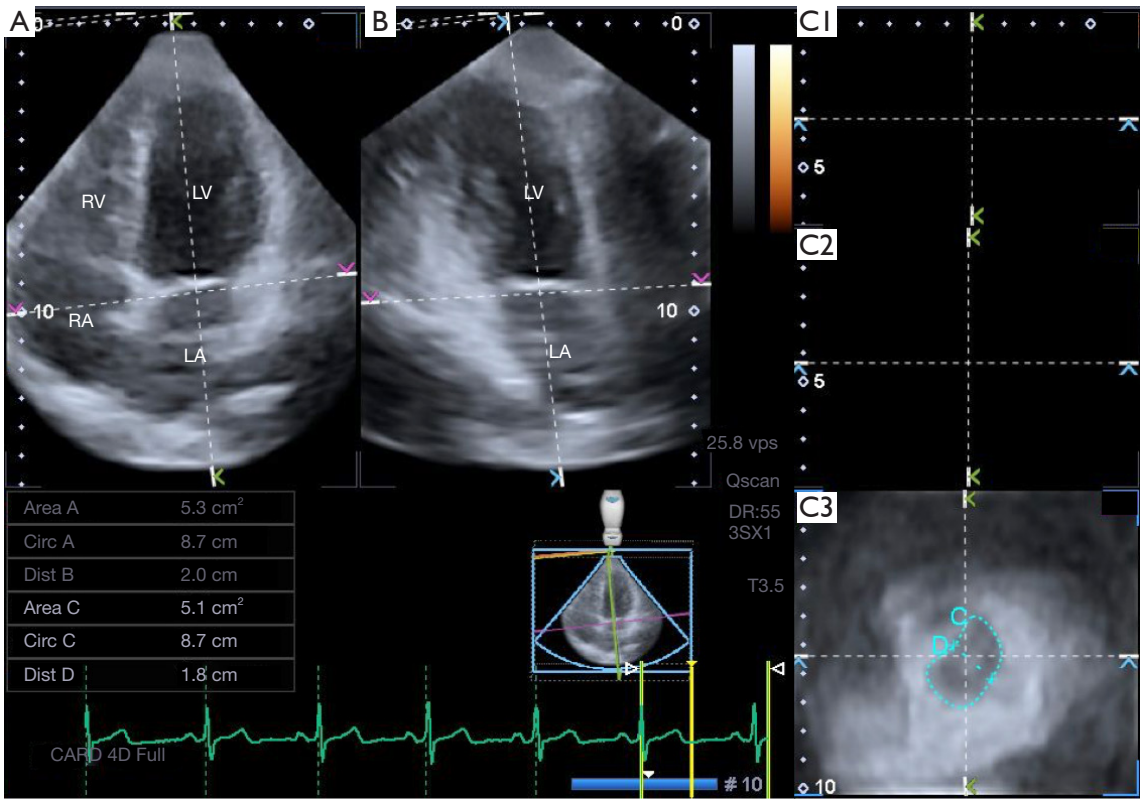

Figure 2 Images from three-dimensional full-volume echocardiographic dataset: apical four-chamber view (A), apical two-chamber view (B) and a cross-sectional view at the level of the mitral annulus (C3) optimized on apical four- and two-chamber views. (C1,C2) Cross-sectional views of different LV levels, not shown during MA measurements. Mitral annular data in end-systole and end-diastole are also presented. Area, MA area; Circ, MA perimeter; Dist, MA diameter; LA, left atrium; LV, left ventricle; RA, right atrium; RV, right ventricle.

featuring MA morphology and global and mean segmental LV-LS and for intraobserver and interobserver correlations. Inter- and intraobserver reproducibility of measurements of end-diastolic and end-systolic MA parameters and LV-LS was tested in healthy subjects. To assess the predictive power of MAFAC, receiver operator curve (ROC) was constructed and the area under the curve was reported with sensitivity and specificity values with 95% confidence intervals. MedCalc software was used for statistical calculations (MedCalc, Mariakerke, Belgium).

Results

Clinical data

Demographic data are presented in *Table 1*. Average height and weight proved to be 172.3±11.1 cm and 71.8±17.7 kg, respectively.

Two-dimensional echocardiographic data

Routine two-dimensional Doppler echocardiography showed normal results including left atrial diameter (36.8±4.0 mm), interventricular septum thickness (9.1±1.5 mm), systolic and diastolic LV diameter (38.4±23.5 and 48.0±3.9 mm, respectively) and LV volume (36.4±9.1 and 97.4±29.4 mL, respectively), LV ejection fraction (65.6%±4.7%), transmitral flow velocity E (72.8±26.0 cm/s) and A (64.3±19.0 cm/s) and their ratio (1.25±0.52). None of the healthy subjects had grade ≥1 valvular regurgitation or significant valvular stenosis.

Three-dimensional speckle-tracking echocardiographic data

The global and mean segmental LV-LS proved to be –16.1%±2.5% and –16.9%±2.4%, respectively (*Table 1*). 3DSTE-derived LV volumetric, LV-LS and MA data are

Table 1 Three-dimensional speckle-tracking echocardiographic data of healthy subjects and their relationship to left ventricular longitudinal strain and mitral annular fractional area change

Variables	All	Global LV-LS		MAFAC	
		>−13%	≤−13%	>44%	≤44%
Demographic data					
N	178 [100]	163 [92]	15 [8]	117 [66]	61 [34]
Age (years)	32.0±11.3	32.7±11.5	23.9±4.6	32.1±11.1	31.8±11.8
Male gender, n [%]	92 [52]	84 [52]	8 [53]	34 [58]	59 [50]
LV volumetric data					
LV end-diastolic volume (mL)	86.1±23.0	85.0±22.2	94.7±28.1*	85.5±23.0	87.3±22.9
LV end-systolic volume (mL)	36.2±10.5	35.7±10.0	42.2±13.9*	35.4±10.5	38.0±10.3
LV ejection fraction (%)	58.2±5.6	58.4±5.5	55.1±5.7	58.6±5.7	57.4±5.3
LV mass (mg)	158.0±31.9	156.3±31.5	168.8±31.1*	156.5±30.9	160.6±33.7
LV longitudinal strain					
Global LV-LS (%)	−16.1±2.5	−16.50±2.10	−11.6±1.6*	−16.5±2.4	−15.5±2.5†
Mean segmental LV-LS (%)	−16.9±2.4	−17.24±2.12	−12.9±1.5*	−17.3±2.4	−16.2±2.2†
MA parameters					
MA end-diastolic diameter (cm)	2.38±0.44	2.45±0.44	2.29±0.45	2.47±0.45	2.21±0.38†
MA end-diastolic area (cm^2)	7.12±2.22	7.39±2.23	6.70±2.62	7.73±2.21	5.93±1.85†
MA end-diastolic perimeter (cm)	10.22±1.49	10.27±1.50	9.89±1.66	10.56±1.47	9.57±1.33†
MA end-systolic diameter (cm)	1.59±0.38	1.59±0.38	1.65±0.41	1.49±0.36	1.80±0.37†
MA end-systolic area (cm^2)	3.44±1.26	3.41±1.26	3.86±1.19	3.09±1.13	4.16±1.23†
MA end-systolic perimeter (cm)	7.08±1.23	7.04±1.23	7.59±1.17	6.74±1.18	7.75±1.06†
MA fractional area change (%)	51.3±15.7	52.5±15.3	39.3±15.3*	60.5±9.2	33.6±9.0†
MA fractional shortening (%)	34.2±15.1	34.3±15.0	27.4±15.2	40.0±13.0	21.4±10.7†
Global LV-LS ≤−13%, n [%]	15 [8]	0 [0]	15 [100]*	5 [4]	10 [16]†
MAFAC ≤44%, n [%]	117 [66]	51 [31]	10 [67]*	0 [0]	61 [100]†

*P<0.05 *vs.* global LV-LS >−13%; †P<0.01 *vs.* MAFAC >44%. LS, longitudinal strain; LV, left ventricular; MA, mitral annular; MAFAC, mitral annular fractional area change.

presented in *Table 1*. In the present study, LV-LS ≤−13% was considered to be reduced. In ROC analysis, the cut-off value for MAFAC to predict impaired LV-LS was ≤44%, with 67% sensitivity (95% CI, 38–88%) and 69% specificity (95% CI, 61–76%) and ROC area under curve 0.73 (P=0.0005) (*Figure 3*). Significantly increased LV volumes and LV mass and reduced MAFAC could be demonstrated in healthy subjects with ≤−13% global LV-LS as compared to cases with global LV-LS >−13%. Significantly larger ratio of subjects with global LV-LS ≤−13% had MAFAC ≤44% as compared to cases with >−13% global LV-LS (31% *vs.* 67%, P=0.009). Patients with MAFAC ≤44% had significantly reduced global and mean segmental LV-LS, reduced end-diastolic and increased end-systolic MA sizes and reduced MAFS. Significantly larger ratio of subjects with MAFAC ≤44% had global LV-LS ≤−13% as compared to cases with MAFAC >44% (4% *vs.* 16%, P=0.009). MAFAC showed no correlations with global or mean segmental LV-LS.

Reproducibility measurements

Table 2 shows the mean ± standard deviation difference in

values obtained by two measurements of the same observer and two observers for the measurements of 3DSTE-derived end-diastolic and end-systolic MA parameters and LV-LS in 20 healthy subjects, along with the respective correlation coefficients.

Discussion

The normal MV apparatus is a dynamic 3D structure which allows normal blood flow during the cardiac cycle: LV inflow from the LA during diastole and LV outflow into the aorta during systole. The key components are the MA, the valve leaflets, the chordae tendineae, and the LV wall with its attached papillary muscles (1). MA plays a significant role in promoting LA and LV filling and emptying, which is dependent on LV functional properties (8). LV strains are quantitative features of LV myocardial contractility. Global LV-LS characterizes LV deformation (lengthening or shortening) in longitudinal direction and has good prognostic value in various disorders (9,10). Moreover, LV-LS is more sensitive than LV-EF in detecting abnormalities in LV systolic function as noted by Carasso *et al.* (3). 3DSTE allows complete non-invasive assessment of the heart chambers in 3D space including parallel evaluation of MA and LV morphology and function (at the same time) from the same 3D dataset. This advantage enables physiologic studies assessing the effects of these components on each other.

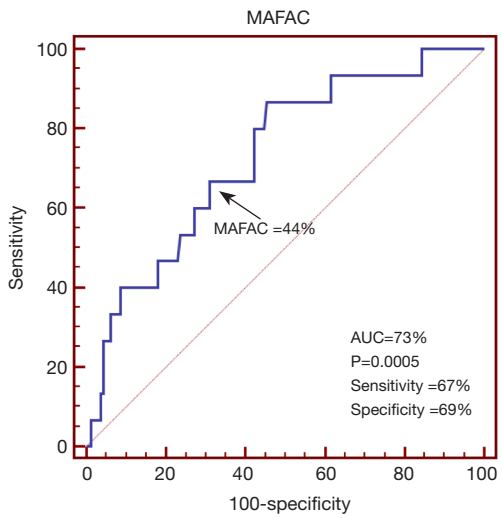

Figure 3 Receiver operating characteristic analysis illustrating the diagnostic accuracy of mitral annular (MA) fractional area change (MAFAC) in predicting reduced (≤–13%) left ventricular longitudinal strain is demonstrated.

In recent studies global LV-LS and MV function have been demonstrated to be associated in several pathological states (11). However, to the best of the authors' knowledge, no clinical studies are available directly assessing a relationship between LV longitudinal deformation and MA functional properties in healthy subjects. Lower global LV-LS was found to be associated with lower MA function. Moreover, impaired LV longitudinal deformation proved to have a prognostic role in the prediction of MAFAC, as well. These results could suggest that subclinical impairment of LV longitudinal function is associated with reduced MA function in otherwise healthy subjects without risk factors

Table 2 Intra- and interobserver variability for the most important parameters

Variables	Intraobserver agreement		Interobserver agreement	
	Mean ± SD difference in values obtained by 2 measurements of the same observer	Correlation coefficient between measurements of the same observer	Mean ± SD difference in values obtained by 2 observers	Correlation coefficient between independent measurements of 2 observers
End-diastolic MAD	0.01±0.25 cm	0.96 (P<0.0001)	0.02±0.21 cm	0.97 (P<0.0001)
End-diastolic MAA	–0.01±1.08 cm^2	0.98 (P<0.0001)	0.00±0.86 cm^2	0.98 (P<0.0001)
End-diastolic MAP	–0.02±1.00 cm	0.93 (P<0.0001)	–0.14±1.06 cm	0.92 (P<0.0001)
End-systolic MAD	–0.02±0.27 cm	0.96 (P<0.0001)	0.01±0.29 cm	0.96 (P<0.0001)
End-systolic MAA	–0.01±0.35 cm^2	0.99 (P<0.0001)	–0.07±0.41 cm^2	0.99 (P<0.0001)
End-systolic MAP	0.08±0.56 cm	0.98 (P<0.0001)	0.07±0.49 cm	0.99 (P<0.0001)
LV-LS	0.08%±0.95%	0.98 (P<0.0001)	0.06%±1.06%	0.96 (P<0.0001)

MAD, mitral annular diameter; MAA, mitral annular area; MAP, mitral annular perimeter; LV-LS, left ventricular longitudinal strain.

or overt cardiovascular diseases. This result is against what could be demonstrated in different disorders. For instance, although type 1 diabetes mellitus is associated with impaired global LV-LS (12), MA functional properties proved to be significantly increased suggesting a compensatory mechanism in these patients (5). Our results suggest that demand for this compensatory mechanism did not reach a certain level required for the mechanism to develop in our healthy subject. Further studies are warranted to confirm our findings and to reveal pathophysiological background of this compensation.

Limitation section

The most important limitations occurring during the 3DSTE studies are listed below:

- Spatial and temporal resolution of the relatively new 3DSTE is low which could affect the results and should be considered when interpreting the results.
- Although 3DSTE could measure LV volumes, its accuracy depends on the quality of the acquired image and particularly on enlargement of the LV (13). This study tried to mirror real life experience, therefore 3DSTE-derived LV volumetric data could be somewhat lower as expected.
- Early stage diseases were not excluded by other imaging or laboratory tests, although lower strain values could indicate subclinical changes.
- LV strain and volumetric and functional data of heart chambers other than the LV were not examined in this study.
- Although the MA geometric shape approximates a hyperbolic paraboloid, only one plane MA motion and function was analysed in this study.
- Spatial longitudinal analysis of the MA movement along its long-axis is also possible (6), it was not aimed to be measured and compared to other parameters in this particular study.

Conclusions

There is a strong relationship between MA and LV longitudinal function. MA fractional area change predicts global LV-LS.

Acknowledgements

None.

Footnote

Conflicts of Interest: The authors have no conflicts of interest to declare.

Ethical Statement: The authors assert that all procedures contributing to this work comply with the ethical standards of the relevant national guidelines on human experimentation and with the Helsinki Declaration of 1975, as revised in 2008, and has been approved by the institutional committee of the University of Szeged. Informed consent was obtained from each patient.

References

1. Dal-Bianco JP, Levine RA. Anatomy of the Mitral Valve Apparatus – Role of 2D and 3D Echocardiography. Cardiol Clin 2013;31:151-64.
2. Zhang HM, Wang XT, Zhang LN, He W, Zhang Q, Liu DW; Chinese Critical Ultrasound Study Group. Left Ventricular Longitudinal Systolic Function in Septic Shock Patients with Normal Ejection Fraction: A Case-control Study. Chin Med J (Engl) 2017;130:1169-74.
3. Carasso S, Cohen O, Mutlak D, Adler Z, Lessick J, Reisner SA, Rakowski H, Bolotin G, Agmon Y. Differential effects of afterload on left ventricular long- and short-axis function: Insights from a clinical model of patients with aortic valve stenosis undergoing aortic valve replacement. Am Heart J 2009;158:540-5.
4. Nemes A, Kalapos A, Domsik P, Forster T. Three-dimensional speckle-tracking echocardiography -- a further step in non-invasive three-dimensional cardiac imaging. Orv Hetil 2012;153:1570-7.
5. Nemes A, Piros GÁ, Domsik P, Kalapos A, Lengyel C, Várkonyi TT, Orosz A, Forster T. Changes in mitral annular morphology and function in young patients with type 1 diabetes mellitus-results from the three-dimensional speckle tracking echocardiographic MAGYAR-Path Study. Quant Imaging Med Surg 2015;5:815-21.
6. Nemes A, Forster T. Recent echocardiographic examination of the left ventricle – from M-mode to 3D speckle-tracking imaging. Orv Hetil 2015;156:1723-40.
7. Biswas M, Sudhakar S, Nanda NC, Buckberg G, Pradhan M, Roomi AU, Gorissen W, Houle H. Two- and three-dimensional speckle tracking echocardiography: clinical applications and future directions. Echocardiography 2013;30:88-105.
8. Silbiger JJ. Anatomy, mechanics, and pathophysiology of

the mitral annulus. Am Heart J 2012;164:163-76.
9. Dandel M, Lehmkuhl H, Knosalla C, Suramelashvili N, Hetzer R. Strain and Strain Rate Imaging by Echocardiography – Basic Concepts and Clinical Applicability. Curr Cardiol Rev 2009;5:133-48.
10. Ng ACT, Prihadi EA, Antoni ML, Bertini M, Ewe SH, Ajmone Marsan N, Leung DY, Delgado V, Bax JJ. Left ventricular global longitudinal strain is predictive of all-cause mortality independent of aortic stenosis severity and ejection fraction. Eur Heart J Cardiovasc Imaging 2018;19:859-67.
11. Witkowski TG, Thomas JD, Debonnaire PJ, Delgado V, Hoke U, Ewe SH, Versteegh MI, Holman ER, Schalij MJ, Bax JJ, Klautz RJ, Marsan NA. Global longitudinal strain predicts left ventricular dysfunction after mitral valve repair. Eur Heart J Cardiovasc Imaging 2013;14:69-76.
12. Jensen MT, Risum N, Rossing P, Jensen JS. Self-reported dyspnea is associated with impaired global longitudinal strain in ambulatory type 1 diabetes patients with normal ejection fraction and without known heart disease - The Thousand & 1 Study. J Diabetes Complications 2016;30:928-34.
13. Kawamura R, Seo Y, Ishizu T, Atsumi A, Yamamoto M, Machino-Ohtsuka T, Nakajima H, Sakai S, Tanaka YO, Minami M, Aonuma K. Feasibility of left ventricular volume measurements by three-dimensional speckle tracking echocardiography depends on image quality and degree of left ventricular enlargement: validation study with cardiac magnetic resonance imaging. J Cardiol 2014;63:230-8.

Cite this article as: Kovács Z, Kormányos Á, Domsik P, Kalapos A, Lengyel C, Ambrus N, Ajtay Z, Piros GA, Forster T, Nemes A. Left ventricular longitudinal strain is associated with mitral annular fractional area change in healthy subjects—Results from the three-dimensional speckle tracking echocardiographic MAGYAR-Healthy Study. Quant Imaging Med Surg 2019;9(2):304-311. doi: 10.21037/qims.2019.02.06

A határérték bal kamrai ejekciós frakció együtt jár a mitralis anulus méretének és funkciójának eltéréseivel

Eredmények a háromdimenziós speckle-tracking echokardiográfiás MAGYAR-Healthy Tanulmányból

Kovács Zsolt dr.[1] ▪ Kormányos Árpád dr.[2] ▪ Domsik Péter dr.[2]
Kalapos Anita dr.[2] ▪ Lengyel Csaba dr.[3] ▪ Ajtay Zénó dr.[4, 5]
Forster Tamás dr.[2] ▪ Nemes Attila dr.[2]

[1]Szent Rókus Kórház, Kardiológiai Osztály, Baja
Szegedi Tudományegyetem, Általános Orvostudományi Kar, Szent-Györgyi Albert Klinikai Központ,
[2]II. Belgyógyászati Klinika és Kardiológiai Központ, [3]I. Belgyógyászati Klinika, Szeged
[4]Zsigmondy Vilmos Gyógyfürdőkórház, Harkány
[5]Pécsi Tudományegyetem, Általános Orvostudományi Kar, Szívgyógyászati Klinika, Pécs

Bevezetés: A mitralis anulus (MA) morfológiája és funkciója számos valvularis (például mitralis regurgitatióban) és nem valvularis betegségben (például bizonyos cardiomyopathiákban, cardialis amyloidosisban) eltéréseket mutathat.
Célkitűzés: A jelen vizsgálat célja az MA morfológiai és funkcionális jellemzői és a háromdimenziós speckle-tracking echokardiográfiával (3DSTE) számított bal kamrai (BK) ejekciós frakció (EF) összefüggéseinek vizsgálata volt normális és határérték-BK-EF-fel bíró esetekben.
Módszer: A jelen vizsgálatba 146 olyan önkéntes eredményeit válogattuk be (átlagos életkor 32,0 ± 11,4 év; 74 férfi), akiknél teljes körű kétdimenziós Doppler-echokardiográfiás vizsgálat történt negatív eredménnyel, melyet 3DSTE-vel egészítettünk ki. A vizsgált populációt két további alcsoportra bontottuk a 3DSTE-vel számított BK-EF-nek megfelelően (határérték 50–54% *versus* ≥55%).
Eredmények: A határérték-BK-EF-fel bíró esetekben magasabb BK-i végszisztolés térfogatot és alacsonyabb BK-i longitudinális straint lehetett mérni. A végszisztolés és végdiasztolés MA-átmérő-, -area- és -kerület-értékek nagyobbnak bizonyultak a határérték-BK-EF-fel bíró esetekben, ekkor az MA funkcionális paraméterek is kisebbek voltak. A fenti összefüggések ellenére a BK-EF nem mutatott korrelációt sem a végszisztolés és végdiasztolés MA-méretekkel, sem az MA funkcionális paraméterekkel.
Következtetések: A 3DSTE-vel meghatározott határérték-BK-EF együtt jár az MA tágulásával és funkciójának romlásával.
Orv Hetil. 2018; 159(50): 2129–2135.

Kulcsszavak: bal kamra, ejekciós frakció, mitralis anulus, háromdimenziós echokardiográfia, speckle-tracking

Borderline left ventricular ejection fraction is associated with alterations in mitral annular size and function

Results from the three-dimensional speckle-tracking echocardiographic MAGYAR-Healthy Study

Introduction: Morphology and function of the mitral annulus (MA) shows alterations in different valvular (for instance in mitral regurgitation) and non-valvular disorders (for instance in certain cardiomyopathies, cardiac amyloidosis).
Aim: The aim of the present study was to examine the relationship between MA morphologic and functional properties and three-dimensional speckle-tracking echocardiography- (3DSTE) derived left ventricular (LV) ejection fraction (EF) in subjects with normal *versus* borderline LV-EF.

Method: The present study comprised 146 volunteers (mean age: 32.0 ± 11.4 years; 74 males) in whom complete two-dimensional Doppler echocardiography was performed with a negative result extended with 3DSTE. The population was further divided into two groups according to their 3DSTE-derived LV-EF (borderline 50–54% *versus* ≥55%).
Results: In cases with borderline LV-EF, higher LV end-systolic LV volumes and lower LV longitudinal strain could be measured. All end-systolic and end-diastolic MA diameter, area and perimeter data proved to be higher in cases with borderline LV-EF. In these subjects, MA functional parameters proved to be lower as well. In contrast, LV-EF showed correlations neither with end-systolic and end-diastolic MA dimensions nor with MA functional parameters.
Conclusions: 3DSTE-derived borderline LV-EF is associated with MA dilatation and functional impairment.

Keywords: left ventricle, ejection fraction, mitral annulus, three-dimensional echocardiography, speckle-tracking

Kovács Zs, Kormányos Á, Domsik P, Kalapos A, Lengyel Cs, Ajtay Z, Forster T, Nemes A. [Borderline left ventricular ejection fraction is associated with alterations in mitral annular size and function. Results from the three-dimensional speckle-tracking echocardiographic MAGYAR-Healthy Study]. Orv Hetil. 2018; 159(50): 2129–2135.

(Beérkezett: 2018. március 28.; elfogadva: 2018. július 17.)

Rövidítések

2D = (two-dimensional) kétdimenziós; 3D = (three-dimensional) háromdimenziós; 3DSTE = (three-dimensional speckle-tracking echocardiography) háromdimenziós speckle-tracking echokardiográfia; ÁOK = Általános Orvostudományi Kar; AP2CH = (apical 2-chamber view) csúcsi 2 üregi nézet; AP4CH = (apical 4-chamber view) csúcsi 4 üregi nézet; BK = bal kamra; BP = bal pitvar; EF = ejekciós frakció; LS = longitudinális strain; MA = mitralis anulus; MAA = MA-area; MAD = (MA diameter) MA-átmérő; MAFAC = (MA fractional area change) az MA frakcionális area változása; MAFS = (MA fractional shortening) MA frakcionális rövidülés; **MAGYAR-Healthy** Tanulmány = **M**otion **A**nalysis of the heart and **G**reat vessels b**Y** three-dimension**A**l speckle-t**R**acking echocardiography in **Healthy** subjects; MRI = (magnetic resonance imaging) mágnesesrezonancia-vizsgálat; RT3DE = (real-time three-dimensional echocardiography) valósidejű 3D-echokardiográfia; STE = speckle-tracking echokardiográfia

A mitralis billentyű a bal pitvar (BP) és a bal kamra (BK) között elhelyezkedő nyereg alakú, komplex szerkezetű, háromdimenziós (3D-) struktúra, melynek szerepe többek között a vér egyirányú áramlásának biztosítása [1, 2]. Fontos alkotóelemei a mitralis anulus (MA), a billentyűlemezek, a papillaris izom és az ínhúrok [1, 2]. Amellett, hogy a billentyűlemezek az MA-hoz rögzülnek, annak szerepe van a BP és a BK telődésének és ürülésének támogatásában is [3]. Ismert tény, hogy az MA morfológiája és funkciója számos valvularis kórképben (például mitralis prolapsusban, mitralis regurgitatio esetén) és nem valvularis betegségben (például bizonyos cardiomyopathiákban, cardialis amyloidosisban) eltéréseket mutathat [4–7]. A fentieknek megfelelően az MA méretének és funkciójának eltérései fontos paraméterek lehetnek a BK méretének és funkciójának változásával járó kórállapotok fennállása esetén azok megítélésében.

A háromdimenziós speckle-tracking echokardiográfia (3DSTE) olyan új noninvazív képalkotó eljárás, mely alkalmas nemcsak bizonyos szívüregek (például a BK, BP) egyidejű volumetrikus és strainalapú funkcionális megítélésére, hanem egyazon 3D virtuális modellt felhasználva egyszerűen lemérhetők az MA szívciklusnak megfelelő méretei is [8]. A jelen vizsgálat célja az MA morfológiai és funkcionális jellemzői és a BK szisztolés pumpafunkcióját jellemző, 3DSTE-vel számított ejekciós frakció (EF) összefüggéseinek vizsgálata volt normális és határérték-BK-EF-fel bíró esetekben.

Betegek és módszer

A vizsgált betegcsoport

A jelen vizsgálatba 146 olyan önkéntest válogattunk be (átlagos életkor 32,0 ± 11,4 év; 74 férfi), akiknél negatív eredményű teljes körű kétdimenziós (2D) Doppler-echokardiográfiás vizsgálat történt. Valamennyi esetben a rutin echokardiográfiás vizsgálatot 3DSTE-vel egészítettük ki. A betegek a vizsgálatok idején panaszmentesek voltak, nem volt ismert cardiovascularis betegségük vagy rizikófaktoruk, gyógyszert nem szedtek. A betegek csoportját két további alcsoportra bontottuk annak megfelelően, hogy a 3DSTE-vel számított BK-EF a teljesen normális tartományba esett-e (BK-EF ≥55%), vagy határértékűnek bizonyult (BK-EF = 50–54%). A jelen vizsgálat a része a Szegedi Tudományegyetem, ÁOK, II. Belgyógyászati Klinika és Kardiológiai Központban megszervezett **MAGYAR-Healthy** Tanulmánynak (**M**otion **A**nalysis of the heart and **G**reat vessels b**Y** three-dimension**A**l speckle-t**R**acking echocardiography in **Healthy** subjects), melynek célja többek között a 3DSTE-vel mért paraméterek normálértékeinek meghatározása mellett fiziológiás összefüggések feltárása egészségesekben. Valamennyi esetben a vizsgálatban részt vevők aláírták a beleegyező nyilatkozatot, a vizsgálati protokoll megfelelt az 1975-ös Helsinki Nyilatkozatban foglaltaknak, és a helyi intézeti etikai bizottság is elfogadta.

Kétdimenziós echokardiográfia

Valamennyi esetben 2D Doppler-echokardiográfiás vizsgálat történt, melyhez Toshiba Artida™ echokardiográfiás készüléket használtunk (Toshiba Medical Systems, Tokió, Japán) 1–5 MHz-es PST-30SBP phased-array transzducerrel. A nemzetközi szakmai irányelvekkel összhangban lemértük a szívciklusnak megfelelő BK-i dimenziókat és térfogatértékeket, valamint a BP-i átmérőt [9]. A valvularis regurgitatiók kizárására színes Doppler-echokardiográfia és vizuális becslés történt, míg a billentyűgradiensek megítélésére folyamatos hullámú Doppler-technikát alkalmaztunk.

Háromdimenziós speckle-tracking echokardiográfia

A vizsgálatok elvégzéséhez ugyanazt a Toshiba Artida™ echokardiográfiás készüléket használtuk 3DSTE során, azonban a 3D echokardiográfiás adatbázisok digitális begyűjtéséhez PST-25SX mátrix phased-array transzducert alkalmaztunk apicalis pozícióból (Toshiba Medical Systems, Tokió, Japán). Az egy lélegzetvételnyi idő és hat szívciklus alatt begyűjtött 3D-részadatbázisokból a szoftver teljes 3D echokardiográfiás adatbázist hozott létre. A vizsgáló az adatok begyűjtése során az optimális képminőség eléréséhez a szükségleteknek megfelelően a mélységet és a szöget optimalizálta.

Az offline kvantitatív analízishez a 3D Wall Motion Tracking szoftver 2.7 verzióját használtuk (Toshiba Artida™; Toshiba Medical Systems, Tokió, Japán) [8, 10]. A szoftver a begyűjtött 3D echokardiográfiás adatbázisok felhasználásával automatikusan a BK különböző szintjeiben három keresztmetszeti képet, valamint apicalis 2 üregi (apical 2-chamber view, AP2CH) és 4 üregi (AP4CH) hossztengelyi nézeteket hozott létre. A virtuális BK-i 3D-modellalkotáshoz szükség van az endocardialis felszín detektálására, amihez a vizsgáló AP2CH- és AP4CH-nézetben definiálta az MA végpontjait és a BK csúcsát. Ezután a szoftver az endocardiumot automatikusan felismerte, majd rekonstruálta a szívciklusnak megfelelően. Vizsgálataink során a BK-i modell segítségével a volumetrikus adatokon túl a globális és átlagos szegmentális BK-i longitudinális strain (LS) paramétereket is kiszámítottuk *(1. ábra)*.

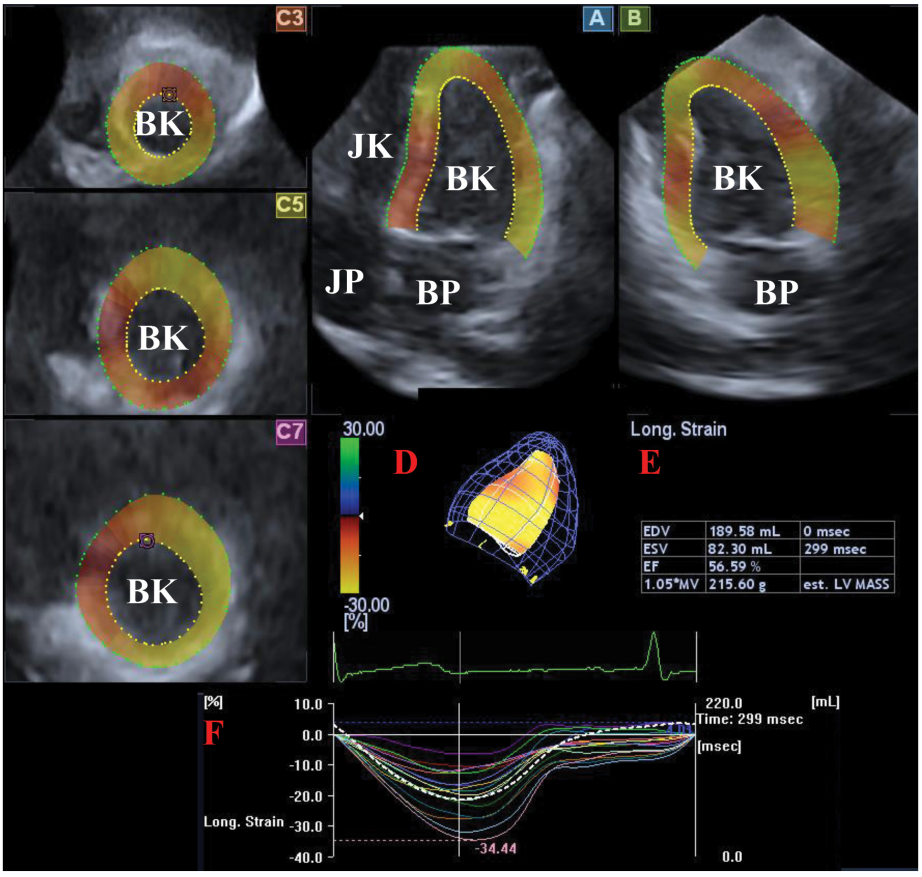

1. ábra Háromdimenziós (3D) speckle-tracking echokardiográfia során begyűjtött 3D-adatbázis felhasználásával a speciális szoftver segítségével a bal kamra (BK) apicalis négyüregi (A) és kétüregi (B), valamint három különböző síkban elkészített keresztmetszeti nézete (C3, C5, C7) ábrázolható. A módszer lehetővé teszi a BK 3D-s modelljének (piros D), volumetrikus adatainak (piros E) és a modell felhasználásával készített idő-BK-i térfogatnak (szaggatott vonal) és idő-BK-i szegmentális (longitudinális) straingörbéknek (színes vonalak) az egyidejű ábrázolását (piros F)

BP = bal pitvar; BK = bal kamra; JP = jobb pitvar; JK = jobb kamra

2. ábra Háromdimenziós speckle-tracking echokardiográfia során létrehozott ábra: apicalis négyüregi nézet (A), apicalis kétüregi nézet (B) és keresztmetszeti nézet a mitralis anulus (MA) szintjében (C7), melyet az apicalis négyüregi és kétüregi nézetekben optimalizáltunk. A kétdimenziós síkba projektált nézeten az MA átmérője, areája és kerülete végdiasztolében és végszisztolében is lemérhető, majd a kapott paraméterekből az MA funkcióját jellemző értékek számíthatók

Area = MA-area; Circ = MA-kerület; Dist = MA-átmérő; MA = mitralis anulus; BP = bal pitvar; BK = bal kamra; JP = jobb pitvar; JK = jobb kamra

Az MA vizsgálata során a C7-es keresztmetszeti képen ábrázoltuk az MA-t végdiasztolében és végszisztolében úgy, hogy közben az AP4CH- és AP2CH-metszetek segítségével igyekeztünk megtalálni az MA optimális keresztmetszeti képét is. A módszer segítségével létrehozott 2D projekciós MA keresztmetszeti képen lemértük a valós MA-átmérőt, -areát és -kerületet végszisztolében és végdiasztolében, majd kiszámítottuk az MA funkcióját jellemző paramétereket *(2. ábra)*.

MA morfológiai paraméterek:
- MA-átmérő (MAD), melyet végszisztolében (a mitralis billentyű nyitódása előtt) és végdiasztolében (a mitralis billentyű záródása előtt) mértünk;
- MA-area (MAA), melyet planimetria során mértünk végszisztolében és végdiasztolében;
- MA-kerület (MAK), melyet szintén planimetria során mértünk végszisztolében és végdiasztolében.

Az MA-funkció jellemzésére számított paraméterek:
- MA frakcionális rövidülés (MAFS) = (végdiasztolés MAD – végszisztolés MAD) / (végdiasztolés MAD × 100)
- MA frakcionális area változása (MAFAC) = (végdiasztolés MAA – végszisztolés MAA) / (végdiasztolés MAA × 100)

Statisztikai analízis

Valamennyi értéket átlag ± standard deviáció, vagy szám és százalék alakban tüntettük fel. A csoportok összehasonlítása során kétmintás t-próbát használtunk, míg a dichotom értékek összehasonlítására X-négyzet-próbát és Fisher-féle egzakt tesztet alkalmaztunk. Pearson-féle koefficienst számítottunk a korreláció jellemzésére. A p kisebb, mint 0,05-ot tekintettük statisztikailag szignifikánsnak. A statisztikai analízisek során MedCalc szoftvert használtunk (MedCalc, Mariakerke, Belgium).

Eredmények

Kétdimenziós Doppler-echokardiográfiás adatok

2D echokardiográfia során normális cardialis méretek voltak mérhetők (bal pitvar: 39,5 ± 2,2 mm, BK-i végdiasztolés átmérő: 47,8 ± 2,3 mm, BK-i végszisztolés átmérő: 33,1 ± 2,2 mm, interventricularis septum: 9,1 ± 0,8 mm, BK-i hátsó fal: 9,0 ± 0,7 mm, BK-EF: 64,5 ± 2,2%). Egyik egészséges egyénnél sem volt igazolható egyes stádiumnál nagyobb mértékű valvularis regurgitatio vagy szignifikáns mértékű valvularis stenosis.

Háromdimenziós speckle-tracking echokardiográfiás adatok

A 3DSTE-vel mért BK-i volumetrikus, BK-LS- és MA-adatokat az *1. táblázat*ban tüntettük fel. A határérték-BK-EF-fel bíró esetekben nagyobb BK-i végszisztolés térfogatot és kisebb BK-LS-t lehetett mérni. A végszisztolés és végdiasztolés MA-átmérő-, -area- és -kerület-értékek nagyobbnak bizonyultak a határérték- (50–54%) BK-EF-fel bíró betegekben a ≥55% BK-EF-fel bíró esetekhez képest. Ezekben az egyénekben az MA funkcionális paraméterek is kisebbnek bizonyultak.

Korrelációk

A teljes populációt vizsgálva a BK-EF nem mutatott korrelációt sem a végszisztolés és végdiasztolés MA-méretekkel, sem az MAFAC-cal (r = 0,21, p = 0,24) és az MAFS-sal (r = 0,19, p = 0,31). Hasonlóan nem volt korreláció igazolható az alcsoportok analízise során sem.

1. táblázat A háromdimenziós speckle-tracking echokardiográfia során mért bal kamrai volumetrikus és longitudinális strain, valamint mitralis anulus paraméterek összefüggései

	Összes adat	BK-EF 50–54%	BK-EF ≥55%
n	146	33	113
Kor (évek)	32,0 ± 11,4	28,6 ± 9,0*	33,0 ± 11,9
Férfinem (%)	74 (51)	23 (70)*	51 (45)
3DSTE-vel mért BK-i volumetrikus adatok			
BK-i végdiasztolés térfogat (ml)	87,0 ± 23,9	84,1 ± 26,6	87,8 ± 23,1
BK-i végszisztolés térfogat (ml)	36,4 ± 10,8	40,9 ± 10,6*	35,1 ± 10,5
BK-i ejekciós frakció (%)	58,5 ± 5,3	52,6 ± 1,3*	60,3 ± 4,8
3DSTE-vel mért BK-i strainadatok			
BK-i globális longitudinális strain (%)	–16,0 ± 2,5	–15,0 ± 2,3*	–16,3 ± 2,4
BK-i átlagos szegmentális longitudinális strain (%)	–16,8 ± 2,4	–15,9 ± 2,1*	–17,1 ± 2,4
3DSTE-vel mért MA-adatok			
MA végdiasztolés átmérő (cm)	2,44 ± 0,43	2,55 ± 0,45†	2,40 ± 0,42
MA végdiasztolés area (cm^2)	7,31 ± 2,21	7,90 ± 2,61†	7,13 ± 2,06
MA végdiasztolés kerület (cm)	10,2 ± 1,5	10,6 ± 1,7†	10,1 ± 1,4
MA végszisztolés átmérő (cm)	1,60 ± 0,39	1,79 ± 0,40*	1,54 ± 0,37
MA végszisztolés area (cm^2)	3,45 ± 1,27	4,21 ± 1,34*	3,23 ± 1,16
MA végszisztolés kerület (cm)	7,06 ± 1,23	7,82 ± 1,25*	6,84 ± 1,14
MA frakcionális area változása (%)	51,5 ± 15,5	44,7 ± 14,8*	53,6 ± 15,1
MA frakcionális rövidülés (%)	34,0 ± 15,1	29,7 ± 12,2*	35,2 ± 15,6

*p<0,05 *versus* BK-EF≥55%
†p = 0,06 *versus* BK-EF≥55%

3DSTE = háromdimenziós speckle-tracking echokardiográfia; BK = bal kamra; EF = ejekciós frakció; MA = mitralis anulus

Megbeszélés

Az echokardiográfos vizsgálatok egyik legfontosabb indikációja a BK szisztolés pumpafunkciójának megítélése, melyre a leggyakrabban alkalmazott paraméter a BK-EF [10]. Ennek oka abban keresendő, hogy számos klinikai vizsgálat igazolta a BK-EF prognosztikus szerepét különböző betegcsoportokban [11]. A BK-EF számos echokardiográfiás módszer segítségével mérhető, beleértve az M-módú, 2D-, 2D speckle-tracking (STE), volumetrikus 3D-echokardiográfiás (RT3DE-) és 3DSTE-eljárásokat [10]. A szakmai irányelvek szerint a jelenleg ajánlott 2D-echokardiográfiás módszer a BK-EF mérésére a módosított Simpson szerinti és az úgynevezett area-length módszerek [9, 10]. Ugyanez a szakmai irányelv azt is megemlíti, hogy a RT3DE-alapú BK-EF-mérés pontos és reprodukálható, és amennyiben elérhető lehetőség, akkor használható [9].

Ismert tény, hogy a 2D-echokardiográfia alulbecsüli a valós MA-átmérőt, amennyiben azt az általunk bemutatott módszertanhoz hasonló, RT3DE és mágnesesrezonancia-vizsgálat (magnetic resonance imaging, MRI) során mért értékekhez hasonlítjuk [12, 13]. A 3D-echokardiogáfiás módszer pontosnak tekinthető, és jól korrelál az MRI-vel mérhető értékekkel [13]. Mivel az MA nem igazi kör alakú képlet, inkább D betűhöz hasonlít, és bizonyos betegségekben torzul, 'gömbölyödik', az MA-átmérőből származtatott paraméterek további torzulást mutathatnak (MA-area, -kerület). Ezen tények ráirányíthatják a figyelmet az echokardiográfiás 3D-képalkotás fontosságára még akkor is, ha a bemutatott módszertan nem veszi számításba az MA 3D-s nyereg alakját, csak annak 2D-be projektált képét.

A 3DSTE egy új, noninvazív diagnosztikus eljárás, mely egyesíti a volumetrikus 3D echokardiográfia és az

STE előnyeit. Egy szívüregről (jelen esetben BK-ról) kreált virtuális 3D-modell segítségével a szívciklusnak megfelelően a BK volumetrikus és strainparaméterei egyidejűleg számíthatók [8]. *Kleijn és mtsai* szerint habár a 3DSTE-vel mért BK-i térfogatok kisebbek az MRI során mértekhez képest, a BK-EF tökéletes egyezést mutat [14]. Igazolást nyert az is, hogy a BK-i térfogatok és a BK-EF mérésében a 3DSTE megbízható [15], és a mért adatok a RT3DE-vel számítottal kicserélhetők [16]. A nemzetközi ajánlások alapján a 2D-echokardiográfia során meghatározott BK-EF határértéke ≥55% [9], míg irodalmi adatok alapján 3D-echokardiográfiával mérve a határérték 47–55% körüli, életkori és nembeli függést is mutat [17]. Irodalmi adatok alapján az is elmondható, hogy az 50% alatti BK-EF csökkentnek tekinthető. A fenti tények figyelembevételével a 3DSTE-vel meghatározott 50–54%-os BK-EF-et borderline, határterületi értéknek tarthatjuk.

A jelen vizsgálatban a BK-EF és az MA morfológiájának és funkciójának összefüggéseit vizsgáltuk. Ebből a célból két populációt hoztunk létre, az elsőben határérték 50–54%-os BK-EF volt mérhető 3DSTE segítségével, míg a másodikban a BK-EF nagyobb-egyenlő volt 55%-nál. Eredményeink azt igazolták, hogy a határérték-BK-EF-fel bíró esetekben a szívciklustól függetlenül az MA tágabb, és funkciója rosszabb a 3DSTE-vel mérve normális tartományba eső BK-EF-fel bíró esetekhez képest. Ez az eredmény rávilágít arra a tényre, hogy a BK-funkció normalitásának határán mozgó esetekben már korán megfigyelhető az MA remodellációja. Ennek oka a a szívüregi volumetrikus változások mellett a BK, és feltételezhetően a BP funkcionális eltéréseiben is keresendő, ahogy ezt a szubklinikusan alacsonyabb BK-i globális LS csökkenése is jelzi. Saját anyagunkban a határérték-BK-EF-et mutató betegekben további vizsgálatok elvégzését tartottuk szükségesnek az esetleges szubklinikus eltérések okának felderítése céljából. A fentieknek megfelelően további vizsgálatok szükségesek a fenti fiziológiai tények még komplexebb megértéséhez.

A vizsgálat korlátai

Vizsgálatunk elvégzésekor számos limitációs tényező merült fel, melyek közül az alábbiakat tartjuk a legfontosabbnak:

- A 3DSTE olyan új klinikai eljárás, mely jelenleg még széles körben nem terjedt el. A jelenleg rendelkezésre álló eszközök mellett a 2D-echokardiográfiához képest csökkent térbeli és időbeli felbontóképességgel rendelkezik, ami eredményeinket befolyásolhatta [8, 10].
- A jelen vizsgálat nem tekintette céljának a 3DSTE-vel mért BK-i volumetrikus adatok és BK-EF-mérés validálását [10, 18]. Fontos tudni, hogy direkt validációs vizsgálat eddig még nem történt, mely a 2D-echokardiográfiával (például Teichholz- vagy Simpson-módszerrel) számított BK-i volumeneket és EF-et a 3DSTE-vel számítottéhoz hasonlította volna. Eddig validációs vizsgálatok cardialis MRI-vel [14] és RT3DE-vel [16] szemben történtek.
- Saját tapasztalataink alapján a jelenleg elérhető 3DSTE-rendszerrel átlagosan 6–8%-kal alacsonyabb BK-EF mérhető a 2D-echokardiográfiás Teichholz-féle módszerrel számítotthoz képest. Ennek megfelelően a 3DSTE-vel mért 50–54%-os BK-EF-csoportba sorolt eseteink 2D-echokardiográfiával mért BK-EF-je valamennyi esetben 55% felett volt.
- 3DSTE segítségével nemcsak a BK, de a pitvarok volumetrikus és strainadatai is korrekt módon mérhetők a szívciklusnak megfelelően, ezek analízisét azonban ebben a tudományos műben nem vizsgáltuk [18].
- Az alcsoportok analízise során különbségeket találtunk az életkor és a nembeli eloszlásban, melyek eredményeinket befolyásolhatták.

Következtetések

A 3DSTE-vel meghatározott határérték-BK-EF együtt jár az MA tágulásával és funkciójának romlásával.

Anyagi támogatás: A közlemény megírása anyagi támogatásban nem részesült.

Szerzői munkamegosztás: K. Zs., K. Á.: A hipotézisek kidolgozása, vizsgálat lefolytatása, statisztikai elemzések, a kézirat megszövegezése. D. P., K. A.: A vizsgálatok lefolytatása. L. Cs., A. Z., F. T.: A kézirat megszövegezése. N. A.: A hipotézisek kidolgozása, a kézirat megszövegezése. A cikk végleges változatát valamennyi szerző elolvasta és jóváhagyta.

Érdekeltségek: A szerzőknek nincsenek érdekeltségeik.

Irodalom

[1] Dal-Bianco JP, Levine RA. Anatomy of the mitral valve apparatus – role of 2D and 3D echocardiography. Cardiol Clin. 2013; 31: 151–164.
[2] Nemes A, Geleijnse ML, Soliman OI, et al. Evaluation of the mitral valve by transthoracic real-time three-dimensional echocardiography. [A mitralis billentyű vizsgálata transthoracalis real-time háromdimenziós echokardiográfiával.] Orv Hetil. 2010; 151: 854–863. [Hungarian]
[3] Silbiger JJ. Anatomy, mechanics, and pathophysiology of the mitral annulus. Am Heart J. 2012; 164: 163–176.
[4] Apor A, Nagy AI, Kovács A, et al. Three-dimensional dynamic morphology of the mitral valve in different forms of mitral valve prolapse – potential implications for annuloplasty ring selection. Cardiovasc Ultrasound 2016; 14: 32.
[5] Antoine C, Mantovani F, Benfari G, et al. Pathophysiology of degenerative mitral regurgitation: new 3-dimensional imaging insights. Circ Cardiovasc Imaging 2018; 11: e005971.
[6] Nemes A, Anwar AM, Caliskan K, et al. Non-compaction cardiomyopathy is associated with mitral annulus enlargement and functional impairment: a real-time three-dimensional echocardiographic study. J Heart Valve Dis. 2008; 17: 31–35.

[7] Nemes A, Földeák D, Kormányos Á, et al. Cardiac amyloidosis associated with enlargement and functional impairment of the mitral annulus: insights from the three-dimensional speckle tracking echocardiographic MAGYAR-Path Study. J Heart Valve Dis. 2017; 26: 304–308.
[8] Nemes A, Kalapos A, Domsik P, et al. Three-dimensional speckle-tracking echocardiography – a further step in non-invasive three-dimensional cardiac imaging. [Háromdimenziós speckle-tracking echokardiográfia – egy újabb lépés a noninvazív háromdimenziós kardiális képalkotásban.] Orv Hetil. 2012; 153: 1570–1577. [Hungarian]
[9] Lang RM, Badano LP, Mor-Avi V, et al. Recommendations for cardiac chamber quantification by echocardiography in adults: an update from the American Society of Cardiology and European Association of Cardiovascular Imaging. J Am Soc Echocardiogr. 2015; 28: 1–39.e14.
[10] Nemes A, Forster T. Recent echocardiographic examination of the left ventricle – from M-mode to 3D speckle-tracking imaging. [A bal kamra korszerű echokardiográfiás vizsgálata – az M-módtól a 3D speckle-tracking képalkotásig.] Orv Hetil. 2015; 156: 1723–1740. [Hungarian]
[11] Prastaro M, Pirozzi E, Gaibazzi N, et al. Expert review on the prognostic role of echocardiography after acute myocardial infarction. J Am Soc Echocardiogr. 2017; 30: 431–443.e2.
[12] Anwar AM, Soliman OI, ten Cate FJ, et al. True mitral annulus diameter is underestimated by two-dimensional echocardiography as evidenced by real-time three-dimensional echocardiography and magnetic resonance imaging. Int J Cardiovasc Imaging 2007; 23: 541–547.
[13] Anwar AM, Soliman OI, Nemes A, et al. Assessment of mitral annulus size and function by real-time 3-dimensional echocardiography in cardiomyopathy: comparison with magnetic resonance imaging. J Am Soc Echocardiogr. 2007; 20: 941–948.
[14] Kleijn SA, Brouwer WP, Aly MF, et al. Comparison between three-dimensional speckle-tracking echocardiography and cardiac magnetic resonance imaging for quantification of left ventricular volumes and function. Eur Heart J Cardiovasc Imaging 2012; 13: 834–839.
[15] Kleijn SA, Aly MF, Terwee CB, et al. Reliability of left ventricular volumes and function measurements using three-dimensional speckle tracking echocardiography. Eur Heart J Cardiovasc Imaging 2012; 13: 159–168.
[16] Kleijn SA, Aly MF, Terwee CB, et al. Comparison between direct volumetric and speckle tracking methodologies for left ventricular and left atrial chamber quantification by three-dimensional echocardiography. Am J Cardiol. 2011; 108: 1038–1044.
[17] Wood PW, Choy JB, Nanda NC, et al. Left ventricular ejection fraction and volumes: it depends on the imaging method. Echocardiography 2014; 31: 87–100.
[18] Piros GÁ, Domsik P, Kalapos A, et al. Relationships between right atrial and left ventricular size and function in healthy subjects. Results from the three-dimensional speckle-tracking echocardiographic MAGYAR-Healthy Study. [A jobb pitvar és a bal kamra méretének és funkciójának összefüggései egészségesekben. Eredmények a háromdimenziós speckle-tracking echokardiográfiás MAGYAR-Healthy Tanulmányból.] Orv Hetil. 2015; 156: 972–978. [Hungarian]

(Nemes Attila dr.,
Szeged, Semmelweis u. 8., 6725
e-mail: nemes@in2nd.szote.u-szeged.hu)

„A józan ész nem ajándék, hanem büntetés, mert meg kell küzdened azokkal, akik nem rendelkeznek vele." (Albert Einstein)

Received: 7 October 2018 | Revised: 5 June 2019 | Accepted: 11 June 2019

DOI: 10.1111/echo.14429

Echocardiography WILEY

The mitral annulus in lipedema: Insights from the three-dimensional speckle-tracking echocardiographic MAGYAR-Path Study

Attila Nemes MD, PhD, DSc[1] | Zsolt Kovács MD[2] | Árpád Kormányos MD[1] | Péter Domsik MD, PhD[1] | Anita Kalapos MD, PhD[1] | Györgyike Á. Piros MD, PhD[1] | Lajos Kemény MD, PhD, DSc[3] | Tamás Forster MD, PhD, DSc[1] | Győző Szolnoky MD, PhD[3]

[1]2nd Department of Medicine and Cardiology Centre, Albert Szent-Györgyi Clinical Center, University of Szeged, Szeged, Hungary

[2]Department of Cardiology, Szent Rókus Hospital, Baja, Hungary

[3]Department of Dermatology and Allergology, Albert Szent-Györgyi Clinical Center, University of Szeged, Szeged, Hungary

Correspondence
Attila Nemes, MD, PhD, DSc, FESC, 2nd Department of Medicine and Cardiology Center, Medical Faculty, Albert Szent-Györgyi Clinical Center, University of Szeged, Semmelweis Street 8, P.O. Box 427, H-6725 Szeged, Hungary.
Email: nemes.attila@med.u-szeged.hu

Abstract

Introduction: Lipedema is a barely recognized and poorly diagnosed, but common disease affecting almost exclusively female patients. The pathomechanism of lipedema is not known, and clinically, it is a bilateral, symmetrical, disproportional fatty enlargement of the lower half of the body, the disease does not affect the feet, and the upper extremities are often involved. Since lipedema is associated with increased aortic stiffness and altered left ventricular (LV) rotational mechanics, the present study was designed to compare the size and function of the mitral annulus (MA) between lipedema patients and controls by three-dimensional speckle-tracking echocardiography (3DSTE).

Methods: Twenty-four patients with stage 2 lipedema and 48 age-, gender-, and body mass index-matched healthy control patients were included in the study. Each person from the lipedema and the control groups underwent two-dimensional Doppler echocardiography and 3DSTE.

Results: Significantly enlarged left atrial diameter, LV end-diastolic diameter and volume, and LV end-systolic volume could be detected in lipedema patients as compared to controls. None of the lipedema patients and controls showed ≥grade 1 mitral or tricuspid regurgitation. Dilated end-systolic and end-diastolic MA diameter, area, and perimeter could be demonstrated in lipedema patients as compared to controls, and these changes were accompanied by impaired MA fractional area change at rest. Following 1-hour use of compression stockings, no significant improvement was seen in these parameters.

Conclusions: Lipedema is associated with MA enlargement and functional impairment. The use of compression stockings does not improve these alterations.

KEYWORDS

echocardiography, lipedema, mitral annulus, three-dimensional

1 | INTRODUCTION

Lipedema is a poorly recognized disease with female predominance, and it is characterized by bilateral, symmetrical, disproportional fatty deposits in the lower body and commonly in the upper extremities.[1] It is usually mistaken with obesity or lymphedema. Lipedema is characterized by nonpitting edema, susceptibility to bruising, and tenderness, and it usually does not respond to various dietary approaches. Underlying causes are mostly unknown; however, hormonal influence is strongly suspected.[1] Recent investigation showed increased aortic stiffness and altered left ventricular (LV) rotational mechanics among patients with lipedema.[2,3] The present study was designed to further examine lipedema-associated cardiac implications and to compare MA size and function between lipedema patients and age-, gender-, and body mass index (BMI)-matched healthy controls by three-dimensional speckle-tracking echocardiography (3DSTE). We were also interested in determining whether 1-hour use of medical compression stockings (MCS) has any effect on MA morphology and functional properties.

2 | METHODS

2.1 | Patient population

The present study comprised 24 patients with stage 2 lipedema without known cardiovascular symptoms. Forty-eight age-, gender-, and BMI-matched healthy volunteers were used as a control group. All lipedema patients and matched controls have undergone two-dimensional (2D) Doppler echocardiography and 3DSTE. This particular study is a part of the MAGYAR-Path Study (Motion Analysis of the heart and Great vessels bY three-dimensionAl speckle-tRacking echocardiography in Pathological cases), which has been organized at the University of Szeged to explore diagnostic and prognostic value of 3DSTE-derived parameters in different pathological states among others ("Magyar" means "Hungarian" in Hungarian language). Ethical guidelines of the 1975 Declaration of Helsinki were applied, and all patients and controls gave informed consent. The institution's human research committee approved the study.

2.2 | Two-dimensional Doppler and speckle-tracking echocardiography

Toshiba Artida™ ultrasound system (Toshiba Medical Systems, Tokyo, Japan) with a PST-30SBP (1–5 MHz) phased-array transducer was used for echocardiographic examinations. Assessment of 2D Doppler echocardiographic studies followed the most recent guidelines.[4] Valvular regurgitations were visually assessed by color Doppler echocardiography. Early and late mitral inflow E and A were measured by pulsed-Doppler echocardiography. To assess LV function, 2D speckle-tracking echocardiographic evaluation of peak systolic LV longitudinal strain (LS) and LS rate was measured in each subject in apical four-chamber view (AP4CH).

2.3 | Three-dimensional speckle-tracking echocardiography

The same Toshiba Artida™ echocardiography machine (Toshiba Medical Systems, Tokyo, Japan) using a PST-25SX matrix-array transducer from apical window during a single breath-hold and constant RR interval on ECG was used for acquisition of six wedge-shaped subvolumes.[5] A full-volume, called as "pyramidal" 3D dataset, was then created by the software in which 3D Wall Motion Tracking software version 2.7 (Toshiba Medical Systems, Tokyo, Japan) was used for 3D analysis. The aim of this analysis was to generate a virtual 3D cast of the LV with the help of automatically selected apical two (AP2CH) and AP4CH views and 3 short-axis views at basal, midventricular, and apical LV levels at end-diastole. Then, image planes were optimized on the endpoints of the MA on AP2CH and AP4CH views and the following measurements were performed on the C7 short-axis view[6] (Figure 1):

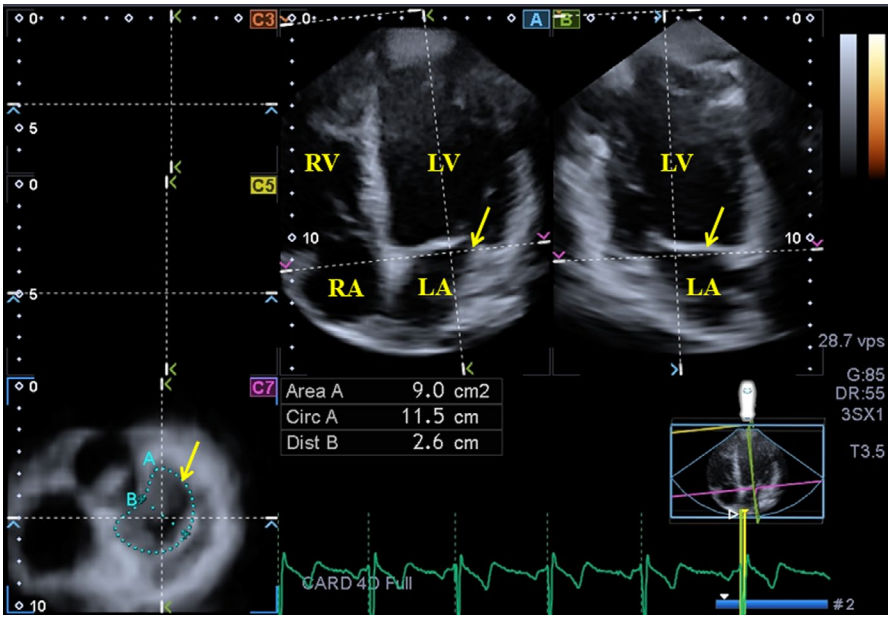

FIGURE 1 Images from three-dimensional full-volume dataset showing mitral annulus in a patient with lipedema: (A) apical four-chamber view, (B) apical two-chamber view and a cross-sectional view at the level of the mitral annulus (C7) optimized in apical four- and two-chamber views. The yellow arrow represents the mitral annular plane on the long- (A, B) and short-axis (C7) images. LA = left atrium; LV = left ventricle; RA = right atrium; RV = right ventricle

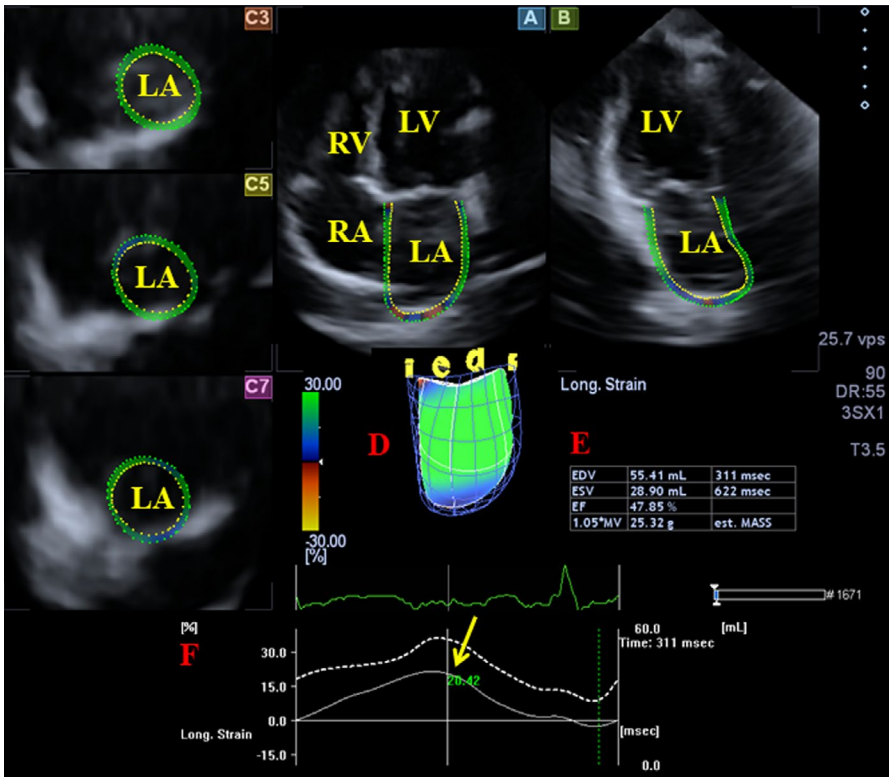

FIGURE 2 Three-dimensional (3D) speckle-tracking echocardiographic evaluation of the left atrium (LA) is displayed in a patient with lipedema. Apical four-chamber (A) and two-chamber (B) views, short-axis views at basal (C3), midatrial (C5), and superior LA level (C7) are shown together with a 3D cast of the LA (D) and calculated volumetric LA data (E). Time—global LA volume change (dashed line) and time—global LA longitudinal strain curves (white line) are also demonstrated (F). The yellow arrow represents global peak LA-LS featuring LA reservoir function. EDV = end-diastolic volume; EF = ejection fraction; ESV = end-systolic volume; LA = left atrium; LV = left ventricle; RA = right atrium; RV = right ventricle

- For the evaluation of MA morphology, MA diameter (MAD) defined as the perpendicular line drawn from the peak of MA curvature to the middle of the straight MA border was measured both at end-diastole and end-systole. MA area (MAA) and perimeter (MAP) were assessed by planimetry.[6-8]
- Using MAD and MAA data, MA functional properties were assessed: MA fractional shortening (MAFS) = [end-diastolic MAD − end-systolic MAD]/end-diastolic MAD × 100 and MA fractional area change (MAFAC) = [end-diastolic MAA − end-systolic MAA]/end-diastolic MAA × 100.[6-8]

To create a 3D virtual LA model, the reader set markers on orthogonal AP2CH and AP4CH views (Figure 2). Following detection of the edge of the septum-MA ring, markers were set in counterclockwise direction around the LA to the edge of the lateral wall-MA ring. LA appendage and pulmonary veins were excluded from the LA cavity. Then, LA was automatically reconstructed and tracked in 3D space throughout the entire cardiac cycle. Using LA 3D cast, peak LA longitudinal strain (LS) characterizing LA reservoir function was calculated for each subject.

2.4 | Experimental protocol

First, patients underwent 2D echocardiography and consecutively 3DSTE. After the echocardiographic measurements, the patients donned their MCSs and applied them for 60 minutes.[3] Postprocedural echocardiography was scheduled at the end of the 60-minute MCS application before the patients took off the MCSs. Patients were not allowed to do any kind of physical exercise or to consume any meal or beverage until the second echocardiographic procedure had been done. During the 60-minute stocking application period, they could sit with straight

TABLE 1 Baseline demographic and two-dimensional echocardiographic data in patients with lipedema and controls

	Controls	Lipedema patients
n	48	24
Risk factors		
Age (y)	41.0 ± 14.0	43.4 ± 11.7
Male gender (%)	0 (0)	0 (0)
Hypertension (%)	0 (0)	0 (0)
Diabetes mellitus (%)	0 (0)	0 (0)
Hypercholesterolemia (%)	0 (0)	0 (0)
Two-dimensional echocardiography		
LA diameter (mm)	35.3 ± 4.2	40.1 ± 4.3*
LV end-diastolic diameter (mm)	46.7 ± 3.6	50.3 ± 3.4*
LV end-diastolic volume (mL)	97.4 ± 21.2	121.4 ± 18.7*
LV end-systolic diameter (mm)	31.3 ± 3.4	31.5 ± 2.7
LV end-systolic volume (mL)	33.4 ± 8.3	40.2 ± 8.4*
Interventricular septum (mm)	8.8 ± 1.6	8.6 ± 0.9
LV posterior wall (mm)	9.1 ± 1.8	8.6 ± 0.9
LV ejection fraction (%)	65.4 ± 4.3	67.4 ± 3.4
E/A	1.3 ± 0.4	1.1 ± 0.3

Abbreviations: E and A = early- and late-diastolic transmitral flow velocities; LA = left atrial; LV = left ventricular.
*$P < 0.05$ vs Controls.

TABLE 2 Comparison of three-dimensional speckle-tracking echocardiography-derived mitral annular morphological and functional parameters between patients with lipedema and controls

	Controls (n = 48)	Lipedema patients at rest (n = 24)	Lipedema patients 1 h after the use of MCS (n = 24)
Morphological parameters			
End-diastolic MA diameter (MAD-D) (cm)	2.42 ± 0.39	2.54 ± 0.51	2.68 ± 0.56*
End-diastolic MA area (MAA-D) (cm^2)	7.33 ± 2.21	8.45 ± 2.43*	9.01 ± 2.77*
End-diastolic MA perimeter (MAP-D) (cm)	10.17 ± 1.54	10.92 ± 1.46*	11.24 ± 1.73*
End-systolic MA diameter (MAD-S) (cm)	1.55 ± 0.39	1.75 ± 0.46*	1.82 ± 0.35*
End-systolic MA area (MAA-S) (cm^2)	3.21 ± 1.12	4.30 ± 1.72*	4.41 ± 1.60*
End-systolic MA perimeter (MAP-S) (cm)	6.75 ± 1.10	7.84 ± 1.40*	8.04 ± 1.38*
Functional parameters			
MAFAC (%)	55.39 ± 14.01	47.78 ± 18.18*	49.08 ± 16.24
MAFS (%)	34.57 ± 15.01	30.16 ± 14.07	30.57 ± 12.53

Abbreviations: MA = mitral annulus; MAFAC = mitral annular fractional area change; MAFS = mitral annular fractional shortening; MCS = medical compression stocking.
*$P < 0.05$ vs Controls.

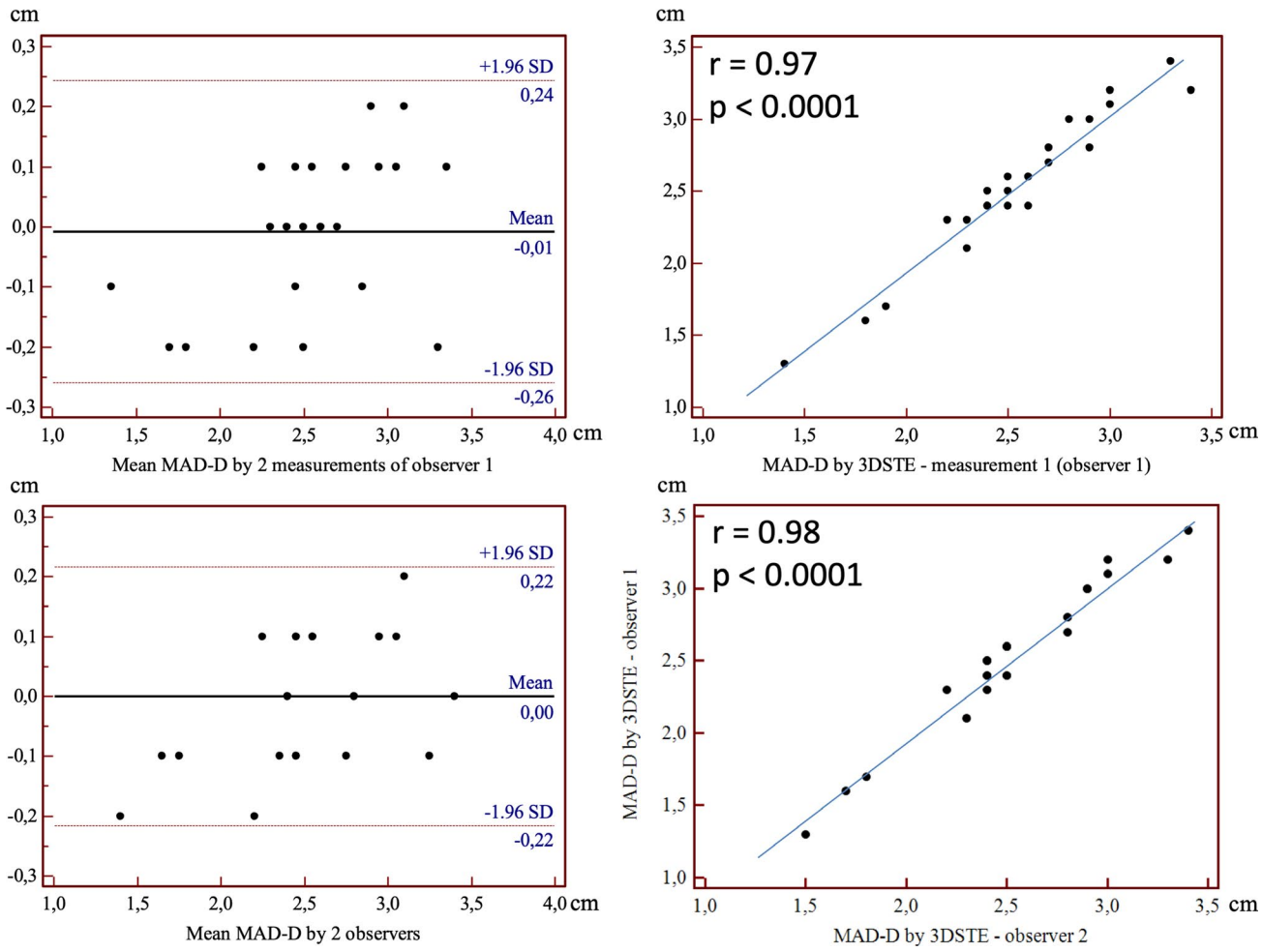

FIGURE 3 Intra-observer (upper graphs) and inter-observer (lower graphs) agreements and correlations for measuring end-diastolic mitral annular diameter (MAD-D) by three-dimensional speckle-tracking echocardiography (3DSTE) are presented

legs or stand. Room temperature and relative humidity were stable at 21–22°C and 45%–50%, respectively. Each garment was used for the first time, and our physiotherapist colleagues assisted donning and doffing, if needed. Participants were informed precisely about the study protocol when the study started.

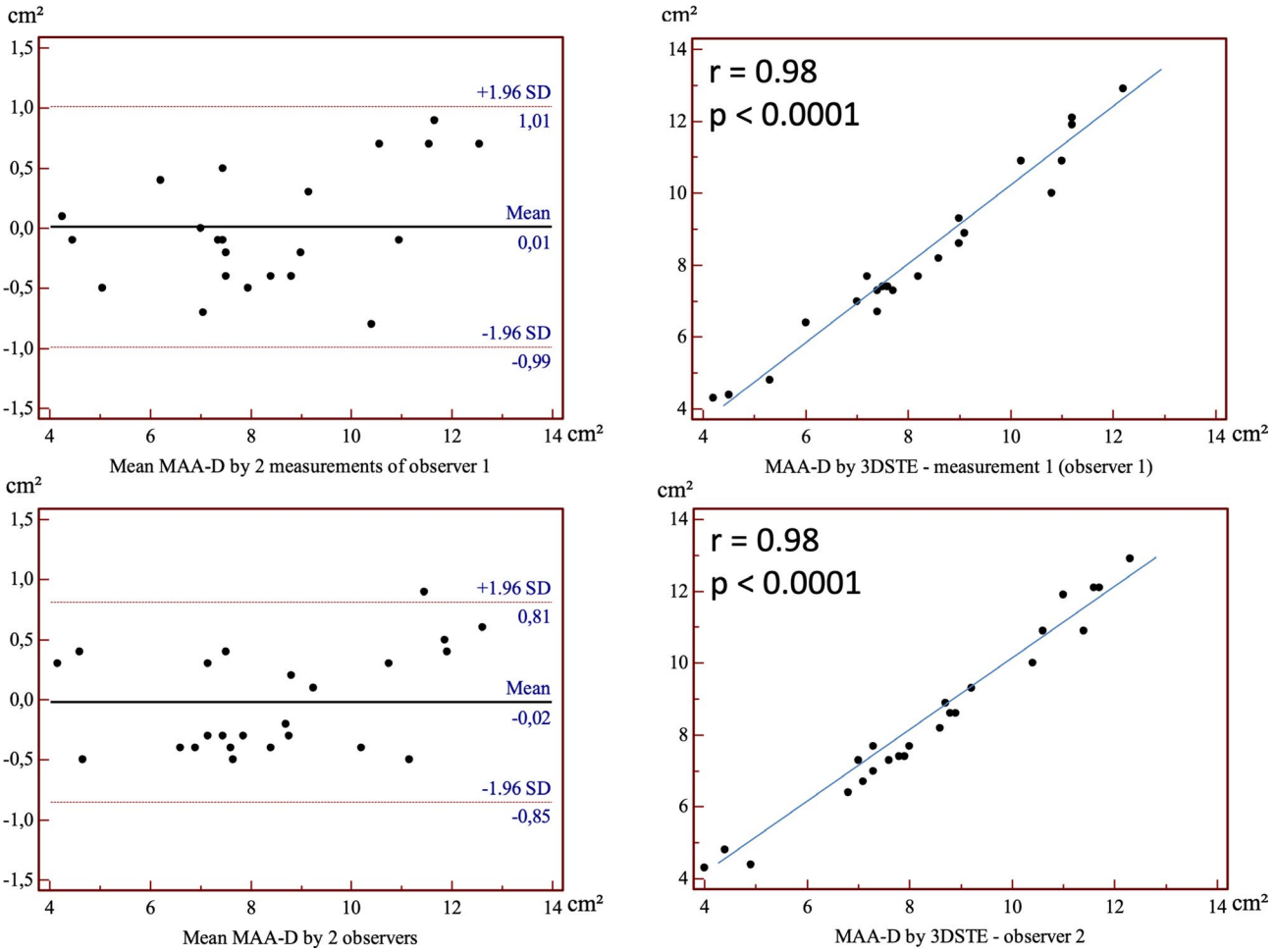

FIGURE 4 Intra-observer (upper graphs) and inter-observer (lower graphs) agreements and correlations for measuring end-diastolic mitral annular area (MAA-D) by three-dimensional speckle-tracking echocardiography (3DSTE) are presented

2.5 | Experimental compression garments

Bauerfeind VenoTrain CuraFlow black-colored flat-knitted ccl 2 (23–32 mm Hg) (Bauerfeind) stocking consisting of 73% polyamide and 27% elastane was used. Interface pressure measurement between skin and compression material using Picopress device (Microlab Elettronica) at B1 point[9] in standing position revealed a mean pressure of 22.79 ± 3.75 mm Hg among patients with lipedema.

2.6 | Statistical analysis

Categorical data were expressed in frequencies and percentage, while continuous data were presented as mean ± standard deviation. Difference was considered to be statistical significant if *P* proved to be <0.05. All tests were two-sided. Kolmogorov–Smirnov test was used for normality of distribution of datasets and was analyzed by Student's *t* test. Non-normally distributed datasets were tested with Mann–Whitney–Wilcoxon test. Fisher's exact test was used for categorical variables. Inter- and intra-observer variability of measurements of MAD, MAA, and MAP was tested in all lipedema patients at rest at end-diastole and end-systole. Agreements were verified using the Bland–Altman method, and Pearson's coefficient was calculated for intra-observer and inter-observer correlations. RStudio was used for statistical analysis (RStudio Team (2015) RStudio: Integrated Development for R. RStudio, Inc). MATLAB version 8.6 software package was used for data analysis (The MathWorks Inc 2015). Medcalc was used for reproducibility measurements (Medcalc).

3 | RESULTS

3.1 | Demographic and two-dimensional echocardiographic data

Enlarged left atrial diameter, LV end-diastolic diameter and volume and LV end-systolic volume respecting cardiac cycle could be demonstrated with preserved LV ejection fraction in lipedema patients as compared to controls (Table 1). None of the lipedema patients and controls showed ≥grade 1 mitral or tricuspid regurgitation. Higher mitral inflow early-diastolic E (77.9 ± 17.4 cm vs 88.2 ± 17.7 cm/s, $P < 0.05$) and late-diastolic A (67.0 ± 17.4 cm/s vs 80.0 ± 16.8 cm/s, $P < 0.05$) velocities could be demonstrated in lipedema patients as compared to controls, which did not change significantly following the

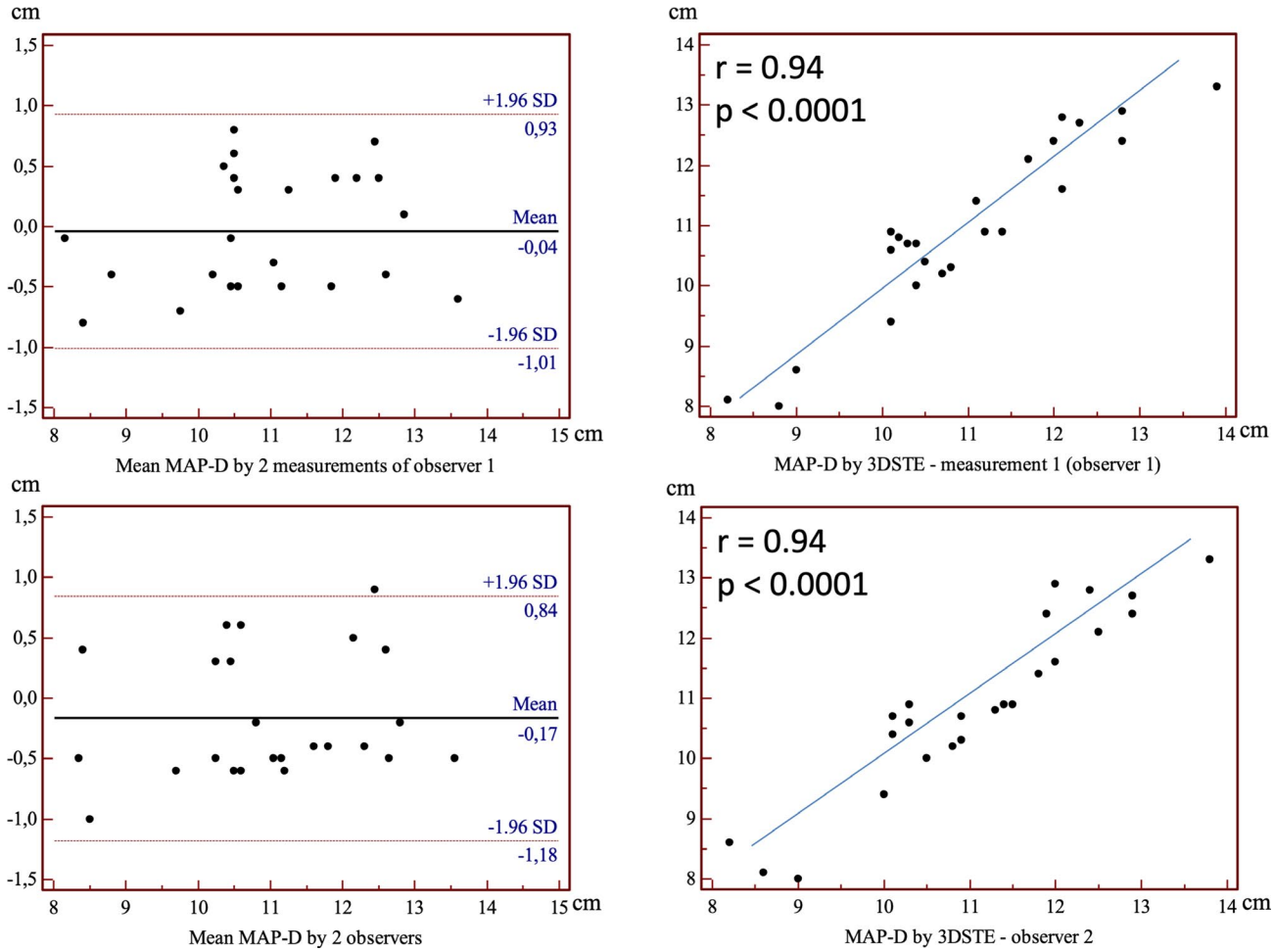

FIGURE 5 Intra-observer (upper graphs) and inter-observer (lower graphs) agreements and correlations for measuring end-diastolic mitral annular perimeter (MAP-D) by three-dimensional speckle-tracking echocardiography (3DSTE) are presented

use of compression stockings (85.2 ± 16.4 cm/s and 77.1 ± 15.9 cm, $P = 0.62$ and $P = 0.56$, respectively). 2D speckle-tracking echocardiography-derived peak systolic LV-LS (−17.8 ± 1.2%. vs −20.5 ± 0.3%, $P < 0.05$) and LV-LS rate (0.79 ± 0.03 1/s vs 0.90 ± 0.04 1/s, $P < 0.05$) proved to be reduced in lipedema patients as compared to controls.

3.2 | Three-dimensional speckle-tracking echocardiography

Dilated end-systolic and end-diastolic MAD, MAA, and MAP could be demonstrated in lipedema patients as compared to matched controls which were accompanied with impaired MAFAC at rest. Following 1-hour use of MCS, these parameters did not show any significant improvement (Table 2).

3DSTE-derived peak global LA-LS characterizing LA reservoir function proved to be 27.6 ± 8.5% at rest and 29.8 ± 7.5% 1 hour after the use of MCS in lipedema patients ($P = 0.14$). At rest, significant correlations could be demonstrated between peak LA-LS and end-systolic MAD ($r = -0.48$, $P = 0.02$), MAA ($r = -0.49$, $P = 0.02$), and MAP ($r = -0.47$, $P = 0.02$) and functional parameters MAFAC ($r = 0.50$, $P = 0.01$) and MAFS ($r = 0.52$, $P = 0.01$). End-diastolic MA parameters did not show any correlations (MAD [$r = -0.07$, $P = 0.75$], MAA [$r = -0.03$, $P = 0.84$], and MAP [$r = -0.02$, $P = 0.91$]). One hour after the use of MCS, only MAFAC ($r = 0.47$, $P = 0.02$) and MAFS ($r = 0.50$, $P = 0.01$) correlated with LA-LS, and none of end-systolic (MAD [$r = -0.35$, $P = 0.09$], MAA [$r = -0.33$, $P = 0.12$], and MAP [$r = -0.36$, $P = 0.08$]) and end-diastolic (MAD [$r = 0.15$, $P = 0.48$], MAA [$r = 0.20$, $P = 0.35$], and MAP [$r = 0.18$, $P = 0.40$]) morphological MA parameters correlated with it.

3DSTE-derived peak LA-RS was −19.8 ± 8.8% at rest and −17.5 ± 6.5% 1 hour after the use of MCS ($P = 0.30$). LA-RS did not correlate with end-systolic and end-diastolic MAD ($r = 0.01$, $P = 0.96$ and $r = 0.02$, $P = 0.92$, respectively), MAA ($r = -0.03$, $P = 0.91$ and $r = 0.25$, $P = 0.24$, respectively), MAP ($r = -0.04$, $P = 0.86$ and $r = 0.26$, $P = 0.22$, respectively), MAFAC ($r = 0.25$, $P = 0.24$), and MAFS ($r = -0.03$, $P = 0.90$) at rest. Similarly, significant correlations could not be detected between LA-RS and end-systolic and end-diastolic MAD ($r = 0.18$, $P = 0.40$ and $r = 0.07$, $P = 0.75$, respectively), MAA ($r = 0.18$, $P = 0.40$ and $r = 0.04$, $P = 0.85$, respectively), MAP ($r = 0.21$, $P = 0.32$ and $r = 0.09$, $P = 0.68$, respectively), MAFAC ($r = -0.16$, $P = 0.46$), and MAFS ($r = -0.11$, $P = 0.61$) 1 hour after the use of MCS.

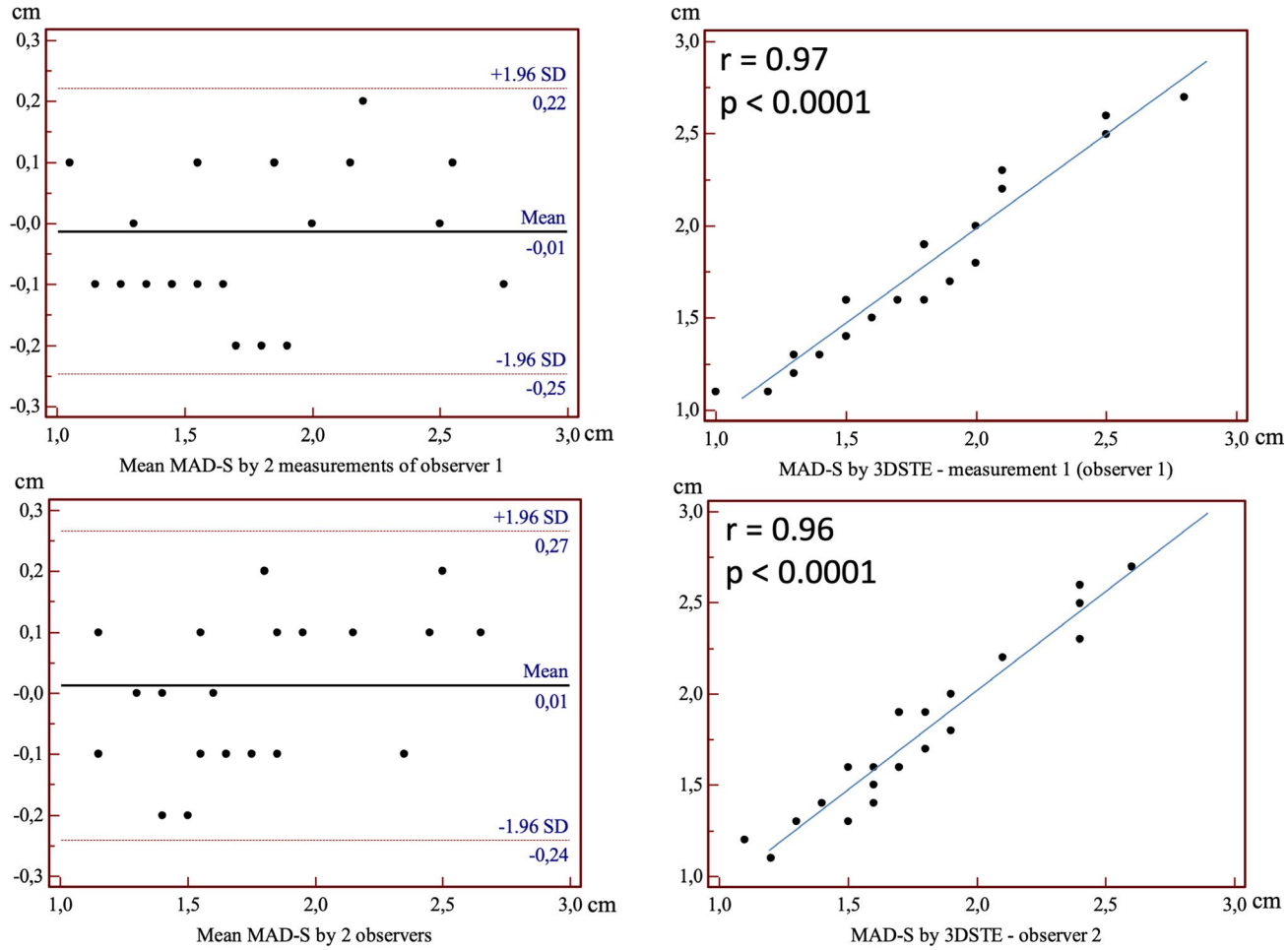

FIGURE 6 Intra-observer (upper graphs) and inter-observer (lower graphs) agreements and correlations for measuring end-systolic mitral annular diameter (MAD-S) by three-dimensional speckle-tracking echocardiography (3DSTE) are presented

3DSTE-derived peak LA-CS was found to be 32.8 ± 10.6% at rest and 34.2 ± 15.9% 1 hour after the use of MCS (P = 0.61). Resting LA-CS did not show correlations with end-systolic and end-diastolic MAD (r = −0.33, P = 0.12 and r = −0.21, P = 0.33, respectively), MAA (r = −0.24, P = 0.25 and r = −0.03, P = 0.89, respectively), MAP (r = −0.25, P = 0.25 and r = −0.07, P = 0.73, respectively), MAFAC (r = 0.23, P = 0.28), and MAFS (r = 0.13, P = 0.56). One hour after the use of MCS, LA-CS correlated with end-systolic MAA (r = −0.48, P = 0.02) and end-systolic and end-diastolic MAP (r = −0.52, P = 0.009 and r = −0.48, P = 0.02, respectively). End-systolic and end-diastolic MAD (r = −0.38, P = 0.07 and r = −0.21, P = 0.32, respectively) and end-diastolic MAA (r = −0.39, P = 0.06) did not correlate with LA-CS.

3.3 | Reproducibility measurements

At rest, the mean ± standard deviation differences in values obtained by two observers for the measurements of end-diastolic MAD, MAA, and MAP were 0.00 ± 0.22 cm, −0.02 ± 0.83 cm^2, and −0.17 ± 1.01 cm, respectively, with a correlation coefficient between these independent measurements of 0.98 (P < 0.0001), 0.98 (P < 0.0001), and 0.94 (P < 0.0001), respectively (inter-observer variability; Figures 3, 4, and 5). At rest, the mean ± standard deviation differences in values obtained by 2 measurements of observer 1 proved to be −0.01 ± 0.25 cm, 0.01 ± 1.00 cm^2, and −0.04 ± 0.97 cm, respectively, with a correlation coefficient between these independent measurements of 0.97 (P < 0.0001), 0.98 (P < 0.0001), and 0.94 (P < 0.0001), respectively (intra-observer variability; Figures 3, 4, and 5).

The same parameters for end-systolic MAD, MAA and MAP were 0.01 ± 0.25 cm, −0.05 ± 0.42 cm^2, and 0.06 ± 0.47 cm with correlation coefficients of 0.96 (P < 0.0001), 0.99 (P < 0.0001), and 0.99 (P < 0.0001), respectively (inter-observer variability; Figures 6, 7, and 8). The same values for 2 measurements of observer 1 proved to be −0.01 ± 0.23 cm, −0.02 ± 0.37 cm^2, and 0.04 ± 0.56 cm, respectively, with correlation coefficients between these independent measurements of 0.97 (P < 0.0001), 0.99 (P < 0.0001), and 0.98 (P < 0.0001), respectively (intra-observer variability; Figures 6, 7, and 8).

4 | DISCUSSION

To the best of the authors' knowledge, this is the first time to assess MA morphology and function in lipedema. Moreover, the effects of lower body compression on MA size and function have not been

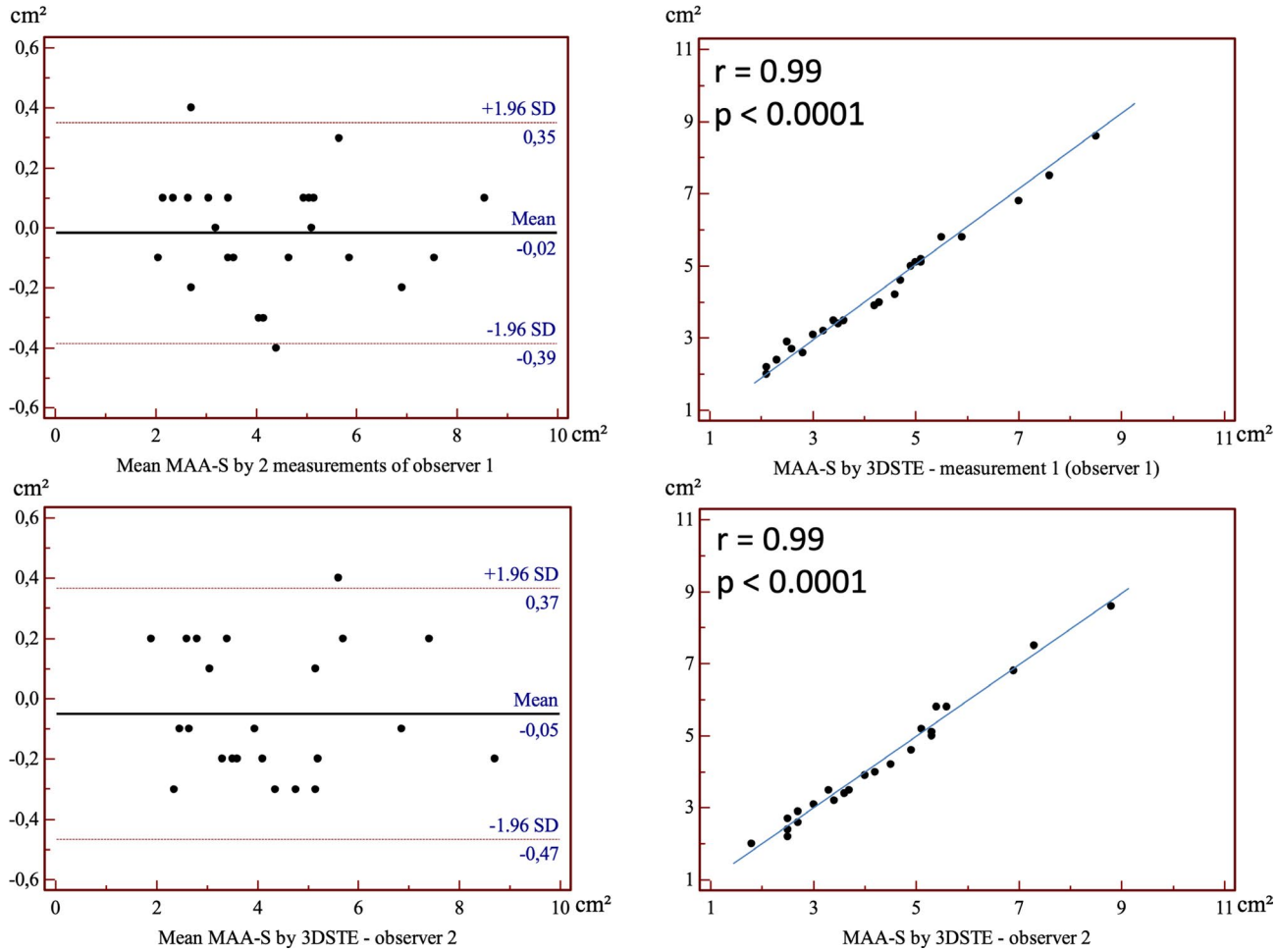

FIGURE 7 Intra-observer (upper graphs) and inter-observer (lower graphs) agreements and correlations for measuring end-systolic mitral annular area (MAA-S) by three-dimensional speckle-tracking echocardiography (3DSTE) are presented

assessed yet. In spite of the absence of valvular regurgitations and stenosis, LV dysfunction, dilated MA parameters and reduced MA functional properties could be demonstrated in lipedema patients as compared to those of controls. These MA morphological and functional alterations showed correlations with LA reservoir function. However, the use of MCS does not have any beneficial effects on these alterations.

Lipedema is a barely known bilateral, symmetrical, disproportional fatty edema which is usually mistaken by obesity or primary or secondary lymphedema. It almost always affects women with a common familial accumulation and fails to respond to standard dietary approaches, but the pathomechanism is still not known. Clinically, lipedema is characterized by nonpitting edema, susceptibility to bruising, and spontaneous or minor trauma-induced pain. The limited number of information is available about lipedema-related cardiac abnormalities. Lipedema patients were found to have increased aortic stiffness and notably altered left ventricular rotational mechanics.[2,3] These results gave rise for further investigations regarding lipedematous cardiovascular implications; therefore, we focused on MA morphology and function. The saddle-shaped MA is an essential part of the mitral valve, and it is a fibrous ring that represents an anatomical junction between the LV and LA. Its shape and size change throughout the cardiac cycle.[10] Similarly to the present findings, MA dilation and functional impairment could be demonstrated in dilated[7] and noncompaction cardiomyopathy[8] and cardiac amyloidosis.[6] Our results could be theoretically explained by deformation abnormalities of the left heart chambers due to increased fluid accumulation capacity of the vascularized lipedematous fatty tissue and interlobular septae.[11] However, the role of increased number of noncardiomyocytes with mesenchymal cells[12] and subclinical epicardial fat deposition of the heart could not be excluded either. Based on the present results, LA and LV dilation and functional impairment could be detected as indirect signs of these alterations.[3] Furthermore, direct infiltration of the fibrous annulus of the mitral valve by lipedematous tissue could not be excluded either. These alterations could lead to further morphological and functional impairment of the heart chambers and MA acting as a vicious circle theoretically leading to earlier development of symptoms in lipedema.

At this moment, limited information is available not only about alterations in MA morphology and function in lipedema, but also

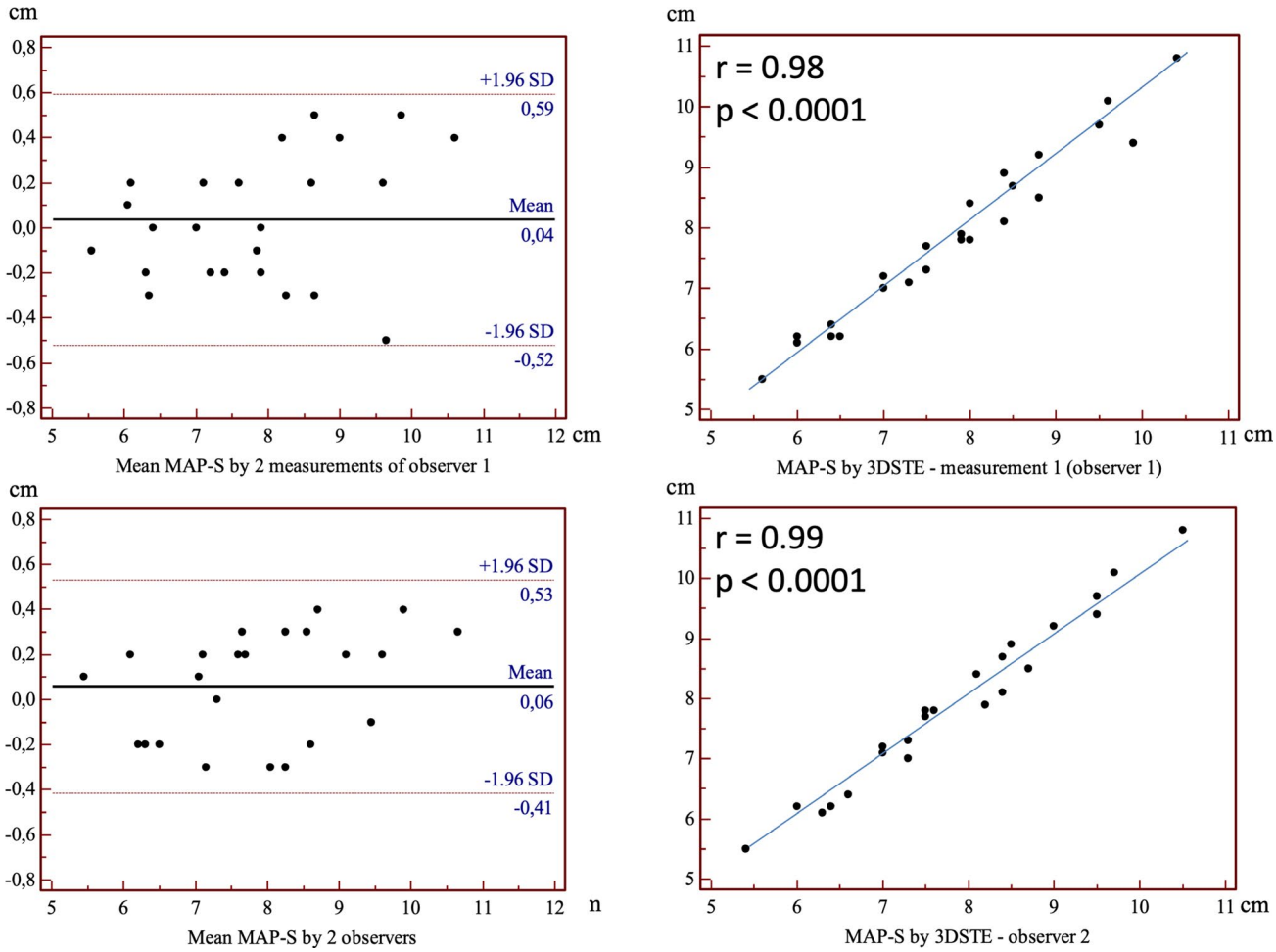

FIGURE 8 Intra-observer (upper graphs) and inter-observer (lower graphs) agreements and correlations for measuring end-systolic mitral annular perimeter (MAP-S) by three-dimensional speckle-tracking echocardiography (3DSTE) are presented

about changes during the progression of the disease. Therefore, exact guideline for its periodic evaluation is not available, but based on the results, annual follow-up could be suggested. Moreover, further diagnostic and prognostic studies are warranted to examine MA-related LV and LA morphological and functional alterations as well.

4.1 | Limitation section

Only projection of the MA to a selected 2D plane could be assessed by the presented method, not the real 3D shape which could be considered as an important limitation of this study. Although 3DSTE is validated for LV and LA volumetric and strain assessments, it was not aimed to be assessed in this study.

5 | CONCLUSIONS

Lipedema is associated with MA enlargement and functional impairment. The use of compression stockings does not improve these alterations.

CONFLICT OF INTEREST

The study was supported by the International Phlebology Union (UIP)—Bauerfeind Award 2015–2017.

ORCID

Attila Nemes https://orcid.org/0000-0002-7570-6214

REFERENCES

1. Lee BB, Andrade M, Antignani PL, et al. International Union of Phlebology. Diagnosis and treatment of primary lymphedema. Consensus document of the International Union of Phlebology (IUP)-2013. *Int Angiol*. 2013;32:541–574.
2. Szolnoky G, Nemes A, Gavallér H, Forster T, Kemény L. Lipedema is associated with increased aortic stiffness. *Lymphology*. 2012;45:71–79.
3. Nemes A, Kormányos A, Domsik P, et al. Left ventricular rotational mechanics differ between lipedema and lymphedema: Insights from the three-dimensional speckle-tracking echocardiographic MAGYAR-Path Study. *Lymphology*. 2018;51:102–108.
4. Lang RM, Badano LP, Mor-Avi V, et al. Recommendations for cardiac chamber quantification by echocardiography in adults: an update

from the American Society of Echocardiography and the European Association of Cardiovascular Imaging. *Eur Heart J Cardiovasc Imaging*. 2015;16:233–271.
5. Nemes A, Kalapos A, Domsik P, Forster T. Three-dimensional speckle-tracking echocardiography – a further step in non-invasive three-dimensional cardiac imaging. *Orv Hetil*. 2012;153:1570–1577.
6. Nemes A, Földeák D, Kormányos Á, et al. Cardiac amyloidosis associated with enlargement and functional impairment of the mitral annulus: Insights from the three-dimensional speckle-tracking echocardiographic MAGYAR-Path Study. *J Heart Valve Dis*. 2017;26:304–308.
7. Anwar AM, Soliman O, Nemes A, et al. Assessment of mitral annulus size and function by real-time 3-dimensional echocardiography in cardiomyopathy: comparison with magnetic resonance imaging. *J Am Soc Echocardiogr*. 2007;20:941–948.
8. Nemes A, Anwar AM, Caliskan K, et al. Non-compaction cardiomyopathy is associated with mitral annulus enlargement and functional impairment: a real-time three-dimensional echocardiographic study. *J Heart Valve Dis*. 2008;17:31–35.
9. Partsch H, Mosti G. Comparison of three portable instruments to measure compression pressure. *Int Angiol*. 2010;29:426–430.
10. Chassagne F, Helouin-Desenne C, Molimard J, Convert R, Badel P, Giraux P. Superimposition of elastic and nonelastic compression bandages. *J Vasc Surg Venous Lymphat Disord*. 2017;5:851–858.
11. Silbiger JJ. Anatomy, mechanics, and pathophysiology of the mitral annulus. *Am Heart J*. 2012;164:163–176.
12. Forner-Cordero I, Szolnoky G, Forner-Cordero A, Kemény L. Lipedema: an overview of its clinical manifestations, diagnosis and treatment of the disproportional fatty deposition syndrome – systematic review. *Clin Obes*. 2012;2:86–95.
13. Varga I, Kyselovič J, Galfiova P, Danisovic L. The non-cardiomyocyte cells of the heart. Their possible roles in exercise-induced cardiac regeneration and remodeling. *Adv Exp Med Biol*. 2017;999:117–136.

How to cite this article: Nemes A, Kovács Z, Kormányos Á, et al. The mitral annulus in lipedema: Insights from the three-dimensional speckle-tracking echocardiographic MAGYAR-Path Study. *Echocardiography*. 2019;36:1482–1491. https://doi.org/10.1111/echo.14429

Original Article

Mitral annulus is enlarged and functionally impaired in adult patients with repaired tetralogy of Fallot as assessed by three-dimensional speckle-tracking echocardiography—results from the CSONGRAD Registry and MAGYAR-Path Study

Attila Nemes[1], Árpád Kormányos[1], Kálmán Havasi[1], Zsolt Kovács[2], Péter Domsik[1], Anita Kalapos[1], István Hartyánszky[1], Nóra Ambrus[1], Tamás Forster[1]

[1]2nd Department of Medicine and Cardiology Centre, Medical Faculty, Albert Szent-Györgyi Clinical Center, University of Szeged, Szeged, Hungary; [2]Department of Cardiology, Szent Rókus Hospital, Baja, Hungary

Contributions: (I) conception and design: A Nemes, Á Kormányos, K Havasi, T Forster; (II) administrative support: N Ambrus; (III) provision of study materials or patients: K Havasi, I Hartyánszky; (IV) collection and assembly of data: Á Kormányos, A Kalapos, P Domsik, Z Kovács; (V) data analysis and interpretation: Á Kormányos, A Nemes; (VI) manuscript writing: all authors; (VII) final approval of manuscript: all authors.

Correspondence to: Attila Nemes, MD, PhD, DSc, FESC. 2nd Department of Medicine and Cardiology Center, Medical Faculty, Albert Szent-Györgyi Clinical Center, University of Szeged, H-6725 Szeged, Semmelweis Street 8, Hungary. Email: nemes.attila@med.u-szeged.hu.

Background: Fibrous mitral annulus (MA) is an important part of the mitral valve having a role in forwarding blood from the left atrium (LA) to the left ventricle (LV). MA can be assessed by three-dimensional speckle-tracking echocardiography (3DSTE) respecting the cardiac cycle. The present study was designed to test whether repaired Tetralogy of Fallot (TOF) is associated with morphological and functional alterations of the MA. The role of the type of treatment (early total reconstruction vs. early palliation, late correction) was also assessed.

Methods: The study population consisted of 29 consecutive adults repaired TOF patients (mean age: 35.4±15.5 years, 18 men), from which 13 patients underwent early total reconstruction (etrTOF), while 16 patients were firstly palliated and later corrected (pcTOF). Their data were compared to that of 76 age- and gender-matched healthy controls (mean age: 35.9±7.6 years, 33 men). All repaired TOF patients and controls were assessed by two-dimensional (2D) Doppler echocardiography and 3DSTE.

Results: Dilated end-systolic and end-diastolic MA diameter, area and perimeter and reduced MA fractional area change and MA fractional shortening could be demonstrated in repaired TOF patients as compared to controls. Increased body surface area-indexed end-diastolic and end-systolic MA diameter and perimeter could be demonstrated in pcTOF patients as compared to that of etrTOF cases.

Conclusions: MA enlargement and functional impairment could be detected in adult patients with repaired TOF regardless of the type of correction. However, pcTOF patients have worse results.

Keywords: Mitral annulus (MA); function; three-dimensional (3D); echocardiography; speckle-tracking

Submitted Mar 27, 2019. Accepted for publication Jun 12, 2019.
doi: 10.21037/cdt.2019.06.08
View this article at: http://dx.doi.org/10.21037/cdt.2019.06.08

Introduction

Tetralogy of Fallot (TOF) is a cyanotic congenital heart disease (CHD) consisting of ventricular septal defect, overriding aorta, pulmonary stenosis, and right ventricular hypertrophy (1,2). Due to the opportunity of early total reconstruction, there is an increasing number of patients with repaired TOF in the adult clinical practice (1). Several echocardiographic methods can be used for

their assessment including three-dimensional speckle-tracking echocardiography (3DSTE), which is a novel echocardiographic modality with capability of 3D volumetric and functional assessment of heart chambers (3-7).

Fibrous mitral annulus (MA) is an important part of the mitral valve having a role in forwarding blood from the left atrium (LA) to the left ventricle (LV) and can be assessed respecting the cardiac cycle by 3DSTE (8). The present study was designed to test whether repaired TOF is associated with morphological and functional alterations of the MA as compared to that of age- and gender matched healthy controls. The role of the type of treatment (early total reconstruction *vs.* early palliation, late correction) was also assessed.

Methods

Patient population

More than 3,000 patients with CHD have been involved into the Registry of C(S)ONGenital caRdiAc Disease patients at the University of Szeged (CSONGRAD Registry), who have been treated and/or operated on since 1961 at the Department of Pediatrics, Department of Cardiac Surgery, and 2nd Department of Medicine and Cardiology Center were collected ("Csongrád" is the name of one of the 19 Hungarian counties where the city of Szeged is placed) (9). From this patient population, 29 consecutive adults repaired TOF patients (mean age: 35.4±15.5 years, 18 men) were recruited, from which 13 patients underwent early total reconstruction (etrTOF), while 16 patients were firstly palliated and later corrected (pcTOF). Early total reconstruction was performed at the age of 5.3±3.2 years in etrTOF patients (mean follow-up period: 29.0±12.0 years). Blalock-Taussig operation (n=15), Brock surgery (n=2), Brock surgery and Blalock-Taussig operation (n=1) were performed as a palliation in pcTOF patients at the age of 4.4±4.2 years. Late correction was performed in pcTOF patients at the age of 12.6±13.1 years (mean follow-up period was 33.7±14.2 years; from early palliation to late correction it proved to be 25.0±11.6 years). Their data were compared to that of 76 age- and gender-matched adult healthy controls (mean age: 35.9±7.6 years, 33 men). All repaired TOF patients and controls were in sinus rhythm and assessed by two-dimensional (2D) Doppler echocardiography and 3DSTE. A special study was organized at the Cardiology Center of the University of Szeged to assess diagnostic and prognostic significance of 3DSTE-derived parameters named MAGYAR-Path Study (Motion Analysis of the heart and Great vessels bY three-dimensionAl speckle-tRacking echocardiography in Pathological cases). All repaired TOF patients and control subjects gave informed consent. The institutional human research committee approved the study which complied with the 1975 Declaration of Helsinki.

2D Doppler and tissue Doppler echocardiography

Toshiba Artida™ echocardiographic device (Toshiba Medical Systems, Tokyo, Japan) with a PST-30SBP phased-array transducer was used for routine 2D Doppler and tissue Doppler echocardiography in all patients. LA and LV dimensions and ejection fraction were assessed according to the guidelines. Doppler echocardiography was used to exclude valvular regurgitations and stenoses as well as for the measurement of early and late diastolic mitral inflow velocities and their ratio.

3D speckle-tracking echocardiography

For 3DSTE-derived data acquisitions, the same Toshiba Artida™ echocardiography machine (Toshiba Medical Systems, Tokyo, Japan) using a PST-25SX matrix-array transducer from apical window was used (10). A full-volume pyramid-shaped 3D dataset was created by the software from separately acquired six wedge-shaped subvolumes during a single breath-hold and constant RR interval on ECG. 3D analysis was performed by 3D Wall Motion Tracking software version 2.7 (Toshiba Medical Systems, Tokyo, Japan). For analysis of MA, a virtual 3D model of the LV was generated by the help of automatically selected apical two- (AP2CH) and four-chamber (AP4CH) views and 3 short-axis views at basal, midventricular and apical LV levels at end-diastole. Following optimization of image planes on the endpoints of the MA on AP2CH and AP4CH views, several measurements were performed on the C7 short-axis view (*Figure 1*) (8):

(I) For morphological assessment of MA, its diameter (MAD), area (MAA) and perimeter (MAP) were measured both at end-diastole and end-systole. MAD was defined as the perpendicular line drawn from the peak of MA curvature to the middle of the straight MA border. MAA and MAP were assessed by planimetry;

(II) For functional assessment of MA, several functional

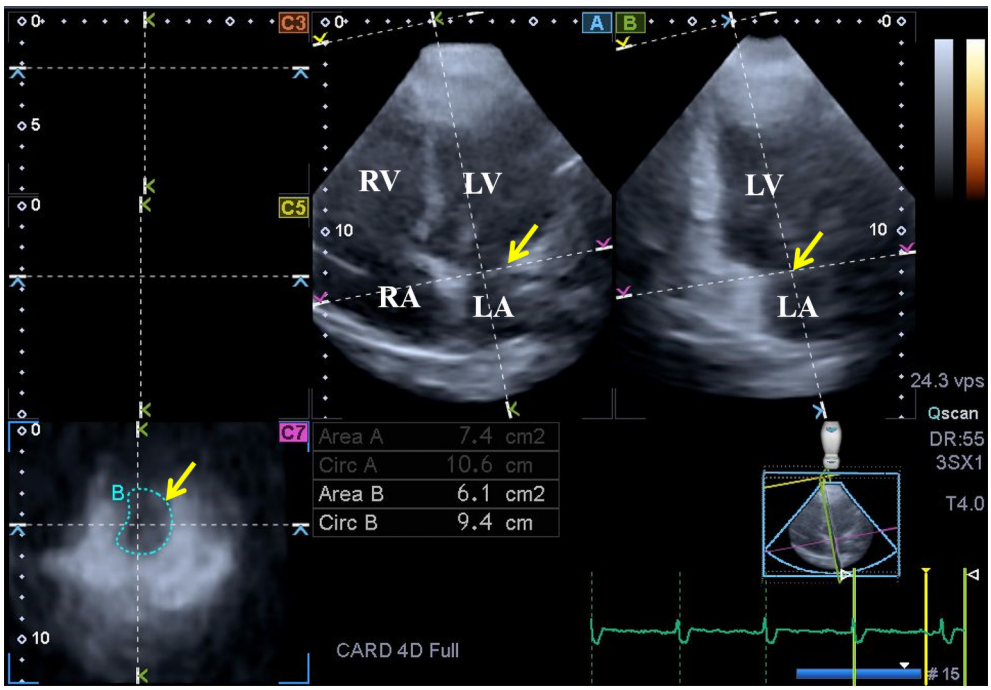

Figure 1 Images from a 3D full-volume dataset presenting the MA in a patient with repaired TOF: (A) Apical four-chamber view; (B) apical two-chamber view and a cross sectional view at the level of the MA (C7) optimized on apical four- and two-chamber views. The yellow arrow represents the mitral annular plane on the long- (A,B) and short-axis (C7) images. MA, mitral annulus; TOF, tetralogy of Fallot; LA, left atrium; LV, left ventricle; RA, right atrium; RV, right ventricle.

properties were calculated using MAD and MAA data: MA fractional shortening (MAFS) = (end-diastolic MAD – end-systolic MAD)/end-diastolic MAD × 100 and MA fractional area change (MAFAC) = (end-diastolic MAA – end-systolic MAA)/end-diastolic MAA × 100.

Statistical analysis

Two-tailed statistical tests were used in all comparisons and a statistical significance was defined with a P value <0.05. Continuous data were presented as mean values ± standard deviation, while categorical data were summarized as a count and percentage. For categorical variables, Fisher's exact test was used. For continuous variables, Shapiro-Wilk test was used to test the normal distribution and if it was confirmed, Student *t*-test was used. If not normally, normally distributed datasets were compared, Mann-Whitney-Wilcoxon test was used. Correlations were assessed by calculating Pearson's correlation coefficients. Data were analysed using Medcalc software (MedCalc, Mariakerke, Belgium).

Results

Demographic and 2D echocardiographic data

Enlarged left atrial diameter and normal LV dimensions and volumes with preserved LV ejection fraction were found in repaired TOF patients regardless of the type of correction as compared to controls (*Table 1*). Tricuspid annular plane systolic excursion (18.4±4.8 *vs.* 16.7±3.5 mm, P=ns) and right ventricular fractional area change (37.1±21.7% *vs.* 43.4±10.6%, P=ns) did not differ between etrTOF and pcTOF patients. Valvular regurgitations and the ratio of their grades are presented in *Table 1*.

3D speckle-tracking echocardiography

Dilated end-systolic and end-diastolic MAD, MAA and MAP could be demonstrated in repaired TOF patients as compared to controls (*Table 2*). MAFAC and MAFS were reduced regardless of the type of treatment. Both BSA-indexed and non-indexed end-systolic MAD, MAA, and MAP were significantly increased in etrTOF patients as compared to that of healthy controls. Almost all BSA-indexed and non-

Table 1 Baseline demographic and 2D Doppler echocardiographic data in patients with repaired TOF and controls

Data	Controls	All repaired TOF patients	etrTOF patients	pcTOF patients
Number	76	29	13	16
Risk factors				
Age (years)	35.9±7.6	35.4±15.5	33.5±14.2	37.1±16.8
Male gender, n [%]	33 [43]	18 [62]	7 [54]	11 [69]
Hypertension, n [%]	0 [0]	8 [28]*	4 [31]*	4 [25]*
Diabetes mellitus, n [%]	0 [0]	0 [0]	0 [0]	0 [0]
Hypercholesterolemia, n [%]	0 [0]	1 [3]	1 [8]	0 [0]
2D echocardiography				
LA diameter (mm)	36.1±3.8	42.0±6.9*	42.0±7.5*	41.9±6.6*
LV end-diastolic diameter (mm)	47.6±4.2	50.3±13.2	47.8±5.8	52.4±17.3*
LV end-diastolic volume (mL)	104.8±23.7	110.1±32.9	108.8±32.7	111.3±34.3
LV end-systolic diameter (mm)	35.5±20.6	31.5±6.3	31.2±5.3	31.7±7.3
LV end-systolic volume (mL)	36.7±9.5	42.2±26.4	39.5±20.3	44.5±31.3
Interventricular septum (mm)	9.3±1.5	9.8±1.5	9.5±1.1	9.9±1.8
LV posterior wall (mm)	9.5±1.7	9.5±1.4	9.4±1.1	9.6±1.5
LV ejection fraction (%)	64.7±3.8	63.9±11.0	65.5±6.1	62.5±14.0
Aortic regurgitation, %				
Grade 1	0 [0]	3 [10]*	1 [8]	2 [13]*
Mitral regurgitation, %				
Grade 1	0 [0]	5 [17]*	2 [15]*	3 [19]*
Grade 2	0 [0]	2 [7]	1 [8]	1 [6]
Tricuspid regurgitation, %				
Grade 1	0 [0]	12 [41]*	6 [46]*	6 [38]*
Grade 2	0 [0]	5 [17]*	3 [23]*	2 [13]*
Grade 3	0 [0]	2 [7]†	0 [0]	2 [13]*
Grade 4	0 [0]	1 [3]	0 [0]	1 [6]

*, P<0.05 *vs.* Controls, †, P=0.07 *vs.* Controls. LA, left atrial; LV, left ventricular; TOF, tetralogy of Fallot; etrTOF, TOF early total reconstruction; pcTOF, TOF early palliation, late correction.

indexed MA parameters were enlarged in pcTOF patients as compared to controls. Increased BSA-indexed end-diastolic and end-systolic MAD and MAP could be demonstrated in pcTOF patients as compared to that of etrTOF cases.

Correlations

MA functional properties (MAFAC, MAFS) did not correlate with 3DSTE-derived LV-EF neither in controls, nor in repaired TOF patients. MAA-S and MAP-S showed correlations with age at the time of the total reconstruction in etrTOF patients (r=0.57, P=0.04 and r=0.57, P=0.04, respectively). The other MA parameters did not show correlations with ages. Similar relationships between ages at the time of early palliation, late correction or difference between these ages and MA dimensions and functional

Table 2 Comparison of 3D speckle-tracking echocardiography-derived mitral annular morphological and functional parameters between patients with repaired TOF and controls

Data	Controls	All repaired TOF patients	etrTOF patients	pcTOF patients
Morphological parameters				
MAD-D (cm)	2.47±0.40	2.65±0.42*	2.62±0.44	2.68±0.41
MAD-D/BSA (cm/m^2)	1.34±0.22	1.48±0.23*	1.40±0.16	1.59±0.25*†
MAA-D (cm^2)	7.62±2.21	8.93±3.09*	8.49±3.03	9.29±3.18*
MAA-D/BSA (cm/m^2)	4.14±1.10	4.88±1.53*	4.47±1.19	5.39±1.76*
MAP-D (cm)	10.41±1.50	11.35±1.93*	11.05±1.91	11.60±1.98*
MAP-D/BSA (cm/m^2)	5.63±0.82	6.29±1.03*	5.88±0.74	6.80±1.08*†
MAD-S (cm)	1.66±0.42	2.16±0.38*	2.08±0.42*	2.22±0.35*
MAD-S/BSA (cm/m^2)	0.90±0.23	1.19±0.22*	1.09±0.17*	1.30±0.21*†
MAA-S (cm^2)	3.55±1.29	6.44±2.54*	5.89±1.96*	6.89±2.92*
MAA-S/BSA (cm/m^2)	1.92±0.66	3.43±1.25*	3.01±0.79*	3.89±1.52*
MAP-S (cm)	7.10±1.19	9.77±1.77*	9.52±1.60*	9.98±1.91*
MAP-S/BSA (cm/m^2)	3.83±0.64	5.36±0.86*	5.01±0.67*	5.78±0.89*†
Functional parameters, %				
MAFAC	52.25±14.24	27.60±13.50*	29.38±13.75*	26.14±13.56*
MAFS	31.98±15.66	18.25±10.56*	20.45±10.40*	16.47±10.68*

*, P<0.05 *vs.* Controls; †, P<0.05 *vs.* etrTOF. MAA-D, end-diastolic mitral annular area; MAA-S, end-systolic mitral annular area; MAD-D, end-diastolic mitral annular diameter; MAD-S, end-systolic mitral annular diameter; MAFAC, mitral annular fractional area change; MAFS, mitral annular fractional shortening; MAP-D, end-diastolic mitral annular perimeter; MAP-S, end-systolic mitral annular perimeter; TOF, tetralogy of Fallot; etrTOF, TOF early total reconstruction; pcTOF, TOF early palliation, late correction.

properties could not be confirmed in pcTOF patients.

Discussion

According to recent findings from imaging studies, significant alterations could be detected in the left heart including LV and LA morphology and function in addition to right heart abnormalities in adults with repaired TOF (3,4,11-13). Most repaired TOF patients show a normal LV twisting pattern, but with a significantly lower LV twist mainly due to decreased apical rotation (11). Almost one-third of the subjects had an abnormal twist pattern due to both abnormal apical and/or basal LV rotations. Over a quarter of the patients had abnormal apical rotation that was associated with larger LV dimensions and decreased biventricular systolic function. Regarding to LV global longitudinal function in repaired TOF, LV global longitudinal strain (LV-GLS) was found to be reduced mainly due to the interventricular septum probably by mechanical coupling of the ventricles (12). In recent 3DSTE-derived atrial studies, both RA and LA volumes seemed to be increased in adult patients with repaired TOF with almost similar deformational abnormalities of RA and LA (3,4).

Mitral valve and its annulus play an important role in regulating blood flow between LV and LA. According to the above-mentioned alterations it could be theorized, that MA could show significant remodelling in repaired TOF. 3DSTE was found to be a valuable tool not only for volumetric and functional assessment of different cardiac chambers (3,4,10), but also for the evaluation of MA dimensions and functional properties respecting the cardiac cycle (8). Although 3DSTE-derived methodology does not assess the 3D spatial saddle shape of MA directly, but only its projection to the chosen 2D plane, dilation of MA dimensions and MA functional impairment could be demonstrated in adult repaired TOF patients, regardless of the type of correction. Moreover, patients who were treated

with the two-step way (early palliation, late correction) showed worse results suggesting clinical benefits of early total reconstruction on late MA morphology and function. Moreover, correlation between the age of early total reconstruction and MA systolic dimensions could confirm these findings. However, further studies are warranted to confirm our findings in a larger patient population evaluating their prognostic significance, as well.

Several important limitations have arisen during the assessments:

(I) A relatively small number of patients from a single center by a single observer (DP) were examined. However, it should be considered that repaired TOF is a relatively rare disease;

(II) Moreover, adult patients with some risk factors were assessed, therefore their effects could also be taken into considerations when interpreting results;

(III) The current image quality of 3DSTE is inferior to that of 2D echocardiography due to poor temporal and spatial image resolutions;

(IV) During the present study, ventricular and atrial volumetric and functional characterization was not aimed to be performed.

Conclusions

MA enlargement and functional impairment could be detected in adult patients with repaired TOF regardless of the type of correction. However, pcTOF patients have worse results.

Acknowledgments

None.

Footnote

Conflicts of Interest: The authors have no conflicts of interest to declare.

Ethical Statement: The authors are accountable for all aspects of the work in ensuring that questions related to the accuracy or integrity of any part of the work are appropriately investigated and resolved.

References

1. Swamy P, Bharadwaj A, Varadarajan P, et al. Echocardiographic evaluation of tetralogy of Fallot. Echocardiography 2015;32 Suppl 2:S148-56.
2. Bedair R, Iriart X. Educational series in congenital heart disease: Tetralogy of Fallot: diagnosis to long-term follow-up. Echo Res Pract 2019;6:R9-23.
3. Nemes A, Havasi K, Domsik P, et al. Evaluation of right atrial dysfunction in patients with corrected tetralogy of Fallot using 3D speckle-tracking echocardiography. Insights from the CSONGRAD Registry and MAGYAR-Path Study. Herz 2015;40:980-8.
4. Havasi K, Domsik P, Kalapos A, et al. Left Atrial Deformation Analysis in Patients with Corrected Tetralogy of Fallot by 3D Speckle-Tracking Echocardiography (from the MAGYAR-Path Study). Arq Bras Cardiol 2017;108:129-34.
5. Nesser HJ, Mor-Avi V, Gorissen W, et al. Quantification of left ventricular volumes using three-dimensional echocardiographic speckle tracking: Comparison with MRI. Eur Heart J 2009;30:1565-73.
6. Saito K, Okura H, Watanabe N, et al. Comprehensive evaluation of left ventricular strain using speckle tracking echocardiography in normal adults: Comparison of three-dimensional and two-dimensional approaches. J Am Soc Echocardiogr 2009;22:1025-30.
7. Yu HK, Li SJ, Ip JJ, et al. Right ventricular mechanics in adults after surgical repair of tetralogy of Fallot: insights from three-dimensional speckle-tracking echocardiography. J Am Soc Echocardiogr 2014;27:423-9.
8. Nemes A, Földeák D, Kormányos Á, et al. Cardiac Amyloidosis Associated with Enlargement and Functional Impairment of the Mitral Annulus: Insights from the Three-Dimensional Speckle Tracking Echocardiographic MAGYAR-Path Study. J Heart Valve Dis 2017;26:304-8.
9. Havasi K, Kalapos A, Berek K, et al. More than 50 years' experience in the treatment of patients with congenital heart disease at a Hungarian university hospital. The basics of the CSONGRAD Registry. Orv Hetil 2015;156:794-800.
10. Nemes A, Kalapos A, Domsik P, et al. Three-dimensional speckle-tracking echocardiography – a further step in non-invasive three-dimensional cardiac imaging. Orv Hetil 2012;153:1570-7.
11. Menting ME, Eindhoven JA, van den Bosch AE, et al. Abnormal left ventricular rotation and twist in adult patients with corrected tetralogy of Fallot. Eur Heart J Cardiovasc Imaging 2014;15:566-74.
12. Menting ME, van den Bosch AE, McGhie JS, et al. Assessment of ventricular function in adults with repaired

Tetralogy of Fallot using myocardial deformation imaging. Eur Heart J Cardiovasc Imaging 2015;16:1347-57.
13. Timóteo AT, Branco LM, Rosa SA, et al. Usefulness of right ventricular and right atrial two-dimensional speckle tracking strain to predict late arrhythmic events in adult patients with repaired Tetralogy of Fallot. Rev Port Cardiol 2017;36:21-9.

Cite this article as: Nemes A, Kormányos Á, Havasi K, Kovács Z, Domsik P, Kalapos A, Hartyánszky I, Ambrus N, Forster T. Mitral annulus is enlarged and functionally impaired in adult patients with repaired tetralogy of Fallot as assessed by three-dimensional speckle-tracking echocardiography—results from the CSONGRAD Registry and MAGYAR-Path Study. Cardiovasc Diagn Ther 2019. doi: 10.21037/cdt.2019.06.08